Dissecting grapevine graft incompatibility with particular reference to its early detection and underlying causes

Sara Tedesco

Dissertation presented to obtain the Ph.D degree in Biology

Instituto de Tecnologia Química e Biológica António Xavier |
Universidade Nova de Lisboa

Oeiras, June, 2021

Work performed at:

Plant Cell Biotechnology Laboratory

Instituto de Tecnologia Química e Biológica António Xavier (ITQB)

Universidade Nova de Lisboa

Av. da República, 2780-157 Oeiras, Portugal

Intercellular Macromolecular Transport Laboratory

Department 2

Max Planck Institute of Molecular Plant Physiology (MPI-MP)

Wissenschaftspark Golm, Am Mühlenberg 1, 14476 Potsdam, Germany

Part of the work was performed at:

Unidad de Hortofruticultura

Centro de Investigación y Tecnología Agroalimentaria de Aragón (CITA)

Av. Montañana, 930, 50059 Zaragoza, Spain

PhD Supervisors:

Professor Pedro Fevereiro

Head of laboratory, Plant Cell Biotechnology Laboratory, Instituto de Tecnologia Química e Biológica António Xavier, Universidade Nova de Lisboa.

CEO of the InnovPlantProtect CoLab, Estrada de Gil Vaz Apartado 72, 7351-901 Elvas, Portugal

Doctor habil. Friedrich Kragler

Head of Intercellular Macromolecular Transport Laboratory, Department 2, Max Planck Institute of Molecular Plant Physiology, Potsdam, Germany

Doctor Ana Pina

Researcher, Unidad de Hortofruticultura, Centro de Investigación y Tecnología Agroalimentaria de Aragón, Zaragoza, Spain.

“Segundo os ensinamentos dos índios norte americanos os seres do Povo em Pé são as árvores, nossos irmãos e irmãs e chefes do reino das Plantas. O Povo em Pé fornece oxigênio ao resto dos filhos da Terra. Através de seus troncos e de seus galhos, as árvores dão abrigo aos seres que têm asas. Nos vãos de suas raízes as árvores fornecem asilo às pequenas criaturas de quatro patas que vivem embaixo da terra. Os Cherokees ensinam que o Povo em Pé e todos os outros povos do reino das plantas são os seres dadivosos que provêem, o tempo inteiro, às necessidades de outros seres.

O Povo em Pé percebe as necessidades de todos os Filhos da Terra e se esforça por atendê-las. Cada árvore e planta possui seus próprios dons, talentos e habilidades a serem compartilhados. Por exemplo, algumas árvores nos dão frutos, enquanto outras fornecem curas para distúrbios em nossos níveis emocionais ou físicos. Porém, cada uma das Pessoas em Pé tem uma lição especial a ser transmitida à humanidade, que vai muito além dos presentes materiais. A Bétula ensina a essência da verdade, nos incita a sermos honestos com nós mesmos ou nos mostra como podemos ser enganados por mentiras alheias. Os Pinheiros são pacificadores. O Pinheiro nos ensina as lições de como estarmos em harmonia com nós mesmos e com os outros, além de nos ensinar a obter uma mente silenciosa. O Plátano ensina-nos a alcançar nossos objetivos e a fazer nossos sonhos se realizarem, a Nogueira nos ensina clareza ou concentração através da utilização de nossos dons mentais, e nos ensina a empregar a nossa inteligência de forma adequada. O Carvalho nos ensina a ter força de caráter e manter nossos corpos fortes e sadios. O Salgueiro é a madeira do amor, e nos ensina a dar, a receber, e a saber ceder, qualidades tão necessárias para que o amor frutifique. A Cerejeira nos ensina a abrir o nosso coração e a nos relacionarmos com os outros usando o sentido da compaixão.

Os Nativos de todas as partes do mundo têm vivido em harmonia com o reino das plantas, em suas respectivas regiões, e têm utilizado o reino vegetal como ajuda à sua sobrevivência. O povo indígena da Mãe Terra só tem usado aquilo de que necessita, e não armazena, por medo de escassez, as oferendas que as árvores lhes proporcionam.

Os Senecas dizem que toda árvore tem mais raízes do que galhos. Este ensinamento nos fala de como cada Pessoa em Pé está ligada profundamente à Mãe Terra.

À semelhança do Povo em Pé, nós, os seres Duas Pernas, temos uma espinha que lembra um tronco, braços que parecem galhos, e cabelos que lembram folhas. Crescemos em direção à luz, da mesma forma que os galhos da árvore esticam-se em direção ao Avô Sol. Nós, os Duas Pernas, também estamos sempre dando e recebendo quando estamos Caminhando em Equilíbrio. A humanidade forma a ponte entre a Mãe Terra e a Nação do Céu, e nós, assim como o Povo em Pé, pertencemos a estes dois mundos. Para conseguir este equilíbrio, devemos viver em harmonia com Todos os Nossos Parentes e estar bem enraizados neste mundo através de nossa Mãe Terra. No momento em que conseguimos retribuir a gratidão pelos presentes que recebemos dos outros, passamos a reconhecer a raiz de cada bênção. Toda vez que retribuímos nossa gratidão à fonte de nossas bênçãos, voltamos a equilibrar o nosso mundo e a reconhecer todas as dádivas que recebemos. A raiz de todas as civilizações que estão por vir já vive neste momento dentro de cada um de nós. Nutrir o futuro equivale a honrar as sementes do presente, permitindo que elas cresçam e se desenvolvam. O Povo em Pé nos pede que nos doemos mais e nos inspira como Guardiãs de nossa Mãe Terra a olhar a raiz de cada bênção para o Bem, de tal forma que a sua dádiva não tenha sido ofertada em vão."

Adaptado de "As cartas do caminho sagrado" de Jamie Sams

Table of contents

Acknowledgements

This work results from the contribution of many people who came to teach and to support me during these years, and without which the realization of this thesis would not have been possible. To all, I would like to express my most sincere gratitude:

- **My PhD advisors**, Professor Pedro Fevereiro, Friedrich (Fritz) Kragler, and Ana Pina for teaching me how to be a researcher. Particularly I want to thank Professor Pedro for accepting me in his lab and providing me with all the necessary means, for the long discussions about incompatibility, to have dressed the lab coat and for coming with me to the grow chamber or the greenhouse and touching by hands the work when I needed an opinion. I also thank him for being an example of hard working addressed to the well of the community. I want to thank Fritz for the opportunity of working with him even if I was not formed in biology and to have personally taught me all I know about molecular biology. For his efforts in making me feel at home in Germany too, and for having patiently endured my temper for over a year sharing the same office. I would also like to thank Ana for being so easy to understand each-other and work together, for having always treated me as a collaborator more than a student and to have never let me alone, nor in reality nor in the empathy. To Ana I own the scientific thinking in conceptualizing, structure and present a research in scientific journals, and I will be always thankful to her for this.

- **All the collaborators**, particularly Dr. Joachim Kopka for his scientific guidance, help in the statistical analysis, and for sincerely support me during the journal revisions' process. A special thanks to Alex Erban, who taught me everything I know about data analysis, for the excel functions and tips, and for his friendly patience and zoom meetings at any day and time (chapter III). To Patricia Irisarri thanks for teaching me histological and histochemistry methods, and for the effort in optimizing the TUNEL

assay for grapevine samples (chapter IV). I want also to thank Dra. Margarida Teixera Santos for sharing with me her knowledge (and materials) about grapevines, their micropropagation, as well as about grapevine viruses and their detection (chapter IV). Thanks also to Pedro Lamosa and Manolis Matzapetakis for their help in NMR spectroscopy, and to Isabel for helping in the collection of the samples (chapter III).

- **All the members of Plant Cell Biotechnology laboratory**: Maria, Sara, Ze', Susana Araujo, Sofia, Ehsan, Claudia, Michela, Margarida, Rita, Diogo and to our neighbour friends from the Plant-X group for being so natural to share and help each other in the lab and making this a so nice, homy, and friendly environment. A special thanks to Maria, for being the best collaborator and friend I could ever find in my PhD, for sharing all the good and bad moments of this journey and for unconditionally help and dedicate herself to others. To Carmen also a special thanks, for her friendships, and to have passionately introduced me in the word of science more than six years ago and to keep doing so even today.

- **All the members of Fritz Kragler's laboratory**: Eleftheria and Eleni for their help and friendship; Ying for her kind hearth; Dana and Cindy for the technical support in several scientific activities and thanks to all others: Lei, Frank, Fede, Saurabh, Yagmur, Dominik, Julia, Andras, Yuan, Anu, and Stephanie for making so nice to work with you.

- **All colleagues from the Plants for life PhD program**: Davide, Pedro, Rui, Filipa, Carlos, and Stefano for helping making this journey a great one, and thanks to Dr. Nelson Saibo to have made possible this outstanding program, and to take care of each student. Thanks to Fundação para a Ciência e a Tecnologia (FCT) to financially support my grant and the institution.

- My family and friends: to my parents, Piero and Renata, for the hard work in educating me, to teach me the integrity and the value of being human. Thanks to my mother for her listening, to my sister Barbara and

Peter for the many English corrections and to support me emotionally every time I needed. To my grandparents, particularly Franco for showing me the secrets for happiness, and to Wanda and Vittorio, my very firsts professors, to have passed me their passion for education. At this regard, thanks to Professor Maria Raffaella Ellero who changed my life by teaching me the deeply mean of the famous Dante's phrase "*Fatti non foste a viver come bruti, ma per seguir virtute e canoscenza*". Thanks to Massimo, for cutting hundreds of leaf discs, to have called every single day when I was in Germany, and to have accompanied me and shared my weight unconditionally. To my friends Nouri, Sara, Pera, Rose, Fede, Ale capo, Robin, Andrea, Ruben, Giacomo, Peppe, Kelly, Fumiko, Ricardo, Carolina, Marta and all the others, thanks to have cheered my days, to understand my "No", to give me the strength of keeping in front, and always be there for me. Finally, a big thank to Portugal for all the professional and personal opportunities of growth I had here. To all of you, my most heartfelt thanks.

List of abbreviations

µg	Microgram
µl	Microliter
µM	Micromolar
µmol	Micromole
µm	Micrometer
µs	Microsecond
^{o}C	Celsius degrees
ABA	Abscisic acid
ACs	Affinity Coefficients
ALF	*Vitis vinífera* cv. Alfrocheiro
ALF/RUP	Alfrocheiro grafted onto RUP rootstock
ANOVA	Analysis of variance
ArMV	Arabis Mosaic Virus
BERL	*Vitis berlandieri*
Bp	Base pair
BSTFA	N,O-bis-(trimethylsilyl)trifluoroacetamide
Carot	Carotenoids
cDNA	Complementary DNA
CF	Carboxyfluorescein
CFDA	Carboxyfluorescein diacetate
$CHCl_3$	Chloroform
Chl(a)	Chlorophyll a
Chl(a+b)	Total Chlorophyll
Chl(b)	Chlorophyll b
cm	Centimeter
cm^2	Square centimeter
cm^3	Cubic centimeter
CK	Cytokinins

CP	coat protein
Ct	Cycle Threshold
cv.	Cultivar
DAG	Days after grafting
DAS-ELISA	Double-antibody sandwich enzyme-linked immunosorbent assay
DASI-ELISA	Double-antibody sandwich indirect enzyme-linked immunosorbent assay
DAW	Days after wounding
dH_2O	Distilled water
DNA	Deoxyribonucleic acid
EDTA	Ethylenediaminetetraacetic acid
EU	European Union
FAA	Formaldehyde - acetic acid – 70% alcohol
FT	FLOWERING LOCUS T
Fv/Fm; Fv/Fo	Maximum quantum yield of photosystem II
GABA	4-amino butanoic acid
GC–EI–TOF/M	Gas chromatography-electron impact ionization-time of flight/mass spectrometry
GFkV	Grapevine fleck vírus
GLRaV1	Grapevine leafroll-associated virus 1
GLRaV2	Grapevine leafroll-associated virus 2
GLRaV3	Grapevine leafroll-associated virus 3
GRSPaV	Grapevine Rupestris Stem Pitting associated Virus
GVA	Grapevine virus A
H	Hour
HCl	Hydrochloric acid
I_2KI	Potassium iodide-iodine reaction
Log10	Logarithm with base 10

log2	Binary logarithm
M	Molar
m	Meter
m5C	5-methylcytosine
MeOH	Methanol
mg	milligram
mM	Millimolar
mm	Millimeter
min	Minute
miRNA(s)	Micro RNA(s)
ml	Milliliter
mol	Mole
mRNA(s)	Messenger RNA(s)
n	Sample size
NA	Not available
NMR	Nuclear Magnetic Resonance
ns	non-significant differences
ng	Nanogram
ns	non-significant
PCA	Principal Component Analysis
PCD	Programmed cell death
PCR	Polymerase chain reaction
PI	Performance Index
PI	Propidium Iodide
Pr	Pearson residuals
PSII	Photosystem II
QTLs	Quantitative trait loci
r	correlation coefficient
Rcf	relative centrifugal force

RNA	Ribonucleic acid
RNAseq	RNA sequencing
ROS	reactive oxygen species
RT-qPCR	real-time quantitative PCR
RUP	Vitis rupestris
SE	Standard error
SEs	Sieve elements
siRNA(s)	Small interfering RNA(s)
sRNA(s)	Small RNA(s)
SYLV	*Vitis vinifera* subsp. sylvestris
SYLV/RUP	Sylvestris grafted onto RUP rootstock
SY	*Vitis vinífera* cv. Syrah
SY383	Syrah clone 383
SY470	Syrah clone 470
SY383/110R	SY383 grafted onto 110R rootstock
SY470/110R	SY470 grafted onto 110R rootstock
TCA cycle	Tricarboxylic acid cycle
TCTP1	Translationally controlled tumor protein 1
TF(s)	Transcription factor(s)
TLS	tRNA-like sequence
TN	Touriga Nacional
TN21	Touriga Nacional clone 21
TN112	Touriga Nacional clone 112
tRNA(s)	Transfer RNA(s)
110R	Ritcher 110
TN21/110R	TN21 grafted onto 110R rootstock
TN112/110R	TN112 grafted onto 110R rootstock
UBI	Ubiquitin-60S ribosomal protein
UV	Ultraviolet

V.	*Vitis*
vs.	versus
Vj	Variable fluorescence at the J step

Summary

Grafting is an ancient agricultural method widely practice already in Greek and Roman times and consists in the joining of two different plant parts, the scion (shoot) and the rootstock (roots), in a way in which they will develop and functioning as a single plant. Over time, grafting evolved from a way of propagating plants to using them to improve their characteristics. For instance, *Vitis vinifera* are grafted since the middle of the 19th century onto American grapevine rootstocks to exploit their resistance to the Phylloxera, which would otherwise be lethal for European vines. One important aspect of grafting is graft incompatibility which refers to the early or later failure of the graft union which delays rootstock breeding selection and causes losses to farmers and nurseries. However, the effects of grafting, its biology, as well as the phenomenon of graft incompatibility are still insufficiently understood by the scientific community and currently largely unpredictable. To deepen our knowledge on the grapevine graft incompatibility phenomenon and to contribute to the goal of early detecting (in)compatible grafting partners – highly auspicated by grapevine breeders and propagators – we made substantial efforts in phenotyping incompatibility in grapevines both *in vivo* and *in vitro,* and we explored the metabolic scion-rootstock profiles in different tissues and phloem exudate across a wide range of different graft combinations.

To identify physiological characters associated with unsuccessful grafting, we used as experimental system two clones of cv. “Touriga Nacional” (clone 21 – TN21, and clone 112 -TN112) and two clones of cv. “Syrah” (clone 470 – SY470 and clone 383 - SY383) showing different compatibility behaviour when grafted onto the same worldwide used rootstock Richter-110 (110R). We monitored several parameters described as predictive of graft incompatibility in other species but that were not yet been simultaneously tested in grapevine grafts, at 21 (callusing stage) and 152

days after grafting (DAG) (hardening stage) of the propagation process. Among the parameters investigated, the grade of *callus* development, as an indicator of graft success, was shown to be the most valuable for practical nursery's applications as it can be evaluated already at early stages (21 DAG). We found the analysis of leaf chlorophyll content a more sensitive parameter to identify changes between different graft combinations than the measurements of chlorophyll fluorescence while Affinity Coefficients (based on stem diameters) calculated for the same graft combination were found to vary according to the formula used, hence we discourage their use as predictors of compatibility. Furthermore, we concluded that incompatibility might not became apparent at 5 months after grafting in grapevines. Despite, important scion-rootstock interactions, such as the control of the rootstock over the growth and the sprouting time of the scion, were revealed already at this stage.

Therefore, to shed light on the early metabolic grapevine scion-rootstock interactions, we investigated changes in the global metabolic profiles in eleven homo- and heterograft combinations in leaves, stem, and phloem exudates collected from both above and below the graft union at 5-6 months after grafting. In particular, we assessed the metabolic profile of homo- and heterografts, the effect of a heterologous grafting partner in the metabolome of a plant, in specific tissues and phloem exudates samples, as well as the metabolic profile of scion and rootstock samples. This approach revealed that although grafting has a minor impact on the metabolome of grafted grapevines comparing to tissues or genotypes, both grafting partners can exert their influence in specific organs and phloem exudates. Furthermore, both scion and rootstock perceive the presence of a heterologous grafting partner leading to the induction of defense-related metabolites which might reflect the perception of a foreign biome and/or the interaction of the grafting partners 'biomes when these belong to different plant species. Leaves were revealed as the best choice

of tissue to search for grafting-related metabolic markers as they showed more consistent changes while the effect of a scion on a rootstock was genotypically-driven and not generalizable. Surprisingly, the phloem exudate composition was significantly altered between scion and rootstock, and sucrose was found specifically depleted in the rootstock phloem exudate of several *V. vinifera* scion when grafted onto 110R rootstock suggesting an impaired translocation across the graft union of these grafts.

Given that *in vitro* micrografting has been used as an experimental system for graft incompatibility studies, we evaluated the use of *in vitro* micrografting, coupled with histology and histochemistry analysis, to unravel physiological markers that forecast incompatible responses in grapevine graft combinations of known compatibility behaviour. Calcofluor cellulose staining used to evaluate the cellular arrangement and potassium iodide-iodine reaction (I_2KI staining) for quantifying starch contents were able to identify the graft combinations with worse graft success rates among heterografts, hence valuable in early predicting grapevine graft compatibility responses. Surprisingly, we found that heterografted grapevine unions showed typical viral symptoms and that successful heterografts displayed a persistent necrotic layer at 49 DAG, a slower vascular differentiation, a lower starch scion-rootstock translocation, and impaired phloem regeneration suggesting translocated incompatibility symptoms in successful heterografts compared to homografts. Levels of Grapevine Rupestris Stem Pitting associated Virus (GRSPaV) infections were correlated with graft (un)-success in two Syrah clones grafted onto 110-Ritcher rootstock under field and *in vitro* conditions. Furthermore, wounded and grafted Syrah plantlets pointed out to an impaired sucrose distribution in these plants, possibly implicated with GRSPaV infections. Given the evidences provided, we suggest that grapevine graft incompatibility might be a virus-induced problem which can arise even

employing certified virus-free plants. Hence, we encourage the use of *in vitro* micrografting to research the viruses that might be responsible for grapevine graft incompatibility in view of strengthening the certification protocols and thereby preserving our grapevine genetic resources.

The insights produced by this research allowed the identification of useful physiological markers *in vivo* and *in vitro* able to forecast graft incompatibility responses in grapevines and to formulate a hypothesis regarding the inner causes of graft incompatibility in grapevines. Additionally, the metabolic profiles analysed in different graft combinations and tissues, allowed the advance of knowledge on the scale and the content of the metabolic scion-rootstock reciprocal interactions in grapevines, which might facilitate future efforts on the identification of metabolic markers for important agronomic traits in grafted grapevines.

Sumário

A enxertia é um método agronómico antigo amplamente praticado já no tempo dos gregos e dos romanos, consistindo na junção de duas partes diferentes da planta, o garfo (parte aérea) e o porta-enxerto (parte radicular), de forma que se desenvolvam e funcionem como uma planta única. Com o tempo, a enxertia evoluiu de um meio de propagação de plantas para ser utilizada no seu melhoramento. Por exemplo, *Vitis vinifera* é enxertada desde meados do século 19 em porta-enxertos de videiras americanas para explorar a sua resistência à Filoxera, que de outra forma seria letal para as vinhas europeias. Um aspeto importante e ainda pouco estudado da enxertia é o fenómeno da incompatibilidade, que se refere à falha precoce ou tardia do sucesso do enxerto, o que retarda a seleção de porta-enxertos melhorados e causa perdas para os agricultores e viveiristas. De facto, os efeitos da enxertia, a sua biologia, bem como o fenómeno da incompatibilidade ainda são pouco compreendidos pela comunidade científica e são atualmente amplamente imprevisíveis. Para aprofundar o nosso conhecimento sobre o fenómeno da incompatibilidade de enxertia de videira e contribuir ao objetivo da deteção precoce de parceiros de enxertia (in)compatíveis – muito pretendido por melhoradores e propagadores de videira – foi feito um esforço substancial na fenotipagem *in vivo* e *in vitro* da incompatibilidade da enxertia em videiras, e explorou-se os perfis metabólicos do garfo e do porta-enxerto em diferentes tecidos e exsudado do floema em uma ampla gama de diferentes combinações de garfo-porta enxerto.

Para identificar os caracteres fisiológicos associados ao insucesso da enxertia, utilizou-se como sistema experimental dois clones da casta “Touriga Nacional” (clone 21 - TN21, e clone 112 -TN112) e dois clones da casta “Syrah” (clone 470 - SY470 e clone 383 - SY383) que apresentam níveis de compatibilidade diferente quando enxertados no mesmo porta-

enxerto, o mundialmente usado, Richter-110 (110R). Aos 21 dias (fase de calogénese) e 152 dias (fase de aclimatação) após a enxertia, foram monitorizados diversos parâmetros descritos como preditivos de incompatibilidade da enxertia em outras espécies, mas ainda não testados simultaneamente em videira. Entre os parâmetros investigados, o grau de desenvolvimento de *callus* como um indicador de sucesso da enxertia revelou-se mais valioso para aplicações práticas em viveiro, uma vez que pode ser avaliado logo nos estágios iniciais (21 dias após a enxertia - DAG). Verificou-se que a análise do conteúdo da folha em clorofila é um parâmetro para identificar variações entre diferentes combinações de enxerto mais sensível do que as medições de fluorescência da clorofila. Por outro lado, os coeficientes de afinidade (com base nos diâmetros do caule) calculados para a mesma combinação de enxerto variam de acordo com o coeficiente utilizado, desencorajando-se, portanto, o seu uso como preditores de compatibilidade. Além disso, apesar de se ter concluído que a incompatibilidade pode não se tornar aparente 5 meses após a enxertia em videira, importantes interações entre garfo e porta-enxerto, como o controle do porta-enxerto sobre o crescimento e o tempo de abrolhamento do garfo, foram revelados já nesta fase.

Para aprofundar o nosso conhecimento sobre as primeiras interações metabólicas entre o garfo e porta-enxerto de videira, investigamos as mudanças nos perfis metabólicos globais em onze combinações de homo- e hétero-enxertos em folhas, caule, e exsudados do floema coletados acima e abaixo da zona de união, 5-6 meses após a enxertia. Em particular, avaliou-se o perfil metabólico de homo- e hétero-enxertos, o efeito de um parceiro heterólogo no metaboloma de uma planta, em tecidos específicos e amostras de exsudados do floema, bem como o perfil metabólico de amostras de garfos e de porta-enxertos. Esta abordagem revelou que, embora o enxerto tenha um impacto menor no metaboloma de videiras enxertadas em comparação com o tecido ou o

genótipo, ambos os parceiros do enxerto podem exercer a sua influência em órgãos e exsudados específicos. Além disso, tanto o garfo como o porta-enxerto reagem à presença de um parceiro heterólogo com a indução de metabolitos relacionados com defesa, o que pode refletir a perceção de um bioma estranho e/ou a interação dos biomas dos parceiros de enxerto quando estes pertencem a diferentes espécies de plantas. As folhas foram identificadas como a melhor escolha para a procura de marcadores metabólicos relacionados com a enxertia, pois mostraram mudanças mais consistentes, enquanto o efeito de um garfo em um porta-enxerto resultou numa resposta genótipo-dependente e não generalizável. Surpreendentemente, a composição do exsudado do floema entre o garfo e o porta-enxerto foi significativamente alterada, e a sacarose foi encontrada especificamente diminuída no exsudato do floema do porta-enxerto de vários enxertos de *V. vinifera* quando enxertado no porta-enxerto 110R, sugerindo que a translocação através da união do enxerto esteja perturbada nestas combinações.

Visto que a microenxertia *in vitro* tem sido usada como um sistema experimental para estudos de incompatibilidade, permitindo aos investigadores contornar várias restrições dos ensaios *in vivo* e permitindo uma avaliação mais precoce, utilizou-se esta técnica, através análise histológica e histoquímica, para desvendar marcadores fisiológicos que pudessem prever respostas incompatíveis em combinações de enxerto de videiras com comportamento de compatibilidade conhecido. A coloração da celulose com calcofluor usada para avaliar a organização celular, e a reação de iodeto de potássio-iodo (coloração com I_2KI) para quantificar o conteúdo de amido, permitiram identificar as combinações de enxerto com piores taxas de sucesso entre hétero-enxertos, portanto, valiosas na previsão precoce da compatibilidade de enxertia em videira. Surpreendentemente, descobrimos que as uniões de hétero-enxertos mostraram sintomas virais típicos, e que os hétero-enxertos bem-

sucedidos exibiram uma camada necrótica persistente aos 49 DAG, uma diferenciação vascular mais lenta, uma menor translocação de amido entre garfo e porta-enxerto, e uma regeneração do floema alterada, sugerindo sintomas de incompatibilidade translocada em hétero-enxertos bem-sucedidos comparados com homo-enxertos. Os níveis de infeção por Grapevine Rupestris Stem Pitting associated Virus (GRSPaV) foram correlacionados com o (não)-sucesso da enxertia em dois clones de Syrah enxertados no porta-enxerto 110-Ritcher em condições de campo e *in vitro*. Além disso, plantulas de Syrah feridas e enxertadas mostraram uma distribuição anómala de sacarose nessas plantas, possivelmente implicada pela infeção com GRSPaV. Dadas as evidências colecionadas, sugere-se que a incompatibilidade da enxertia em videira possa ser um problema induzido por vírus, que pode surgir mesmo empregando plantas certificadas por serem livres de vírus e encoraja-se o uso da microenxertia *in vitro* para pesquisar a presença de vírus que possam ser responsáveis pela incompatibilidade, com o objetivo de fortalecer os protocolos de certificação e, assim, preservar os recursos genéticos de videira.

As evidencias produzidas no âmbito desta investigação permitiram identificar marcadores fisiológicos úteis, quer *in vivo* quer *in vitro* para prever respostas de incompatibilidade de enxertia em videira, e formular uma hipótese sobre as causas internas da incompatibilidade. Além disso, os perfis metabólicos analisados em diferentes combinações de enxertos e tecidos, permitiram avançar o conhecimento sobre a escala e o conteúdo das interações metabólicas recíprocas entre garfo e porta-enxerto em videiras, o que pode facilitar futuros esforços na identificação de marcadores metabólicos para importantes características agronómicas em videiras enxertadas.

Chapter I

General Introduction

This chapter was prepared to be submitted for future publication.

More information can be found in the following publication:

Assunção, M.; **Tedesco, S.**; Fevereiro, P. Molecular Aspects of Grafting in Woody Plants. In *Annual Plant Reviews Online*, 1st ed.; Wiley Online Library: New York, NY, USA, 2021; Volume 4, pp. 87–126. doi: 10.1002/9781119312994. apr0751

Abstract

Grafting is a method for plant propagation and improvement. In the European viticulture, grafting is the sole control strategy against the Phylloxera injuries, being of crucial importance for sustainable grape production. Despite these benefits, grafting is also source for disease dissemination and graft incompatibility results in propagation losses. However, the physiology of grafting, such as compatibility factors, healing processes and the components of signaling between scion and rootstock, are still insufficiently understood by the scientific community. Advances in grafting research hint at a complex scion-rootstock communication. Mobile molecules, such as hormones, metabolites proteins and RNAs, and also coordinated gene expression and regulation between plant parts are suspected to modulate the healing of the union and the regeneration of vascular tissues. Among some graft partners such processes result in a successful graft but in other cases, the graft develops distress symptoms, early or in the long term, eventually leading to graft incompatibility. It is not known whether the cause of incompatibility is based on a rejection of the opposing partners or on the stress induced by the grafting itself. The recognition of graft-transmissible RNA signals as important players in regulating coordinated developmental and environmental shoot-root responses opens a new path towards understanding grafting physiology and perhaps incompatibility. This chapter summarizes the current knowledge on grafting from the perspective of viticulture, discusses the hypotheses behind graft incompatibility, and matters related to the molecular effects of grafting, as well as current and novel research perspectives that might help to unveil this millenary mystery.

Key words: Graft Incompatibility, Grafting, RNA signaling, Rootstock-scion communication, *Vitis vinifera*

1. Introduction

Grafting refers to the union of plant body parts so that vascular continuity is established between them and the resulting composite organism functions as a single plant body [1]. Usually, the upper shoot portion of one plant ("scion") is grafted onto the lower portion of another plant ("rootstock") (Figure 1).

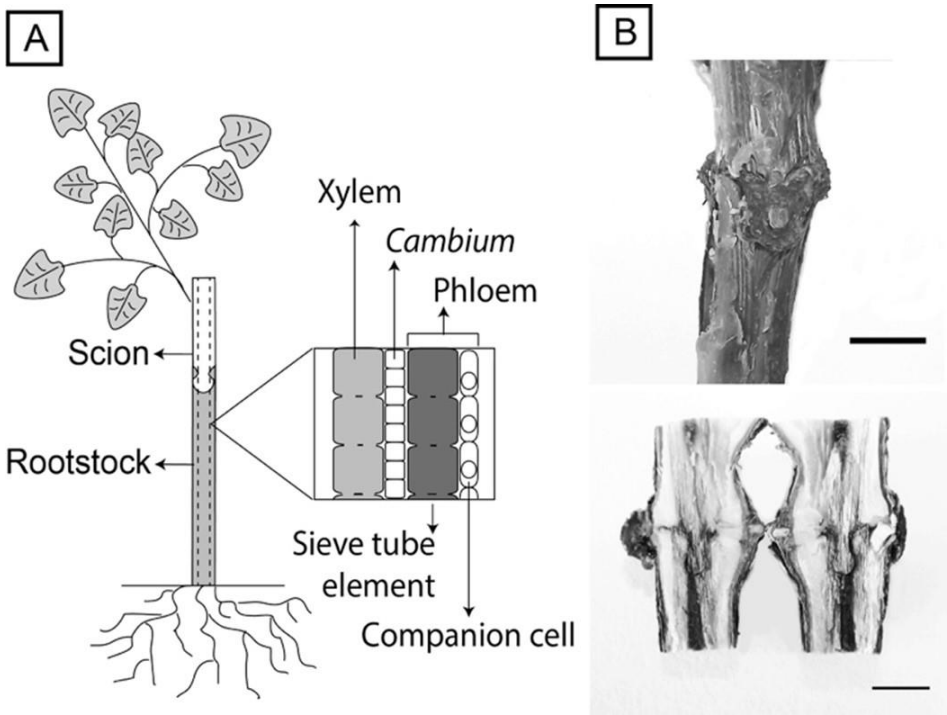

Figure 1. Anatomy of a grafted grapevine: (**A**) Illustration of the vascular system of a grafted grapevine, (**B**) Pictures of an Omega-cut grapevine graft. External view (above) and internal section (below) (scale bar = 1 cm).

Grafting is an ancient vegetative propagation and plant improvement technique largely used in fruit trees and in horticulture to induce beneficial

phenotypical traits to the scion, such as the control of the size, improved yield and fruit quality, and resistance to biotic and abiotic stresses [2].

In European grapevines, grafting is almost a mandatory technique as it rescued the vineyards and the wine industry from the devastating effects of Phylloxera already few years after its introduction to Europe, in the middle of the 19th century. Phylloxera is a sap-sucking insect that destroys the root system of *Vitis vinifera*. Nevertheless, American vine species have evolved resistance against Phylloxera, so that the grafting of *Vitis vinifera* scions onto genotypes of American species (including *V. riparia*, *V. berlandieri*, and *V. rupestris*) or their hybrid rootstocks is still the only effective solution against this pest. In fact, it is the most long-term use of a biological control strategy, and it completely revolutionized the grapevine world [3]. Since the application of grafting, not only grapevine propagation in the field changed radically but also viticulture has been forced to consider the specific traits of different heterograft combinations (i.e., a graft between two different genotypes). In fact, the rootstock influences many aspects of the vine growth [4] by altering yield, fruit composition, as well as plant vigor and canopy configuration [3,5].

In the post-Phylloxera era, several grafting techniques have been gradually developed in the search for the perfect union of scion and rootstock. Nowadays, the main technique used to graft grapevine is the bench grafting using a grafting machine. However, variable degrees of grafting success and poor graft unions, often associated with phytosanitary aspects, contribute to the current concerns about the limited longevity of vineyards. Notwithstanding, poor sanitation at the nurseries, bad choice of cuttings, and poor grafting practices lead to inferior planting material affecting the productive life of a vineyard [6,7].

The success of grafting does not only depend on technical and phytosanitary issues, but also on the levels of compatibility (i.e., the capacity of a graft to develop successfully) between the rootstock and the scion. Despite the essential impact of grafting on viticulture only recently graft compatibility among *Vitis* species is being addressed [8,9]. Traditionally, grapevine grafting research has focused on the influence of rootstocks on scion traits such as plant vigor [10], yield [11], fruit quality [12], cold tolerance [13], and drought stress [14].

The aim of this chapter is to: (a) highlight the specificity of grafting in grapevine, (b) review the phenomenon of graft incompatibility and its main hypothesis, (c) discuss a possible role for nucleic acids trafficking in graft success, and (d) highlight new (and suggest novel) research perspectives to unveil the incompatibility phenomenon in woody species.

2. Grapevine grafting: a unique symbiosis

With the introduction of Phylloxera in Europe, growers had to change their propagation methods in affected areas. At the early days, the common practice was the budding of grape cultivars onto resistant pre-rooted rootstocks in the field. Nevertheless, the field-budding method was expensive and slow so that bench grafting was developed where grafting machines allow the mass production of grafted vines and the saving of labor costs for experienced grafters [15]. Several grafting machines, including the whip-type, the saw-type, and the V-shape type have been developed and currently, the German omega-cut is the most widely used grafting machine in Europe since it seems to produce the highest rate of successful grafts [15]. Despite, contrasting results have also been reported [16]. Today, differently from other woody species, grapevine grafts are performed in modern nurseries, which evolved to function like factories with streamlined production lines. Typically, a one-bud *Vitis vinifera* wood cutting is grafted onto a selected American or hybrid rootstock cutting, both

dormant. Then, the grafts are incubated for callusing for 2–3 weeks under controlled temperature and after rooted on the field or in the greenhouse [7] (Figure 2).

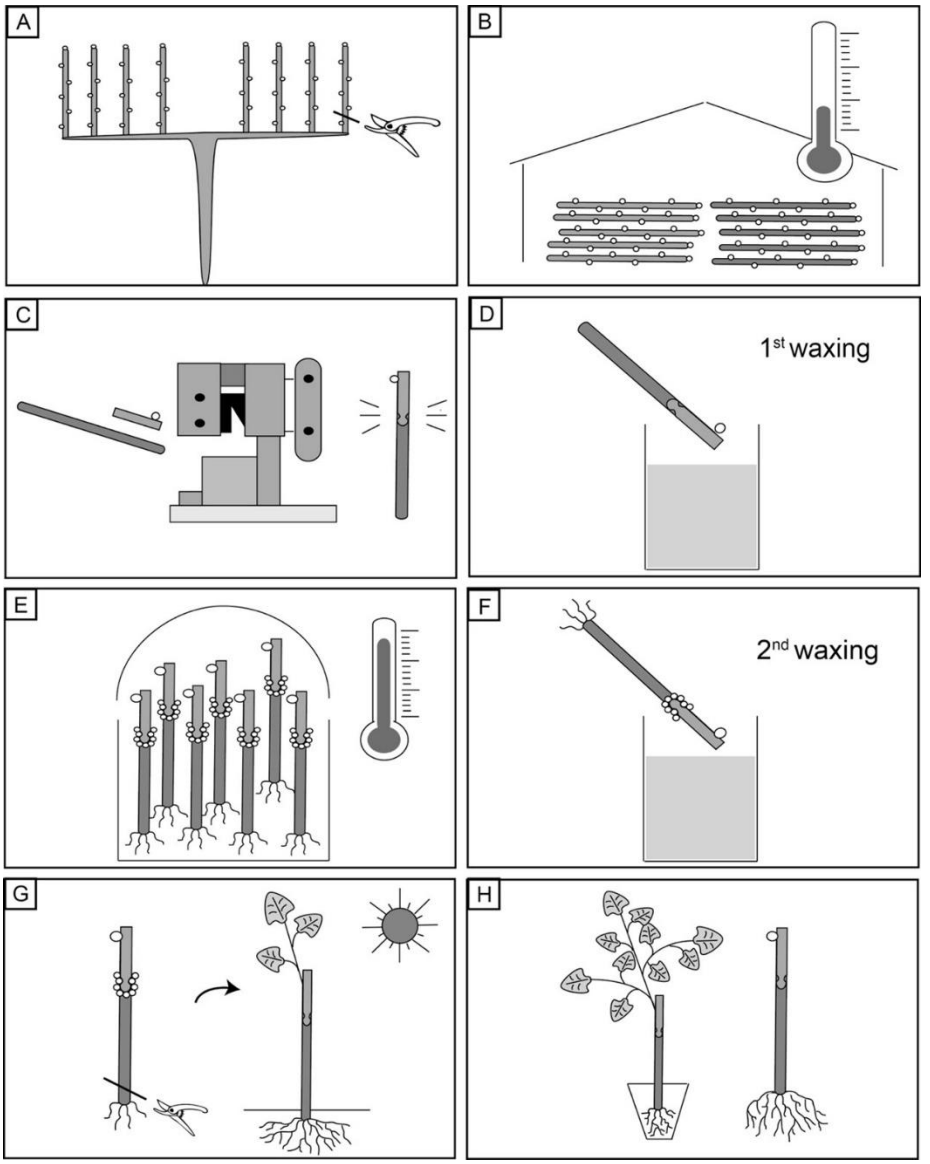

Figure 2. Grapevine graft propagation. (**A**) Winter collection of scion and rootstock cuttings; (**B**) Cold storage of cuttings; (**C**) Omega-cut bench grafting; (**D**) Waxing; (**E**) Callusing stage (28ºC and relative humidity

>90%); (**F**) Waxing; (**G**) In-field rooting stage; (**H**) Green grafted grapevine for summer plantation (left) and grafted dormant grapevine for winter plantation (right).

The preparation of cuttings and the formation of *callus* tissue between the grafting partners are critical stages in the propagation process since incompletely sealed or healed grafts are prone to infections and create structural weaknesses at the graft junction. Indeed, symptoms of trunk diseases in nursery vines include poorly healed graft unions with abnormal dark brown or black staining wounds [6,7]. A proper healing of the graft is likely to occur with highly compatible partners. Likewise, good grafting practices are fundamental to prevent the infection of the propagation material, including: (i) the frequent cleaning of grafting rooms and the disinfection of grafting machines, benches and tools [7], (ii) the protection of the graft union avoiding heavy waxing that may penetrate the junction and impede the graft union to form [17], (iii) performing the callusing under controlled conditions since the high density of the cuttings in callusing boxes prevents the oxygenation of the union and favors the spread of pathogens [7].

Anatomically, the *cambium* of the scion and the rootstock must be in close contact to form a union. During the grafting process of adult grapevines, the vessels adjacent to the graft interface are described to be sealed by tyloses and gum, cambial activity commences close to the bud of the scion, and undifferentiated *callus* cells are formed, which will differentiate into periderm, cortex and vascular strands [18]. Although few differences exist in the way grapevines are grafted, there appear to be no differences regarding the formation of a graft comparing to other plant species. In fact, the majority of reports on grafting point out very similar structural events taking place during the stages of graft formation in woody and herbaceous

species including the adhesion of scion and rootstock upon grafting, the proliferation of *callus* cells, the differentiation and functional connection of vascular elements among the partners [2,19–21].

At the molecular level, the sequence of events underlying graft union formation remains largely uncharacterized but it likely requires extensive re-programming of gene expression, protein translation, and metabolism [22]. Transcriptomic approaches applied in *Vitis* autografts have reported the upregulation of many genes involved in cell wall synthesis and phloem and xylem development. Wounding and defense responses were also specifically changed at the graft interface from 3 to 28 days after grafting (DAG) [22]. More recently, a set of potential expression markers for successful grapevine grafting were identified by analyzing gene expression in compatible and incompatible graft combinations at different stages of the propagation process [8]. Specifically, compatible grapevines were shown to present an enhanced and prompter expression of genes signaling the metabolic and hormonal pathways coupled with a lower expression of oxidative stress genes and of genes from the phenolic metabolism at the callusing stage when compared to incompatible grapevines. While at later stages, at 80 DAG, compatible grapevines shown an upregulation of Transcription Factors (TFs), such as Lateral organ boundaries protein 4 (LBD4), Homeobox-leucine zipper protein ATHB-6 (HB6), and Ethylene-responsive transcription factor (ERF3), involved in the regulation of vascular differentiation, which seem to be important in driving grapevine graft success [8].

Noticeably, numerous scion-rootstock interactions respond simultaneously to grafting such as the reactivation of stem growth after the dormancy period, the wound reaction shared by both partners, and the interaction of the grafted vine with the environment, which hinder the identification of the mechanisms of graft formation, as well as what drives

to an incompatible graft. Therefore, predicting graft outcome is a challenge (for example, what degree of dwarfism will be obtained), as is to study interactions between the scion and the rootstock. Indeed, given the phenotypic variability in a non-grafted plant reflects the genotype x environment interactions (GxE), in grafted plants the phenotype results from the interaction between both the scion (S) and the rootstock (R) genotypes coupled with their individual and combined interactions with the environment, reflecting a higher order interaction which could range from RxSxE [23] to (RxE)x(SxE)x(RSxE).

It is well established that in a grafted plant the scion and the rootstock maintain their own genetic integrity [23,24] meaning that a grapevine scion taken from the European species and grafted onto an American species will develop *Vitis vinifera* branches and not American nor hybrid branches. Nevertheless, in virtue of the wide range of mutual scion-rootstock influences, the end-product of a graft can be considered as a new “bi-member” individual functioning as a unique symbiotic relationship [25,26].

Some authors have used the term “chimera” to refer to a grafted plant [27,28]. In botany, the term refers to an adventitious bud that arises from the junction of the scion and the rootstock and contains tissues of both plants, as originally observed by Hans Winkler, who gave the suggestive name “chimera” to these particular structures [29]. Chimeras have been explained as a special type of genetic mosaic whereby genetically different apical cells continues into developing plant organs [30]. Based on the structure of their meristem, chimeras have been classified into mericlinal, sectorial, and periclinal [31] (Figure 3).

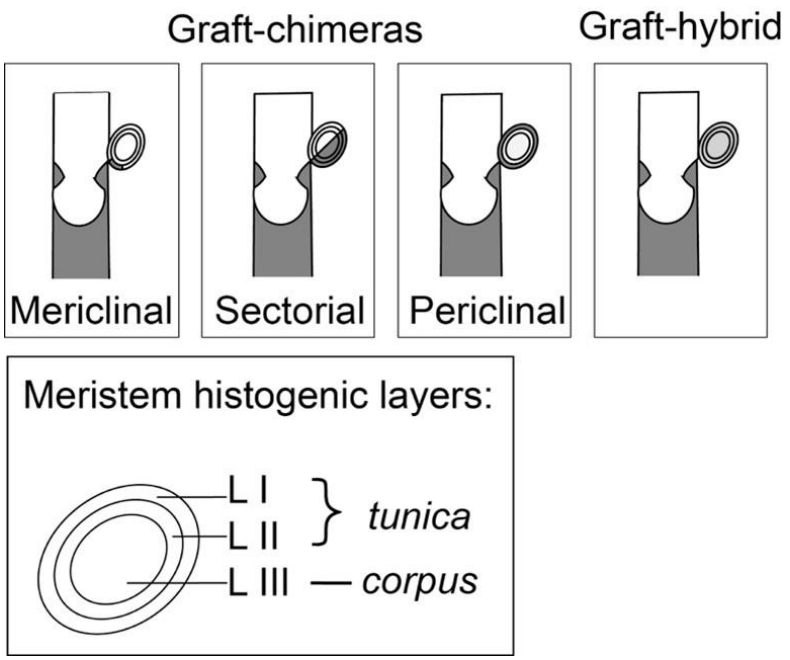

Figure 3. Graft chimeras and graft hybrid. Chimeras have been classified as “mericlinal chimeras” when a mutation is present just in a smaller part of one of the tissue layers of the meristem, “sectorial chimeras” when a mutation is carried by a section of multiple layers and “periclinal chimeras”, when one or two entirely mutated layers are present in the meristem. According to the graft hybrid hypothesis, a graft-hybrid arises from the junction, as the mixture product of the scion and rootstock genotypes.

Periclinal are the most stable chimeras thus are frequently clonally propagated as commonly performed in *Vitis* species. Indeed, the cultivars ‘*Pinot moure’*, ‘*Pinot noir’*, ‘*Pinot gris’*, ‘*Pinot blanc’*, ‘*Pinot Meunier’*, ‘*Chardonnay’*, and ‘*Greco di Tufo’* were identified as grapevine chimeras by microsatellite marker studies [31]. Nevertheless, already at the time of their discovery, chimeras have been confused with graft hybrids giving

support to a historical controversy regarding whether a new plant species can be produced asexually by grafting or not.

Although graft hybrids are a “rarity” and the vast majority of graft-induced sports are chimeras, it has been demonstrated that cellular and nuclear fusions does occur at the graft junction and can serve as a route for the asexual generation of allopolyploids [29]. Since it appeared to be in contrast with Mendelian genetics, a widespread skepticism accompanies Darwin’s concept of graft hybridization. Despite, it was verified that it was possible to obtain graft hybrids but using very special grafting methods, which are totally different from the ordinary methods applied in graft propagation [32]. The most well-known method for graft hybridization is the mentor grafting developed by the Russian breeder Michurin, which consists in grafting a young scion, which is continually defoliated, onto a mature rootstock, in order to turn the scion as a sink tissue for the rootstock [30]. The new characteristics induced by the mentor grafting have been observed in the scion and these were transmitted to the progeny in some cases, even though the transmission frequency was often below 1% [23,30,33]. Moreover, the grafting partners’ exchange of mRNAs and small RNAs-mediating silencing and epigenetic alterations are emerging as an important scion-rootstock communication mechanism which may be crucial to understand the physiology of grafted plants [34,35]. These findings hint a number of opportunities for plant improvement and agriculture [reviewed in 23,36].

Despite grafting has been used for millennia to propagate plants and to indirectly manipulate the scion phenotype, the mechanisms of graft formation remain vague and to date, no molecular or genetic mechanisms required for this process has yet been completely identified [37]. Clearly, genetic implications related to grafting such as graft hybridization, as well as the phenomenon of graft incompatibility are even more shrouded in

mystery although the endless potential of this ancient technique for modern breeding certainly deserve more attention.

3. Compatibility and incompatibility are not synonymous of graft success and graft failure

A major difficulty in approaching the incompatibility phenomenon lies in its definition. Indeed, there is not a clear definition of graft compatibility and incompatibility, rather they are generally defined respectively as the ability or inability to produce a successful graft [33,38] (Table 1).

Table 1. List of statements addressing a definition for graft incompatibility

Defining citations for graft incompatibility	**Reference**
"The only certain criterion of incompatibility is the characteristic interruption in cambial and vascular continuity which leads to the spectacular smooth breaks at the point of union".	[39]
"Incompatibility (…) shall refer only to mutual physiological influences (or lack of them) between tissues of stock and scion that culminate in unsuccessful graft unions".	[40]
"The structural event critical to compatibility occurs when the new cells generated from the periphery of the faces of stock and scion protrude and come into physical contact".	[41]
"It is the failure to achieve vascular continuity which appears to be the critical event determining whether a graft is compatible or not".	[42]
"Incompatibility, with respect to grafted fruit trees, is defined as a phenomenon of premature senescence of the tree caused by physiological and biochemical processes".	[43]
"Failure of a graft combination to form a strong union and to remain healthy due to cellular, physiological intolerance resulting from metabolic, developmental, and/or anatomical differences".	[38]

"Incompatibility is a complex physiological state of a plant defined by: adjustment of the metabolisms of the grafting union partners, growth conditions, presence of viruses and other factors (nutrition, stress …)".	[44]
"Is an interruption in cambial and vascular continuity leading to a smooth break at the point of the graft union, causing graft failure. It is caused by adverse physiological responses between the grafting partners, disease, or anatomical abnormalities".	[45]
"Graft incompatibility is an extremely complex phenomenon that involves anatomical, physiological, biochemical and molecular interactions between scion and rootstock".	[46]
"Compatibility is defined as a sufficiently close genetic (taxonomic) relationship between stock and scion for a successful graft union to form, assuming that all other factors (technique, temperature, etc.) are satisfactory".	[47]

However, there are several requirements to achieve a successful graft, and compatibility is only one of the essential criteria [45]. Likewise, incompatibility is just one of the causes of graft failure. Beside incompatibility, the use of desiccated or diseased scions, a faulty grafting technique, bad vascular *cambium* alignment, and adverse environmental conditions, among other causes all contribute to the failure of the graft [45]. There is a long-term general consensus that the greater the taxonomic distance between a scion and a rootstock, the greater the possibility to produce an incompatible graft [19,33]. Nevertheless, relatedness of species has just recently been experimentally tested in legumes and it was proved that this is not a good predictor of graft compatibility [48]. In woody species, although exceptions have been found, graft compatibility is described to be maximum in autografted plants, high among species within the same *genus*, moderate among related *genera* and minimum or null when the grafted partners belong to different families [34]. In addition, compatibility or incompatibility gradients were found rather than a clear distinction between compatible and incompatible graft combinations. [33,49].

In incompatible grafts, not all the mentioned steps of graft formation occur. Adhesion and *callus* proliferation between the scion and the rootstock occur in both compatible and incompatible combinations resulting from a wound response rather than from the perception of the non-self grafting partner [50]. However, the strength of attachment is lower and phloem and xylem differentiation is limited or may not occur in incompatible grafts [21,51]. The initial healing of the graft union does not itself ensure long-term compatibility [33] as the initial establishment of the vascular continuity among the grafted partners can take days in the case of herbaceous plants, to more than a year in the case of some woody perennials. In some other cases, incompatibility may not become apparent for several years

and are therefore often referred to as "delayed incompatibility" [21]. In *Vitis*, 5 months' time-cycle of the grafting process was considered enough to assess levels of incompatibility in the field [52], although it was found that graft healing was not yet complete at this stage by analyzing the internal anatomy of the graft union [9]. The assessment of compatibility levels between the grafting partners is often performed at the nurseries at two time points: after the callusing stage and at the end of the growing season [8,53,54]. The important events for the establishment of a compatible or an incompatible graft seem to be starting at the formed *callus* bridge among the partners. However, the variability required for each developmental stage and the occurrence of delayed manifestations make it difficult to establish when the determining reactions for incompatibility have taken place, which would substantially aid researchers to define a time window where to focus.

Over the years, several ways of classifying graft incompatibility have been proposed, most of them trying to interpret incompatibility based on observed external symptoms [46]. However, among the classifications already proposed, the one of Mosse (1962) [39] is the most used today. In this classification, the author divided the incompatibility of grafting into two types: "translocated" and "localized" [39]. "Translocated" incompatibility has been associated with (1) starch accumulation above the union and its absence below, (2) phloem degeneration, (3) normal vascular continuity at the union, although overgrowth of the scion might be present, and (4) early effects on growth. This type of incompatibility has been observed among peach and plum [46,39], among *Jaoumet* (*Vitis vinifera* cultivar) and 57-Ritcher (*V. berlandieri* x *V. rupestris*) [55], and also among *V. rotundifolia* and *V. vinifera*, although in this case some vascular continuity may be incomplete [52]. According to Zarrouk and collaborators (2006), the analysis of chlorophyll concentration in the leaves is indicative of this type

of incompatibility in *Prunus* [56], and the same was also confirmed in grapevines [9]. “Localized” incompatibility, can be observed among apricot and plum combinations and is characterized by (1) breaks in cambial vascular continuity which causes mechanical weakness to the union, (2) gradual starvation of the roots with slow development of external symptoms, and (3) the immediate or delayed break of the union [2,46]. To identify localized incompatibility, an internal observation of the graft union is usually performed [9,56,57]. Nevertheless, X-ray 3D tomography, have been applied to investigate “bad” and “good” grapevine grafts, being a valuable example, together with magnetic resonance imaging technique, of non-destructive methods that can be used instead [58,59].

Notwithstanding, the classification of incompatibility into two types has already been questioned since symptoms are often similar and both types have been found to coexist [46]. It is believed that, once the mechanisms underlying graft incompatibility is understood, the classification may be altered mainly taking into account its true causes [46,60].

Previous to the classification of Mosse, another classification included graft failure due to virus and phytoplasma as one type of incompatibility [61]. It is likely that this classification, together with the remarkably similar symptoms found among virus-infected and incompatible plants [39], led to the adoption of the term “graft incompatibility” in the case of graft failures due to viral infections. The terminology has been reported for several plant grafts, such as orange trees, sweet cherry, walnut trees, and for certain apple varieties on the rootstock Spy 227 [39]. However, it is particularly widespread in grapevines, probably due to their high susceptibility to viruses [62–66].

Although it has been reported that among *Euvitis* sub-species of genus *Vitis* do not display absolute incompatibility [67], different levels of

incompatibility between grapevine rootstocks and *Vitis vinifera* cultivars have been reported [8,49,68,69]. It is likely that incompatibility is partly responsible for the graft failures occurring at the nursery employing certified virus-free plants. Indeed, it has been reported that 39% of bench grafted vines are deemed defective at the nursery [7] and incompatibility are mentioned for several cultivars and rootstocks on nationals and nurseries catalogues of registered vines (Table 2).

Table 2. Technical reports on graft incompatibility in grapevines

Scion	Rootstock	Rootstock characteristics	References
Rootstock clones: *V. Berlandieri x V. Rupestris*			
Pinot Noir N, Syrah N	110-Richter	It is moderately vigorous to vigorous, has a very long vegetative cycle and delayed maturity. It is well suited to all kinds of soils especially in warm areas [70]. It has good resistance to *radicicolae phylloxera* and is sensitive to *gallicolae phylloxera*. It is highly resistant to downy mildew.	[71,72]
Jaoumet B	57-Richter	Not available	[71]
Tempranillo N	1103-Paulsen	It is moderately vigorous, has a long vegetative cycle and a delayed ripening. It is adapted to a wide range of soil conditions [70]. It has high resistance to *radicicolae phylloxera* and is moderately susceptible to *gallicolae phylloxera*. It is highly resistant to downy mildew.	[71]
Antão Vaz, Caladoc N, Carignan N,	140-Ruggeri	It is a vigorous rootstock with a long vegetative cycle and delayed maturity [70]. It has good resistance to *radicicolae*	[71–73]

Garnacha Tinta, Itália, Marselan N, Mourvèdre N, Négrette N, Syrah N, Sultanina, Tempranillo N,		*phylloxera* but is sensitive to *gallicolae phylloxera.* It is highly resistant to downy mildew.	
Garnacha Tinta and several other unspecified cultivars	779-Paulsen	It is a very vigorous rootstock, rustic and adapted to poor soil. Highly resistant to droughts. It is currently underused, due to poor graft compatibility with many cultivars.	[73]
Rootstock clones: *V. Berlandieri x V. Riparia*			
Alfonso Lavallée, Antão Vaz, Cabernet franc N, Cabernet Sauvignon N, Malbech (French clones), *Moscatel Hamburgo,*	Kober 5 BB	It has a very high vigor inducing a delayed ripening. In very wet years there have been cases of no fruit-set [70]. It has a high tolerance to *radicicolae phylloxera* and to nematodes. It is moderately sensitive to *gallicolae phylloxera* and highly resistant to downy mildew.	[71–73]

Sauvignon B, Victoria.			
Garnacha Tinta, Sultanina	Selection Oppenheim SO4	It develops slowly and shows low vigor in the first years, but vigor increases significantly thereafter. It favors early maturity [70]. It has high tolerance to *radicicolae phylloxera* and good tolerance to nematodes. It is medium susceptible to *gallicolae phylloxera* and anthracnosis but highly resistant to downy mildew.	[73]
Carignan, Gamay, *Servant*	161-49 Couderc	It has moderate vigor, low growth and moderate to good drought resistance. It has a high tolerance to *radicicolae phylloxera* and medium to nematodes. It is moderately susceptible to *gallicolae phylloxera* but highly resistant to downy mildew.	[71]
Rootstock clones: *V. Riparia x V. Rupestris*			
Barbera, Cabernet Sauvignon, Chasselas dorato, Sauvignon.	101-14 Millardet et de Grasset	It induces moderate vigor in scions and low yield-to-pruning ratios. It is best suited to moist, deep soils [70]. It has good tolerance to *radicicolae phylloxera* and nematodes but moderate	[73,74]

		tolerance to *gallicolae phylloxera*. It has good resistance to downy mildew.	
Barbera, Cabernet Sauvignon N, Chardonnay, Chasselas dorato, Chenin B, Dattier de Beyrouth B, Pineau d'Aunis N, Sauvignon B, Syrah N,	3309 Couderc	It imparts low to moderate vigor to grafted vines, early fruit ripening and high yield-to-pruning ratio [70]. It has good tolerance to *radicicolae phylloxera* but it is susceptible to nematodes, to *gallicolae phylloxera* and to anthracnosis but shows good resistance to downy mildew.	[73,74]
Rootstock clones: *161-49 Couderc x 3309 Couderc*			
Chardonnay	Gravesac	It is adapted to sandy or gravel soil and induces high and steady yields. It has a high tolerance to *radicicolae phylloxera* but is susceptible to nematodes. It is moderately sensitive to *gallicolae phylloxera* but shows good resistance to downy mildew and anthracnosis.	[73]

Therefore, incompatibility contributes to the reasons for grapevine nurseries to double the production of grafts to guarantee their contracts. Although incompatibility has been just recently addressed in grapevines, graft incompatibility has been widely associated with altered biochemical processes such as the increased production of reactive oxygen species (ROS) and a lower expression of antioxidant genes [75–78] in other species. Programmed cell death (PCD) was also involved since *in situ* DNA fragmentation was detected [77,79]. A number of authors linked compatibility responses to quantitative and qualitative differences in phenolic compounds in the grafted partners [60,80,81]. Several phenolic compounds, including gallic, sinapic and ferulic acids have been proposed as markers to detect incompatible grapevine grafts at different stages of the propagation cycle [49,68]. In this regard, a follow-up investigation, identified catechin as a relevant compound in graft union success and confirmed the validity of gallic and sinapic acids as important chemical markers of cv. Touriga Nacional compatibility [82]. Interestingly, the same was confirmed at the molecular level where an increased expression of genes of the phenolic metabolism were associated to incompatible grapevine grafts [8]. As pointed-out by Melnyk (2017) [27], the insights produced by comparing different levels of graft compatibility suggest that overall incompatibility is an enhanced stress response, but whether it is a cause or a consequence of graft failure is still not determined [27].

4. The hypothesis behind graft incompatibility

Historically, the study of incompatibility focused on the phenomenon of cell recognition and graft rejection by the partners. Already in the ’20s, Kostoff (1928) [83] suggested that the scion and the rootstock communicate at the graft interface and induce an immune response. By performing several precipitation experiments, Kostoff observed that in most cases, extracts collected from plants belonging to different genera and tested against each

other produced a precipitation ring. He also observed that the precipitation potency of specific combinations is increased after grafting and observed that in some cases the capacity to produce “precipitins” (= an antibody that reacts with its specific antigen to form an insoluble precipitate) is acquired during grafting development, being highest between 30 to 45 DAG [83]. Given his experimental data, Kostoff concluded that a higher plant may acquire immunity and that grafting may induce it. Although it is now well accepted that no antibodies are formed in plants and that other publications have refuted that grafting could induce acquired immunity between the rootstock and the scion [84], the idea of Kostoff has resurfaced in the literature. Indeed, transcriptomic approaches revealed the upregulation of genes from numerous stress responses, such as the induction of oxidative stress, the expression of pathogen-related proteins and secondary metabolites in hetero- versus autografted grapevines suggesting that the heterograft response potentially reflects the detection of a non-self partner, which may trigger an “immune” type of response [85]. Furthermore, recent metabolic profiles on 11 grapevine graft combinations confirmed that the presence of a heterologous grafting partner increases defense-related compounds in both scion and rootstocks at short and longer distance from the graft [86]. Hence, it would be interesting to verify whether or not the putative “immune” graft incompatibility response could be explained by the detection of a different biome composition of the grafting partners rather than by the detection of a taxonomically different grafting partner. Indeed, it was already highlighted that by grafting, the fungal, bacterial, and viral biomes of the grafted plant parts also interact and might have a role in the healing of the graft union and the final performance of the plant [86]. In the ’80s, Yeoman and collaborators (1982, 1984) [41,42] suggested that the success or failure of the graft union depends on the outcome of cell-cell recognition events occurring when proliferated *callus* cells from the scion and the rootstock come into

physical contact [41,42]. According to these authors, the exchange of a diffusible messenger molecule takes place between the opposing cells, leading to wall thinning and secondary plasmodesmata connections forming between genetically distinct cells at the graft junction [87]. Furthermore, the formation of plasmodesmata, which are intercellular symplasmic channels, provide a pathway for cell-to-cell transmission of small and large molecules acting as signals, that could constitute an added recognition event involved in graft incompatibility [41].

An alternative model for graft incompatibility without the involvement of cellular recognition was proposed by Randy Moore (1984) [88]. According to this author, the development of a compatible graft starts with the wounding and the proliferation of *callus* cells with varying fate depending on transmitted and receiving signals. Such signals could be auxin inducing vascular differentiation across the interface and leading to the formation of a functional graft. Contrarily, incompatibility would occur when toxins override morphogens (e.g., auxins) thereby preventing the formation of a compatible graft [88]. As an example, in incompatible pear/quince grafts, Prunasin, a cyanogenic glycoside, is produced by the quince rootstock and ascends into the pear scion where it is enzymatically broken down to liberate hydrocyanic acid at the graft interface where it is responsible for cellular necrosis and incompatibility [89]. According to Moore the taxonomic distance associated with graft incompatibility is not indicative of cellular non-recognition but rather convey metabolic disharmony [88].

Interestingly, it seems that the enhanced stress response in incompatible unions is the cause of graft failure for Moore's hypothesis, while incompatibility is a consequence of early non-recognition events for Yeoman.

Currently, all theories, particularly the ones of Yeoman and Moore, remain valuable and are still being investigated, both suggesting the presence of mobile signals suspected to be responsible for graft incompatibility. Advances in the graft incompatibility research, further support the hypothesis of Yeoman by pointing out a pivotal role of *callus* cells in graft union formation, strengthening the idea of an early predetermination of the future incompatibility reaction [50]. Additionally, *callus* differentiation into *cambium* and vascular tissue is delayed in incompatible grafts, an enhanced metabolism and anatomical abnormalities have been found [50, 79,90,91]. Mismatched, discontinuous half plasmodesmata were observed [92], and intercellular transport of factors via plasmodesmata was significantly lower. According to Pina (2009) [93], this suggested the presence of a signal that may be reaching the other partner and change its innate rate of communication [93].

As hypothesized by Moore, several studies proposed hormones as being the endogenous factors underlying scion-rootstock communication during grafting. Hormonal signaling, including auxin, cytokinin, and gibberellins, play an important role in the shoot-to-root interactions during graft union formation [94]. In Arabidopsis micrografts, ethylene and jasmonic acid [95] and, in grapevine, also abscisic acid (ABA) seem to be involved [22,96]. Although hormones were considered as non-essential for vascular reconnection and ultimate graft success [reviewed in 97], Melnyk and collaborators (2015) [37] showed that blocking auxin responses in the rootstock is sufficient to delay graft formation suggesting that a local and tissue-specific recognition system exists in the rootstock to perceive a systemically produced signal from the scion. This indicates that both local recognition and long-distance signaling are important for the formation of a graft [37].

5. Scion-rootstock communication through nucleic acids trafficking

Recent grafting studies points out to a complex communication between the scion and the rootstock mainly involving mobile signals. For the proper survival and development of a plant, the shoot and the roots need to communicate through the vasculature. For this reason, plants evolved the capacity for mobile signals to traffic through the phloem stream [98]. Besides long-distance transported hormones and metabolites, also nucleic acids and entire organelles can be exchanged between attached cells at the graft interface [99,100]. In recent years, long-distance phloem transport of functional proteins and RNAs such as small, micro, and large messenger RNAs (mRNAs) indicate their potential role as regulatory signals mediating the scion-rootstock communication and have become major research domains [33,35].

The exchange of DNA at the graft interface has been investigated mainly in the context of the graft hybridization hypothesis. Applying the mentor grafting method, histological evidence for the root-to-shoot transfer of chromatin through the vasculature has been provided [101]. In fact, results from Bock's group (2009, 2012) [24,99] surprisingly showed that large DNA pieces or entire plastid genomes can be bi-directionally transferred locally across cells at the graft interface. Nevertheless, heritability is largely prevented since the phenomenon is restricted to opposing cells at the graft junction [24,99]. Further research showed that even entire nuclear genomes can be transferred among genetically different plant cells upon grafting. As evidence, a new, fertile, allopolyploid plant species between a woody and an herbaceous plant has been produced suggesting that grafting could be used as a renewed tool for crop improvement and biotechnological applications [102]. Recently, the cellular structures underlying the horizontal transfer of plastid genomes was uncovered [100].

It was described to start after the callusing stage with the formation of very large symplasmic pores in the plasma membrane and cell walls, which are morphologically distinct from plasmodesmata, that allow the passage of cytoplasmic material and of plastids with altered morphology [100].

In addition to the transfer of DNA itself, increasing efforts have been made to determine how RNA molecules are transferred between the scion and the rootstock and their hypothetical role on the graft-induced changes in plant traits. Mobile RNAs have been associated with signals that can travel from cell-to-cell through plasmodesmata and over long distances, through the phloem, in order to coordinate growth and development with environmental and stress cues [103] (Figure 4).

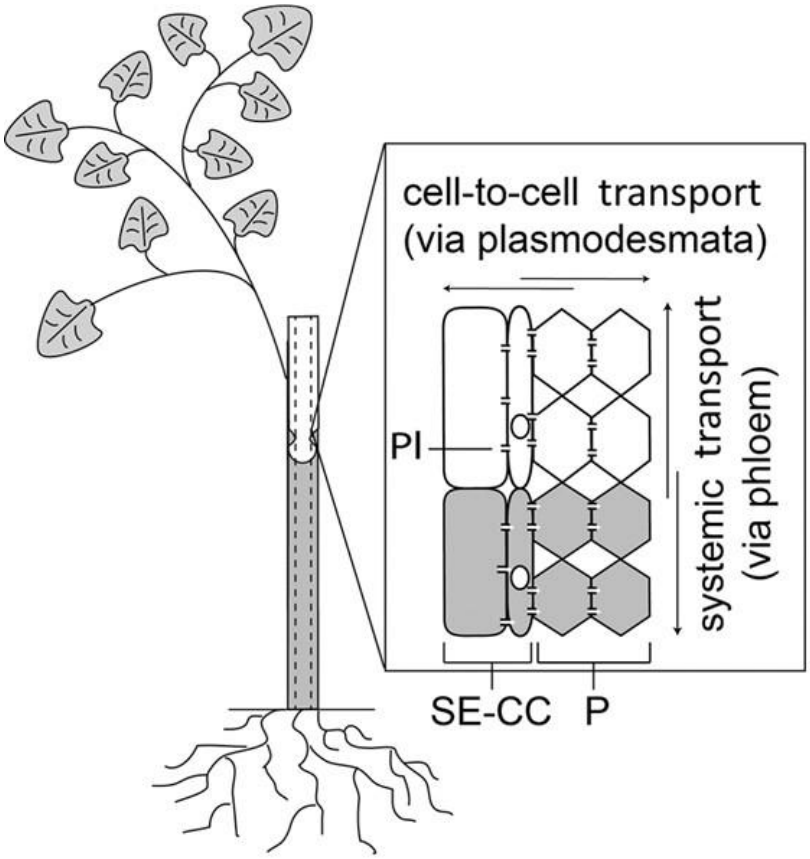

Figure 4. Direction of the RNA trafficking spread through a grafted plant. The RNA signal can travel cell-to-cell through plasmodesmata (Pl). Eventually, it can cross parenchyma cells (P) and the companion cells (CC) to reach the sieve elements (SE) and thus spread over long distances via the phloem stream and even over the graft junction to distant plant body parts.

Compelling evidences support that RNA trafficking in plants is not driven by simple diffusion but rather by a selective and active transport mechanism, through the formation of unique ribonucleoproteins. These proteins allow the selective delivery of macromolecules to specific plant

organs [104]. Recently, 5-methylcytosine (m5C) modification of mobile mRNAs proved to play a crucial role in facilitating their transport. Indeed, the mobile TRANSLATIONALLY CONTROLLED TUMOR PROTEIN 1 (TCTP1) transcript was shown loose its mobility over graft junctions in methylation-deficient mutants [105]. Furthermore, beside enrichment in m5C modification, mobile mRNAs were also found enriched in specific motifs such as tRNA-like sequence (TLS) which were shown to mediate transport when fused to otherwise non-mobile transcripts [106,107].

For more than 20 years, research has focused on the biological function of mobile mRNAs demonstrating that mobile transcripts can impact development by producing functional proteins in the targeted destination tissue [107,108]. Phloem transport of mRNAs was found to be responsive to growth conditions and environmental stress in grafted grapevines [109], to regulate leaf morphology in tomato [110], tuberization in potato [111,112], and root architecture and root growth in Arabidopsis [105,113]. Actually, mobile mRNAs represent approximately one-fourth of plants transcriptome suggesting an extensive communication through RNAs across the plant body [104]. Indeed, more than 2000 genes were identified to encode mobile mRNAs in Arabidopsis and they were shown to be responsive to different nutritional conditions, being some of them able to move bi-directionally (i.e., shoot-to-root and root-to-shoot) and to produce functional proteins in specific destination tissues, including flowers [114]. Another focus of research has been addressed to several classes of phloem-mobile non-coding small (typically 21–24 nucleotides) RNAs (sRNAs) [115] considered key molecules governing development and stress responses. Evidence for graft transmission of specific microRNAs (miRNAs) has been accumulating in recent years, in various plant species [reviewed in 35]. Tzarfati and collaborators (2013) [116] showed involvement of specific miRNAs in engendering physiological effects of

grafting in *Citrus* and also revealed differences in the expression pattern of smaller, specific miRNAs among *Citrus*' scion-rootstock combinations. In the last years, a lower expression of miRNAs, potentially targeting transcription factors related to vascular development, was associated to good graft compatibility in grapevines suggesting that incompatibility might be associated to the regulation in the expression of specific genes [8].

Small interfering RNAs (siRNAs) are highly abundant in the phloem exudate [115,117] and functional siRNA molecules can move over graft junctions to reproductive cells in flowers [118] in line with a possible involvement of epigenetic inheritance in grafting [28,33]. Heritable alterations in DNA methylation induced by grafting have been reported in several heterografted plants [reviewed in 35] and have been claimed as the explanation for the graft hybrid controversy [119]. Researchers from Cambridge University further confirmed that sRNAs are mobile among the grafted partners and mediate epigenetic changes in the recipient cells [120,121]. Follow-up investigations in collaborations with the Salk Institute in California, found out that such changes affect thousands of *loci* [122] raising surprise for the scale of this phenomenon.

Analyzing the thousands of mobile transcripts, as well as the function of mobile sRNA populations, will be the next step for the RNA signaling research and to elucidate whether it might be involved in graft formation and graft incompatibility. Indeed, the genetic limits of grafting, which manifest incompatibility when taxonomically distant partners are grafted together, suggest that the scion-rootstock communication underlying compatibility and incompatibility should involve genetic signals. Even in legumes, where phylogenetic relatedness was found not to be indicative of graft success, directional physiological differences, or scion-derived signals, possibly mobile RNAs, proteins, and hormones, were suggested as drivers of graft success [48]. Although some aspects suggest a

signaling role of mobile RNAs whether the trafficking of RNAs is involved in successful graft formation or not remains to be shown. It has been proposed that the unique population of phloem mobile RNAs could represent a mechanism to coordinate vascular development with environmental inputs [123]. According to Lucas et al. (2001) [123], the phloem content derives from the rootstock acting as source tissue in a stem-grafted heterograft, which is proposed to exert control over the operations of the sieve element-companion cell complexes in the apical sink scion. In fact, heterografting experiments with a cucumber scion and a pumpkin rootstock showed that scion sink tissue phloem contained pumpkin specific transcripts and proteins but it was devoid of its own phloem orthologous proteins. Therefore, it was suggested that the rootstock is the regulator of the synthesis/transport of the scion phloem stream [123].

In addition, transfer RNA (tRNA) halves, a less characterized class of graft-transmissible small RNA that inhibit protein translation, have been proposed as a systemic apoptotic signal triggering differentiation of provascular tissue [124]. Considering that both xylem tracheary elements and phloem sieve tube elements require respectively full and partial developmental programed cell death to occur in order to become functional [123,125], it is possible to envisage how such sRNAs might impact vascular graft formation and eventually incompatibility.

Although grafting has been extensively used as an experimental system in the RNA mobility research, mainly to analyse the long-distance transport capacity of RNAs, surprisingly little work was addressed towards the grafting process itself and towards the compatibility/incompatibility phenomenon. In summary, although the involvement of graft-mobile RNAs has been mentioned in several reviews as owning widespread implications

for understanding grafting mechanisms [23,28,33,35] their involvement still remains to be experimentally addressed.

6. Future research perspectives and concluding remarks

Grafting has been used for millennia to produce desired alterations to the scions such as the overcoming of soil-borne diseases in grapevines. Despite this, graft beneficial applications are limited by graft incompatibility and may constitute a door for pathogens to infect the graft product. This may affect the agricultural applications of grafting, slowing down the selection of elite rootstock genotypes, and resulting in frequent graft failures in the nurseries. It also introduces drawbacks at the growers' level since poor grafts affect the vineyards longevity and force producers to frequently substitute unproductive vines. Certainly, one of the most important application of graft incompatibility studies would be to early predict whether a proposed scion-rootstock combination is compatible, especially in woody species. This year, Pina and collaborators (2021) [126] have advanced the field of compatibility research by producing the first report on quantitative trait loci (QTLs) for graft incompatibility in *Prunus* species exemplifying the steps and the direction that the graft compatibility research should follow [126]. Graft incompatibility in *Prunus* has been studied for a long time [61,127,128] with special attention to its physiological characteristics and to the challenges associated to the quantification and the evaluation of the graft incompatibility trait itself. Therefore, the establishment of adapted phenotypic protocols to quantify incompatibility, as done in *Prunus* [129], is fundamental for mapping QTLs associated with graft incompatibility, although this is missing in other woody plants. For instance, internal anatomical characterization of the graft union (necrotic layer, bark and wood discontinuity) allows the screening of compatible and incompatible *Prunus* graft combination [57,129] but in grapevines the method was not discriminative of

compatibility [9]. Therefore, more efforts in phenotyping graft incompatibility in other woody species need to be done to apply the QTLs approach, which would be tremendously useful for breeders to early screen incompatible grafting partners through marker assisted selection. Interestingly, the same researchers have also tested whether, given the similarity found in their biological mechanisms, floral self-incompatibility and graft incompatibility traits would be related at the genetic level [129]. Therefore, they have screened the inheritance of these traits in a F1 apricot population, and found that they are genetically independent, although they do not exclude that some overlapping mechanism may be found between these two processes at the molecular level [129].

Another breakthrough in the graft incompatibility field of research, explored the consensus that phylogenetic relatedness and differences in stem anatomy might underlie incompatibility [48]. Despite the surprise of their findings, the completeness of the experimental design and the systematicity of the methods were applied to experimentally test the proposed drivers of the graft incompatibility response. Beside phylogeny and vascular patters, the authors found that neither germination type, nor the type of tissue can explain interspecies graft success, although whether the same might also be applied to woody grafts, still remains to be shown. Furthermore, the fact that *sweet pea* grafted onto *pea* was able to produce a successful graft but the same did not happen in reciprocal grafts (i.e. *pea* grafted onto *sweet pea*), led the authors to suggest directional physiological differences or a scion-derived signal as possible drivers [48]. Certainly, as proposed since some time, graft-mobile sRNAs might be involved in epigenetic and/or post-transcriptional regulations underlying the compatibility response of proposed graft combinations [33]. Hence, it is expected that this hypothesis will be soon experimentally tested. However, there is a general consensus that graft incompatibility is an

enhanced stressed response coupled with the wide-spread occurrence of virus-induced graft incompatibility detected in several graft systems, suggesting that the hypothesis of Kostoff of incompatibility as an “immune” (defense) reaction might deserve more attention**.** For instance, one cannot excluded the possibility that the putative “scion-derived signal” might appear within or across its own biome which might induce an incompatibility response when put into contact with the foreign biome of the rootstock partner, or more simply, when this is grafted to a susceptible grafting partner. Similarly, it is not excluded that the panoply of RNAs travelling across the graft union might reflect a plant/microbe-virus-fungal battle (or a biome/biome battle) perhaps mediated also by RNA silencing or mRNA signalling. Metagenomic analysis (of fungi, bacteria, and virus) applied onto a range of interspecies heterograft combinations showing different levels of compatibility, such as the experimental design exemplify by Wulf (2020) [48], might help to verify whether differences in the biomes’ communities of the grafting partners, or specific microorganisms, might induce graft incompatibility. In case of grapevines, where viruses are known to frequently induce graft incompatible responses [130], *in vitro* micrografting systems were recently validated as valuable methods to identify the viral susceptibility of different scion–rootstock combinations [131]. Nevertheless, given that more than 65 viruses infect grapevines [132] but just a few of them are tested in the EU certification schemes, it would be important to verify whether any of the not-certificated viruses might be responsible for incompatibility manifestations with regards to specific graft combinations.

Grafting and incompatibility have almost been ignored by the scientific community for a long time, but researchers started to re-evaluate this ancient technique and to see it as a renewed tool for plant improvement in recent years [reviewed in 36]. As a result of this increased interests, these

latest years were marked by important break-through results, new approaches and hypothesis which came to enrich our perspectives about the graft incompatibility phenomenon. Although it is expected that more will come in the following years, the field of research has still a long path to go before the exciting perspective of deliberately tune plant phenotypes via grafting, of allowing the early detection of incompatible grafting partners, and perhaps, one day, of broadening the useful application of grafting towards more distant graft combinations.

Research objectives and thesis layout

Graft compatibility is essential to establish successful grafts, however the range of graft application is restricted by still unknown anatomical, physiological, and molecular features leading to incompatibility and the ultimate failure of the graft. This problem is crucial particularly for the European viticulture, as grafting with resistant rootstocks is still the most effective solution to overcome the devastating effects of Phylloxera. Since the introduction of new varieties requires the knowledge of (in)compatible combinations, incompatibility delays rootstock breeding, further slowing-down the release of improved genotypes. In particular, the delayed manifestation of incompatibility causes drawbacks for farmers productivity and threats the longevity of their vineyards. Hence, understanding the early phases of graft development would be important for the early detection of incompatible partners. The identification of physiological, metabolic, and molecular markers of incompatibility, coupled with the implementation of reliable phenotypic schemes that would permit us to quantify this complex trait, are necessary steps that the research field still need to make to advance breeding selection for the incompatibility trait. To address this lack of knowledge, the main objective of this thesis is to deepen our understanding onto the phenomenon of graft incompatibility in grapevine by exploring *in vivo* and *in vitro* early physiological indicators of

graft incompatibility in grapevine, and by exploring early metabolic scion-rootstock interactions with the aim to gain insights on the metabolic effects of grafting in different tissues and graft combinations. To achieve this, three specific aspects were addressed:

1. Identify optimal phenotypic parameters related to grapevine graft incompatibility in several graft compatible and incompatible *Vitis vinifera* scions grafted onto Ritcher-110 (110R) rootstock under field conditions at early stages of the propagation process.
2. Elucidate the scale and the content of the scion-rootstock metabolic interactions in several grapevine graft combinations by measuring the metabolic profile of their leaves, stems, and phloem exudates collected both above and below the graft union at early stages of graft formation.
3. Evaluate the use of *in vitro* micrografting to unravel physiological markers of early incompatible responses in grapevines via histological and histochemical observations of the events of graft formation in *Vitis vinifera* scions grafted onto 110R rootstock.

The gained insights represent a substantial advancement in our knowledge about *in vivo* and *in vitro* detection methods to early detect graft incompatible grapevine partners, and in the effect of early metabolic scion-rootstock interactions in specific tissues and phloem exudates of grafted grapevines. In summary, the findings produced during this research led us to suggest that graft incompatibility in grapevine might be a virus-induced problem which can arise even when using certified virus-free plants.

The thesis is structured as follows:

To identify phenotypic parameters discriminative of graft success, in **Chapter II** we used four clones of two *V. vinifera* cultivars (cv. Touriga Nacional and cv. Syrah) that show different compatibility behaviour when grafted onto the same rootstock (110R). We have monitored several physiological parameters, the internal anatomy of the graft union, chlorophyll fluorescence, and pigment contents of homo- and heterografts

at 2 times of graft formation in a nursery-grafting context. The data collected permitted us to identify useful phenotypic parameters that can be used to early screen grapevine compatible partners and to propose that grapevine graft success correlates with the improvement of the scion–rootstock translocation via vasculature. Furthermore, grapevine scion-rootstock interactions were found to affect important developmental decisions and growth habits of the scion already at 5 months after grafting, when the healing of the graft is not yet completed.

Therefore, 5 months after grafting was used as a time-point in **Chapter III** to shed light on the early metabolic grapevine scion-rootstock interactions. We explored differences in the global metabolic profiles of 11 homo- and heterograft combinations in different tissues and phloem exudates collected from both above and below the graft union. Such analysis permitted to verify that the presence of a heterologous grafting partner increases defense-related compounds in both scion and rootstocks at short and longer distance from the graft leading to hypothesize whether such defense response might reflect differences between the grafting partners 'biomes. Furthermore, the rootstock phloem exudate was found significantly depleted in sucrose (the main transported sugar in plants) particularly when *V. vinifera* scions are heterografted onto 110R rootstock, further supporting the previous suggestion (Chapter II) of an impaired vascular translocation in these grafts.

In **Chapter IV** we applied *in vitro* micrografting techniques to the *V. vinifera*/110R graft combinations studied in Chapter II and included in Chapter III, coupled with histological and histochemistry analysis, aiming to identify physiological markers able to forecast incompatible responses in these grapevine grafts. We have characterized the timeframe of graft formation in successful grapevine homografts and identified several histochemistry dies able to reveal physiological parameters indicative of grapevine graft incompatibility. Furthermore, the system used permitted to

observe that heterografts failures displayed viral symptoms while translocated incompatibility symptoms were observed in successful heterografts. This led us to verify that levels of Grapevine Rupestris Stem Pitting associated Virus (GRSPaV) infections correlated with graft (un)-success in Syrah clones grafted onto 110-Ritcher rootstock under field (Chapter II and III) and *in vitro* conditions, suggesting that GRSPaV, a virus not included in the EU certification schemes, might be involved in the graft incompatibility of Syrah grafted onto 110R.

Finally, in **Chapter V**, the main achievements, conclusions, and futures perspectives are discussed.

References

1. Mudge, K.W. Grafting: theory and practice. In *Plant Propagation Concepts and Laboratory Exercises*, Beyl, CA, Trigiano, R.N. Eds.; CRC Press: Boca Raton, FL, USA, 2008, pp. 273–292.
2. Gainza, F.; Opazo, I.; Muñoz, C. Graft incompatibility in plants: Metabolic changes during formation and establishment of the rootstock/scion union with emphasis on Prunus species. *Chil. J. Agric. Res.* **2015**, 75, 28–34.
3. Tandonnet, J.P.; Cookson, S.J.; Vivin, P.; Ollat, N. Scion genotype controls biomass allocation and root development in grafted grapevine. *Aust. J. Grape Wine Res.* **2010**, 16, 290–300.
4. Hellman, W.E. Grapevine Structure and Function. In *Oregon Viticulture*; Hellman, E.W. Eds.; Corvallis: Oregon State University Press, 2003, pp. 5–19.
5. Keller, M.; Mills, L.J.; Harbertson, J.F. Rootstock Effects on Scion Vigor and Fruit and Wine Composition in a Dry Climate. *Am. J. Enol. Vitic.* **2011**, 62, 388a-388a.
6. Stamp, J.A. The contribution of imperfections in nursery stock to the decline of young vines in California. *Phytopathol. Mediterr.* **2001**, 40, 369–375.
7. Waite, H.; Whitelaw-Weckert, M.; Torley, P. Grapevine propagation: principles and methods for the production of high-quality grapevine planting material. *New Zeal. J. Crop Hortic. Sci.* **2015**, 43, 144–161.
8. Assunção, M.; Santos, C.; Brazão, J.; Eiras-Dias, J.E.; Fevereiro, P. Understanding the molecular mechanisms underlying graft success in grapevine. *BMC Plant Biol.* **2019**, 19, 1–17.
9. Tedesco, S.; Pina, A.; Fevereiro, P.; Kragler, F. A Phenotypic Search on Graft Compatibility in Grapevine. *Agronomy* **2020**,10, 706.
10. Jones, T.H.; Cullis, B.R.; Clingeleffer, P.R.; Rühl, E.H. Effects of novel hybrid and traditional rootstocks on vigour and yield components of Shiraz grapevines. *Aust. J.*

Grape Wine Res. **2009**, 15, 284–292.
11. Pulko, B.; Vršic, S.; Valdhuber, J. Influence of various rootstocks on the yield and grape composition of sauvignon blanc. *Czech J. Food Sci.* **2012**, 30, 467–473.
12. Ozden, M.; Vardin, H.; Simsek, M.; Karaaslan, M. Effects of rootstocks and irrigation levels on grape quality of *Vitis vinifera* L. cv. Shiraz. *African J. Biotechnol.* **2010**, 9, 3801–3807.
13. Sabbatini P.; Howell, G.S. Rootstock Scion Interaction and Effects on Vine Vigor, Phenology, and Cold Hardiness of Interspecific Hybrid Grape Cultivars (Vitis spp.). *Int. J. Fruit Sci.* **2013**, 13, 466–477.
14. Ali, S. Physiological and morphological responses of grapevine (V. vinifera L. cv. 'ITALIA') leaf to water deficit under different rootstock effects. *Acta Sci. Pol. Hortorum Cultus* **2016**, 15, 135–148.
15. Alley, C. Propagation of grapevines. *Calif. Agric.* **1980**, 34, 29–30.
16. Çelik, Ü. The effects of different grafting methods applied by manual grafting units on grafting success in grapevines. *Turkish J. Agric. For.* **2000**, 24, 499–504.
17. Fourie, P.H.; Halleen, F. Chemical and biological protection of grapevine propagation material from trunk disease pathogens. *Eur. J. Plant Pathol.* **2006**, 116, 255–265.
18. Mullins, M.G.; Bouquet, A.; Williams, L.E. Biology of the grapevine. Cambridge University Press: Cambridge, Massachusetts, USA, 1992.
19. Pina, A.; Errea, P. A review of new advances in mechanism of graft compatibility-incompatibility. *Sci. Hortic. (Amsterdam)* **2005**, 1–11.
20. Koepke, T.; Dhingra, A. Rootstock scion somatogenetic interactions in perennial composite plants. *Plant Cell Rep.* **2013**, 32, 1321–1337.
21. Pina, A.; Cookson, S.; Calatayud, A.; Trinchera, A.; Errea, P. Chapter 5—Physiological and molecular mechanisms underlying graft compatibility. In *Vegetable Grafting Principles and Practices*; Colla, G., Perez-Alfocea, F., Schwarz, D., Eds.; CABI Oxfordshire: Wallingford, UK, 2017; pp. 132–154.
22. Cookson, S.J.; Ollat, N. Graft union formation in grapevine induces transcriptional changes related to cell wall modification, wounding, hormone signalling, and secondary metabolism. *J. Exp. Bot.* **2013**, 64, 2997–3008.
23. Albacete, A.; Martínez-Andújar, C.; Martínez-Pérez, A.; Thompson, A.J.; Dodd, I.C.; Pérez-Alfocea, F. Unravelling rootstock×scion interactions to improve food security. *J. Exp. Bot.* **2015**, 66, 2211–2226.
24. Stegemann, S.; Bock, R. Exchange of Genetic Material Between Cells in Plant Tissue Grafts. *Science* **2009**, 324, 649–651.
25. Kozo-Polianskiĭ, B.M. Symbiogenesis: a new principle of evolution; Harvard University Press: Cambridge, Massachusetts, USA, 2010.
26. Warschefsky, E.J.; Klein, L.L.; Frank, M.H.; Chitwood, D.H.; Londo, J.P.; von Wettberg, E.J.B.; Miller, A.J. Rootstocks: Diversity, Domestication, and Impacts on Shoot Phenotypes. *Trends Plant Sci.* **2016**, 21, 418–437.
27. Melnyk, C.W. Plant grafting: insights into tissue regeneration. *Regeneration* **2017**, 4, 3–14.
28. Wang, J.; Jiang, L.; Wu, R. Plant grafting: how genetic exchange promotes vascular

reconnection. *New Phytol.* **2017**, 214, 56–65.
29. Frank, M.H.; Chitwood, D.H. Plant Chimeras : the good , the bad , and the ' Bizzaria' *Developmental Biology* **2016**, 314, 41-53.
30. Mudge, K.; Janick, J.; Scofield, S.; Goldschmidt, E.E. A History of Grafting. *Hortic. Rev. (Am. Soc. Hortic. Sci)* **2009**, 35, 437–493.
31. Stenkamp, S.H.G.; Becker, M.S.; Hill, B.H.E.; Blaich, R.; Forneck, A. Clonal variation and stability assay of chimeric Pinot Meunier (*Vitis vinifera L.*) and descending sports. *Euphytica* **2009**, 165, 197–209.
32. Liu, Y. Historical and Modern Genetics of Plant Graft Hybridization. *Adv. Genet.* **2006**, 101–129.
33. Goldschmidt, E.E. Plant grafting: new mechanisms, evolutionary implications. *Front. Plant Sci.* **2014**, 5, 1–9.
34. Rasool, A.; Mansoor, S.; Bhat, K.M.; Hassan, G.I.; Rehman Baba, T.; Nasser Alyemeni, M.; Alsahli, A.A.; El-Serehy, H.A.; Paray, B.A.; Ahmad, P. Mechanisms Underlying Graft Union Formation and Rootstock Scion Interaction in Horticultural Plants. *Front. Plant Sci.* **2020**, 11, 590847.
35. Kapazoglou, A.; Eleni, T.; Avramidou, E.V.; Abraham, E.M.; Gerakari, M.; Megariti, S.; Doupis, G.; Doulis, A.G. Epigenetic Changes and Transcriptional Reprogramming Upon Woody Plant Grafting for Crop Sustainability in a Changing Environment. *Front. Plant Sci.* **2021**, 11, 1–16.
36. Assunção, M.; Tedesco, S.; Fevereiro, P. Molecular Aspects of Grafting in Woody Plants. In *Annual Plant Reviews Online*, 1st ed.; Wiley Online Library: New York, NY, USA, 2021; Volume 4, pp. 87–126.
37. Melnyk, C.W.; Schuster, C.; Leyser, O.; Meyerowitz, E.M. A developmental framework for graft formation and vascular reconnection in arabidopsis thaliana. *Curr. Biol.* **2015**, 25, 1306–1318.
38. Andrews, P.K.; Serrano Marquez, C. Volume 15—Graft incompatibility. In *Horticultural Reviews*; Janick, J., Ed.; John Wiley & Sons, Inc.: Oxford, UK, 1993; pp. 183–232.
39. Mosse, B. Graft-Incompatibility In Fruit Trees With Particular Reference To Its Underlying Causes. Technical Communication No. 28. Kent: Farnham Royal, Bucks: Commonwealth Agricultural Bureaux, England, 1962.
40. Moore, R. Graft Compatibility and Incompatibility in Higher Plants. *Dev. Comp. Immunol.* **1981**, 5, 377–389.
41. Jefree, M.M.; Yeoman, C.E. Development of intercellular connections bteween opposing cells in a graft union. *New Phytol.* **1982**, 93, 491–509.
42. Yeoman, M.M. Cellular Recognition Systems in Grafting. In *Cellular Interactions*, Linskens H.F., Heslop-Harrison J. Eds.; Springer Berlin Heidelberg: Heidelberg, DE, 1984; pp. 453–472.
43. Feucht, W. Graft incompatibility of the tree crops: An overview of the present scientific status. *Acta Horticulturae* **1988**, 227.
44. Usenik, V.; Štampar, F. Influence of various rootstocks for cherries on p-coumaric acid, genistein and prunin content and their involvement in the incompatibility process.

Gartenbauwissenschaft **2000**, 65, 245–250.
45. Hartman, H.T.; Kester, D.E.; Davies, F.T.; Geneve, R.G. Principles of grafting and budding. In *Hartmann and Kester's Plant Propagation: Principles and Practices*; Prentice Hall: Upper Saddle River, NJ, USA, 2011; pp. 415–463.
46. Pereira, I.D.S.; Antunes, L.E.C.; Picolotto, L.; Fachinello, J.C. Incompatibilidade de enxertia em *Prunus* Graft incompatibility in *Prunus*. *Cienc. Rural* **2014**, 449, 1519–1526.
47. Mudge, K. "The How, When, and Why of Grafting" web-course, department of Horticulture of the Cornell university. Available at: https://courses.cit.cornell.edu/hort494/mg/specific.grafting/compatibility.html (accessed on 30.03.21)
48. Wulf, K.E.; Reid, J.B.; Foo, E. What drives interspecies graft union success? Exploring the role of phylogenetic relatedness and stem anatomy. *Physiol. Plant.* **2020**, 170, 132–147.
49. Assunção, M.; Canas, S.; Cruz, S.; Brazão, J.; Zanol, G.C.; Eiras-Dias, J.E. Graft compatibility of *Vitis spp.*: The role of phenolic acids and flavanols. *Sci. Hortic. (Amst.)* **2016**, 207, 140–145.
50. Pina, A.; Errea, P.; Martens, H.J. Graft union formation and cell-to-cell communication via plasmodesmata in compatible and incompatible stem unions of *Prunus spp. Sci. Hortic. (Amsterdam)* **2012**, 143, 144–150.
51. Melnyk, C.W.; Meyerowitz, E.M. Plant grafting *Curr. Biol.* **2015**, 25, R183–R188.
52. Bouquet, A. Differences observed in the graft compatibility between some cultivars of Muscadine grape (*Vitis rotundifolia Michx.*) and European grape (*Vitis vinifera L.* cv. Cabernet Sauvignon). *Vitis* **1980**, 19, 99–104.
53. Hamdan, A.S.; Basheer-Salimia, R. Preliminary Compatibility between Some Table-Grapevine Scion and Phylloxera- Resistant Rootstock Cultivars. *Jordan J. Agric. Sci.* **2010**, 6, 1–10.
54. Vršič, S.; Pulko, B.; Kocsis, L. Factors influencing grafting success and compatibility of grape rootstocks. *Sci. Hortic. (Amsterdam)* **2015**, 181, 168–173.
55. D'Khili, S.G.B.; Michaux-Ferrière, N. Etude histochimique de 1 ' incompatibilite au microgreffage et greffage de boutures herbacees chez la vigne. *Vitis* **1995**, 34, 135–140.
56. Zarrouk, O.; Gogorcena, Y.; Moreno, M.A.; Pinochet, J. Graft compatibility between peach cultivars and *Prunus* rootstocks. *HortScience* **2006**, 41, 1389–1394.
57. Irisarri, P.; Pina, A.; Errea, P. Evaluación del comportamiento vegetativo y compatibilidad de injerto de variedades de peral sobre los patrones 'BA-29' y 'OHF-87' ITEA *Inf. Tec. Econ. Agrar.* **2016**, 243–254.
58. Milien, M.; Renault-Spilmont, A.S.; Cookson, S.J.; Sarrazin, A; Verdeil, J.L. Visualization of the 3D structure of the graft union of grapevine using X-ray tomography. *Sci. Hortic. (Amsterdam)* **2012**, 144, 130–140.
59. Bahar, E.; Korkutal, I. Using magnetic resonance imaging technique (MRI) to investigate graft connection and its relation to reddening discoloration in grape leaves. *JFAE* **2010**, 8, 293–297

60. Zarrouk, Y.; Testillano, O.; Risueño, P.S.; Moreno, M.C.; Gogorcena, M.A. Changes in Cell/Tissue Organization and Peroxidase Activity as Markers for Early Detection of Graft Incompatibility in Peach/Plum Combinations. *J. Am. Soc. Hortic. Sci.* **2010**, 135, 9–17.
61. Herrero, J. La compatibilite entre les sujets porte-greffes et les varieies fruitieres. In Congr. Pomol. Intern., session 87, 1956, Namur 17–28.
62. Uyemoto, J.K.; Rowhani, A.; Luvisi, D.; Krag, C.R. New closterovirus in 'Redglobe' grape causes decline of grafted plants. *Calif. Agric.* **2001**, 28–31.
63. Meng, B.; Li, C.; Goszczynski, D.E.; Gonsalves, D. Genome Sequences and Structures of Two Biologically Distinct Strains of Grapevine leafroll-associated virus 2 and Sequence Analysis. *Virus Genes* **2005**, 31, 31–41.
64. Beuve, M.; Sempé, L.; Lemaire, O. A sensitive one-step real-time RT-PCR method for detecting Grapevine leafroll-associated virus 2 variants in grapevine. *J. Virol. Methods* **2007**, 141, 117–124.
65. Bertazzon, N.; Borgo, M.; Vanin, S.; Angelini, E. Genetic variability and pathological properties of Grapevine Leafroll-associated Virus 2 isolates. *Eur. J. Plant Pathol.* **2010**, 127, 185–197.
66. Al Rwahnih, M.; Rowhani, A.; Smith, R.J.; Uyemoto, J.K.; Sudarshana, M.R. Grapevine Necrotic Union, A Newly Recognized Disease of Unknown Etiology In Grapevines Grafted On 110 Richter Rootstock In California. *J. Plant Pathol.* **2012**, 94, 149–156.
67. Gargin, S.; Altindisli, A. A Research on the affinity coefficients of Red Globe grape variety with 140 R, 41 B rootstocks. *BIO Web Conf.* **2014**, 3, 01004.
68. Canas, S.; Assunção, M.; Brazão, J.; Zanol, G.; Eiras-Dias, J.E. Phenolic compounds involved in grafting incompatibility of *vitis spp:* Development and validation of an analytical method for their quantification. *Phytochem. Anal.* **2015**, 26, 1–7.
69. Gökbayrak, Z.; Söylemezoğlu, G.; Akkurt, M.; Çelik, H. Determination of grafting compatibility of grapevine with electrophoretic methods. *Sci. Hortic. (Amsterdam)* **2007**, 113, 343–352.
70. Goldammer, T. Grape Grower's Handbook A Guide To Viticulture for Wine Production. Apex Publishers: Colchester, GB, 2015.
71. Plantgrape project database. Available at: http://plantgrape.plantnet-project.org (accessed on 3.06.21)
72. Instituto da Vinha e do Vinho I.P. Catálogo das castas para vinho cultivadas em Portugal. Chaves Ferreira press, Lisboa, Portugal, 2011.
73. Overview of the characteristics of the vine rootstock. "Rauscedo" nurseries cooperative catalogue, available at: https://www.vivairauscedo.com/en/portinnesti (accessed on 3.06.2021)
74. Italian national catalog of grapevine varieties. Available at http://catalogoviti.politicheagricole.it/catalogo.php (accessed on 3.06.2021)
75. Aloni, B.; Karni, L.; Deventurero, G.; Levin, Z.; Cohen, R.; Katzir, N.; LotanPompan, M.; Edelstein, M.; Aktas, H.; Turhan, E.; Joel, D.M.; Horev, C.; Kapulnik, Y. Physiological and biochemical changes at the rootstock-scion interface in graft

combinations between Cucurbita rootstocks and a melon scion. *J. Hortic. Sci. Biotechnol.* **2008**, 83, 777–783.

76. Nocito, F.F.; Espen, L.; Fedeli, C.; Lancilli, C.; Musacchi, S.; Serra, S.; Sansavini, S.; Cocucci, M.; Sacchi, G.A. Oxidative stress and senescence-like status of pear calli co-cultured on suspensions of incompatible quince microcalli. *Tree Physiol.* **2010**, 30, 450–458.
77. Irisarri, P.; Binczycki, P.; Errea, P.; Martens, H.J.; Pina, A. Oxidative stress associated with rootstock-scion interactions in pear/quince combinations during early stages of graft development. *J. Plant Physiol.* **2015**, 176, 25–35.
78. Xu, Q.; Guo, S.R.; Li, L.; An, Y.H.; Shu, S.; Sun, J. Proteomics analysis of compatibility and incompatibility in grafted cucumber seedlings. *Plant Physiol. Biochem.* **2016**, 105, 21–28.
79. Espen, L.; Cocucci, M.; Sacchi, G.A. Differentiation and functional connection of vascular elements in compatible and incompatible pear/quince internode micrografts. *Tree Physiol.* **2005**, 25, 1419–1425.
80. Pina, A.; Errea, P. Differential induction of phenylalanine ammonia-lyase gene expression in response to *in vitro callus* unions of *Prunus spp. J. Plant Physiol.* **2008**, 165, 705–714.
81. Hudina, M.; Orazem, P.; Jakopic, J.; Stampar, F. The phenolic content and its involvement in the graft incompatibility process of various pear rootstocks (*Pyrus communis L.*). *J. Plant Physiol.* **2014**, 171, 76–84..
82. Assunção, M.; Pinheiro, J.; Cruz, S.; Brazão, J.; Queiroz, J.; Eduardo, J.; Dias, E.; Canas, S. Gallic acid, sinapic acid and catechin as potential chemical markers of *Vitis* graft success. *Sci. Hortic.* **2019**, 246, 129–135.
83. Kostoff, D. Induced immunity in plants. In Proceedings of National Academy of Sciences, March 1928, pp. 14.3: 236-237.
84. Whitaker, S.; Chester, W.T. Studies on the precipitin reaction in plants. IV. The question of acquired reactions due to grafting. *Am. J. Bot.* **1933**, 297–308.
85. Cookson, S.J.; Clemente Moreno, M.J.; Hevin, C.; Nyamba Mendome, L.Z.; Delrot, S.; Magnin, N.; Trossat-Magnin, C.; Ollat, N. Heterografting with nonself rootstocks induces genes involved in stress responses at the graft interface when compared with autografted controls. *J. Exp. Bot.* **2014**, 65, 2473–2481
86. Tedesco, S.; Erban, A.; Gupta, S.; Kopka, J.; Fevereiro, P.; Kragler, F.; Pina, A. The Impact of Metabolic Scion–Rootstock Interactions in Different Grapevine Tissues and Phloem Exudates. *Metabolites* **2021**, 11, 349.
87. Kollmann, R.; Glockmann, C. Studies on graft unions. I. Plasmodesmata between cells of plants belonging to different unrelated taxa. *Protoplasma* **1985**, 124, 224–235.
88. Moore, R. A Model for Graft Compatibility-Incompatibility in Higher Plants. *Am. J. Bot.* **1984**, 71, 752–758.
89. Gur, A.; Samish, R.M.; Lifshitz, E. The role of the cyanogenic glycoside of the quince in the incompatibility between pear cultivars and quince rootstocks. *Journal Hortic. Sci.* **1968**, 26, 186–237.
90. Wang, Y.; Kollmann, R. Vascular Differentiation in the Graft Union of *in-vitro* Grafts

with Different Compatibility. — Structural and Functional Aspects. *J. Plant Physiol.* **1996**, 147, 521–533.
91. Errea, P. Implications of phenolic compounds in graft incompatibility in fruit tree species. *Sci. Hortic. (Amsterdam)* **1998**, 74, 195–205.
92. Ehlers, K.; Kollmann, R. Primary and secondary plasmodesmata: structure, origin, and functioning. *Protoplasma* **2001**, 216, 1–30.
93. Pina, A.; Errea, P.; Schulz, A.; Martens, H.J. Cell-to-cell transport through plasmodesmata in tree *callus* cultures. *Tree Physiol.* **2009**, 29, 809–818.
94. Aloni, B.; Cohen, R.; Karni, L.; Aktas, H.; Edelstein, M. Hormonal signaling in rootstock-scion interactions. *Sci. Hortic. (Amsterdam)* **2010**, 127, 119–126.
95. Yin, H.; Yan, B.; Sun, J.; Jia, P.; Zhang, Z.; Yan, X.; Chai, J.; Ren, Z.; Zheng, G.; Liu, H. Graft-union development: a delicate process that involves cell–cell communication between scion and stock for local auxin accumulation. *J. Exp. Bot.* **2012**, 63, 4219–4232.
96. Chitarra, W.; Perrone, I.; Avanzato, C.G.; Minio, A.; Boccacci, P.; Santini, D.; Gilardi, G.; Siciliano, I.; Gullino, M.L.; Delledonne, M.; et al. Grapevine Grafting: Scion Transcript Profiling and Defense-Related Metabolites Induced by Rootstocks. *Front. Plant Sci.* **2017**, 8, 654.
97. Wulf, K.E.; Reid, J.B.; Foo, E. Auxin transport and stem vascular reconnection - has our thinking become canalized? *Ann. Bot.* **2019**, 123, 429–439. doi: 10.1093/aob/mcy180.
98. Harada, T. Grafting and RNA transport via phloem tissue in horticultural plants. *Sci. Hortic. (Amsterdam)* **2010**, 125, 545–550.
99. Stegemann, S.; Keuthe, M.; Greiner, S.; Bock, R. Horizontal transfer of chloroplast genomes between plant species. *Proc. Natl. Acad. Sci.* **2012**, 109, 2434–2438.
100. Hertle, A.P.; Haberl, B.; Bock, R. Horizontal genome transfer by cell-to-cell travel of whole organelles. *Sci. Adv.* **2021**, 7.
101. Ohta, Y. Graft-transformation, the mechanism for graft-induced genetic changes in higher plants. *Euphytica* **1991**, 55, 91–99.
102. Fuentes, I.; Stegemann, S.; Golczyk, H.; Karcher, D.; Bock, R. Horizontal genome transfer as an asexual path to the formation of new species. *Nature* **2014**, 511, 232–235.
103. Notaguchi, M.; Higashiyama, T.; Suzuki, T. Identification of mRNAs that move over long distances using an RNA-seq analysis of *Arabidopsis*/*Nicotiana benthamiana* heterografts. *Plant Cell Physiol.* **2015**, 56, 311–321.
104. Saplaoura, E.; Kragler, F. Mobile Transcripts and Intercellular Communication in Plants; In *The Enzymes*, Lin, C.; Luan, S. Eds.; Academic Press: Cambridge, Massachusetts, USA, 2016; pp. 1–29.
105. Yang, L.; Perrera, V.; Saplaoura, E.; Apelt, F.; Bahin, M.; Kramdi, A.; Olas, J.; Mueller-Roeber, B.; Sokolowska, E.; Zhang, W.; Li, R.; Pitzalis, N.; Heinlein, M.; Zhang, S.; Genovesio, A.; Colot, V.; Kragler, F. m5C Methylation Guides Systemic Transport of Messenger RNA over Graft Junctions in Plants. *Curr. Biol.* **2019**, 29, 2465-2476.e5.

106. Guan, D.; Yan, B.; Thieme, C.; Hua, J.; Zhu, H.; Boheler, K.R.; Zhao, Z.; Kragler, F.; Xia, Y.; Zhang, S. PlaMoM: A comprehensive database compiles plant mobile macromolecules. *Nucleic Acids Res.* **2017**, 45, D1021–D1028.
107. Zhang, W.; Thieme, C.J.; Kollwig, G.; Apelt, F.; Yang, L.; Winter,N.; Andresen, N.; Walther, D.; Kragler, F. tRNA-Related Sequences Trigger Systemic mRNA Transport in Plants. *Plant Cell* **2016**, 28, 1237–1249.
108. Kim, M.; Canio, W.; Kessler, S.; Sinha, N. Developmental Changes Due to Long-Distance Movement of a Homeobox Fusion Transcript in Tomato. *Science* **2001**, 293, 287–289.
109. Yang, Y.; Mao, L.; Jittayasothorn, Y.; Kang, Y.; Jiao, C.; Fei, Z.; Zhong, G.-Y. Messenger RNA exchange between scions and rootstocks in grafted grapevines. *BMC Plant Biol.* **2015**, 15, 251.
110. Haywood, V.; Yu, T.-S.; Huang, N.-C.; Lucas, W. J. Phloem long-distance trafficking of GIBBERELLIC ACID-INSENSITIVE RNA regulates leaf development. *Plant J.* **2005**, 42, 49–68.
111. Banerjee, A.K.; Chatterjee, M.; Yu, Y.; Suh, S.-G.; Miller, W.A.; Hannapel, D. J. Dynamics of a Mobile RNA of Potato Involved in a Long-Distance Signaling Pathway. *PLANT CELL ONLINE* **2006**, 18, 3443–3457.
112. Mahajan, A.; Bhogale, S.; Kang, I.H.; Hannapel, D.J.; Banerjee, A.K. The mRNA of a Knotted1-like transcription factor of potato is phloem mobile. *Plant Mol. Biol.* **2012**, 79, 595–608.
113. Notaguchi, M.; Wolf, S.; Lucas, W.J. Phloem-Mobile Aux / IAA Transcripts Target to the Root Tip and Modify Root Architecture F. *J. Integr. Plant Biol.* **2012**, 54, 760–772.
114. Thieme, C.J.; Rojas-Triana, M.; Stecyk, E.; Schudoma, C.; Zhang, W.; Yang, L.; Miñambres, M.; Walther, D.; Schulze, W.X.; Paz-Ares, J.; Scheible, W.-R.; Kragler, F. Endogenous Arabidopsis messenger RNAs transported to distant tissues. *Nat. Plants* **2015**, 15025.
115. Yoo, B.-C. A Systemic Small RNA Signaling System in Plants. *Plant Cell Online* **2004**, 16, 1979–2000.
116. Tzarfati, R.; Ben-Dor, S.; Sela, I.; Goldschmidt, E.E. Graft-induced Changes in MicroRNA Expression Patterns in *Citrus* Leaf Petioles. *Open Plant Sci. J.* **2013**, 7, 17–23.
117. Buhtz, A.; Springer, F.; Chappell, L.; Baulcombe, D.C.; Kehr, J. Identification and characterization of small RNAs from the phloem of *Brassica napus*. *Plant J* **2008**, 53, 739–749.
118. Zhang, W.; Kollwig, G.; Stecyk, E.; Apelt, F.; Dirks, R.; Kragler, F. Graft-transmissible movement of inverted-repeat-induced siRNA signals into flowers. *Plant J.* **2014**, 80, 106–121.
119. Wu, R.; Wang, X.; Lin, Y.; Ma, Y.; Liu, G.; Yu, X.; Zhong, S.; Liu, B. Inter-Species Grafting Caused Extensive and Heritable Alterations of DNA Methylation in *Solanaceae* Plants. *PLoS One* **2013**, 8.
120. Molnar, A.; Melnyk, C.W.; Bassett, A.; Hardcastle, T.J.; Dunn, R.; Baulcombe, D.C. Small Silencing RNAs in Plants Are Mobile and Direct Epigenetic Modification in

Recipient Cells. *Science* **2010**, 328, 872–875.
121. Melnyk, C.W.; Molnar, A.; Bassett, A.; Baulcombe, D.C. Mobile 24 nt Small RNAs Direct Transcriptional Gene Silencing in the Root Meristems of Arabidopsis thaliana. *Curr. Biol.* **2011**, 21, 1678–1683.
122. Lewsey, M.G.; Hardcastlec, T.J.; Melnykc, C.W.; Molnarc, A.; Vallic, A.; Uricha, M.A.; Nerya, J.R.; Baulcombec, D.C.; Ecker, J.R. Mobile small RNAs regulate genome-wide DNA methylation. *Pnas* **2015**, E801–E810.
123. Lucas, W.J.; Yoo, B.C.; Kragler, F. RNA as a long-distance information macromolecule in plants. *Nat. Rev. Mol. Cell Biol.* **2001**, 2, 849–857.
124. Zhang, S.; Sun, L.; Kragler, F. The Phloem-Delivered RNA Pool Contains Small Noncoding RNAs and Interferes with Translation. *Plant Physiol.* **2009**, 150, 378–387.
125. Iakimova, E.T.; Woltering, E.J. Xylogenesis in zinnia (*Zinnia elegans*) cell cultures: unravelling the regulatory steps in a complex developmental programmed cell death event. *Planta* **2017**, 245, 681–705.
126. Pina, A.; Irisarri, P.; Errea, P.; Zhebentyayeva, T. Mapping Quantitative Trait Loci Associated With Graft (In) Compatibility in Apricot (*Prunus armeniaca L.*). *Front. Plant Sci.* **2021**, 12.
127. Herrero, J. Studies of Compatible and Incompatible Graft Combinations With Special Reference to Hardy Fruit Trees. *J. Hortic. Sci.* **1951**, 26, 186–237.
128. Errea, P.; Felipe, A.; Herrero, M. Graft establishment between compatible and incompatible *Prunus spp*. *J. Exp. Bot.* **1994**, 45, 393–401. doi: 10.1093/jxb/45.3.393.
129. Irisarri, P.; Zhebentyayeva, T.; Errea, P.; Pina, A. Inheritance of self- And graft-incompatibility traits in an F 1 apricot progeny. *PLoS One* **2019**, 14, 1–14.
130. Rowhani, A.; Uyemoto, J.K.; Golino, D.A.; Daubert, S.D.; Al Rwahnih, M. Viruses Involved in Graft Incompatibility and Decline. In *Grapevine Viruses: Molecular Biology, Diagnostics and Management*; Meng, B., Martelli, G.P., Golino, D.A., Fuchs, M., Eds.; Springer International Publishing: Cham, Switzerland, 2017; pp. 289–302.
131. Cui, Z.H.; Agüero, C.B.; Wang, Q.C.; Walker, M.A. Validation of micrografting to identify incompatible interactions of rootstocks with virus-infected scions of Cabernet Franc. *Aust. J. Grape Wine Res.* **2019**, 25, 268–275.
132. Martelli, G.P. Directory of virus and virus-like diseases of the grapevine and their agents. *J. Plant Pathol.* **2014**, 96, 1–36.

Chapter II

A Phenotypic Search on Graft Compatibility in Grapevine

This chapter was published in the *Agronomy* journal:
Tedesco, S.; Pina, A.; Fevereiro, P.; Kragler, F. A Phenotypic Search on Graft Compatibility in Grapevine. *Agronomy* 2020, *10*, 706. doi: 10.3390/agronomy10050706

In this research paper, Sara Tedesco performed the phenotyping methods, the data analysis, and participated in the writing of the manuscript.

Abstract

Grafting is the most used propagation method in viticulture and is the unique control strategy against Phylloxera. Nevertheless, its practice remains limited mainly due to inconsistent graft success and difficulties in predicting graft compatibility responses of proposed scion–rootstock combinations, slowing down the selection of elite rootstocks. Aiming to identify optimal phenotypic parameters related to graft (in)compatibility, we used four clones of two grapevine cultivars that show different compatibility behavior when grafted onto the same rootstock. Several physiological parameters, internal anatomy of the graft union, chlorophyll fluorescence, and pigment contents of homo- and heterografts were monitored in a nursery-grafting context. The measurements highlighted enhanced performance of the heterografts due to rooting difficulties of *Vitis vinifera* homografts. This suggests that in viticulture, homografts should only be used as compatibility controls regarding qualitative attributes. By observing the internal anatomy of the union, we found that grapevines might require longer times for graft healing than anticipated. While Affinity Coefficients were not informative to assess incompatibility, leaf chlorophyll concentration analysis proved to be a more sensitive indicator of stress than the analysis of chlorophyll fluorescence. Overall, we conclude that graft take correlated best with *callus* formation at the graft junction three weeks after grafting.

Key words: grafting; graft incompatibility; graft success prediction; grapevine; Richter 110; rootstock; rootstock breeding; Syrah; Touriga Nacional; *Vitis*

1. Introduction

Grafting is an ancient method for plant propagation and plant improvement. During recent decades, the use of grafting expanded to commercially propagate horticultural crops [1] and it is currently applied in orchards, greenhouses, and gardening. For grapevines, grafting represents the longest use of a biological control strategy ever applied, as it saved and keeps saving viticulture and the wine industry from the devastating effects of the soil-borne aphid Phylloxera (*Daktulosphaira vitifoliae Fitch*). Since American vines showed resistance to Phylloxera, *Vitis vinifera* scions started to be grafted onto American resistant rootstocks or their hybrids, and nowadays, more than 80% of all vineyards worldwide are composed of heterografted *Vitis* species [2]. Although the use of grafted crops is increasing, its practice remains limited mainly due to inconsistent graft success with variant scion and rootstock species [3]. It has been reported that 39% of bench grafted vines are deemed defective at the nursery [4]. Consequently, nurseries are frequently required to double the production of grafted vines to guarantee their contracts. Graft incompatibility can be defined as the failure to form a successful graft union between two plant parts when all other requirements, such as technique, timing, phytosanitary and environmental conditions are satisfied [5].

Both compatible and incompatible plants are defined in the graft research field in such that they can be grafted and form a vascular connection [6]. Nevertheless, incompatible grafted plants do not exhibit normal growth behavior and lifespans whereas compatible grafted plants demonstrate normal growth behavior. Measurements for the degree of (in)compatibility are often based on graft success rates or other sometimes not well defined physiological and morphological indicators. In general, compatibility measurements include indicators

related to growth behavior and stress symptoms. All of these can be displayed immediately or delayed and in some cases, they can take as long as 20 years to manifest, as seen in conifers and oaks [7]. Although it is believed that the likelihood of graft success is higher when scion and rootstock are closely related or of the same species, graft compatibility between scion and rootstock can vary greatly even between related species and grapevine clones [5]. Inline, predictive and standardized measurements to evaluate compatibility levels would be useful for breeders when considering the use of a rootstock with a specific graft combination [3], particularly in the case of new genotypes under selection with unknown grafting properties [8–10]. Indeed, to release a new grapevine rootstock into the market, several traits need to be evaluated including “Phylloxera” and nematode resistance, salt and drought tolerance, and last but not least, graft compatibility with scion species need to be assessed [11].

Considering that grapevine breeding has generation cycles that may last 25 years [12], it is obvious how incompatibility could impede the effort of breeding programs, slowing-down the selection of elite genotypes. Despite the importance of grafting and high graft success rates for many crop plants and its unavoidability in grapevine propagation, surprisingly little is understood, even with over one hundred years of scientific research [3]. Intending to unveil graft biology and incompatibility, a number of reports exist on (i) the phenotypic traits and field performances of several graft combinations [13–15]; (ii) the anatomy of grafted grapevines [16,17]; (iii) the biochemistry of grapevine grafts with focus on phenolic compounds [18,19] and on isoenzymes [20]; (iv) the molecular aspects concerning the transcriptome of different graft combinations [5,21,22]; and (v) total protein profiles [20]. Although numerous detection methods have been employed, no simple indicator seems to accurately predict compatibility behavior of variant scion–

rootstock combinations, which would be valuable to shorten breeding cycles and to limit the production losses of nurseries and growers.

To address the known limitations in graft success predictions, we evaluated several methods that have been described as predictive for graft (in)compatibility in different plant species. Aiming to screen for suitable indicators of successful grapevine grafts, we employed the rootstock Richter 110 (110R) that was reported to have different graft success rates when combined with clones of Touriga Nacional, one of the most important Portuguese cultivar [5,19], and of cv. Syrah [23]. In particular, Syrah clone 383, one of the most susceptible to the reported vine decline, is no longer available for the market [24]. To further address the parameters regarded as indicative for scion–rootstock incompatibility, we re-evaluated reported methods and monitored several physiological indicators at the early callusing stage, 3 weeks after grafting (21 days after grafting – DAG), and at the hardening stage, 5 months after grafting (152 DAG), of cv. Syrah and cv. Touriga Nacional grafted onto 110R rootstock, known to have a different degree of compatibility with these plants [5,18,19,23]. We compared also reported Affinity Coefficient calculations based on stem growth measurements as a measure for graft compatibility. Furthermore, we analyzed the internal anatomy of the graft union and the leaf chlorophyll and carotenoid content and chlorophyll fluorescence parameters serving as plant stress indicators.

2. Material and methods

2.1. Plant Material and Experimental Details

Cuttings of certified virus-free plants of four registered *V. vinifera* clones cv. “Syrah”, clone 383 and 470 (SY383 and SY470, ENTAV-INRA/FR clones) and cv. “Touriga National”, clone 21 and 112 (TN21 and TN112,

ISA/PT and JBP/PT clones, respectively) and cuttings of the rootstock 110R (*V. berlandieri* X *V. rupestris,* JBP/PT clone) were used. Graft combinations were selected according to the incompatibility reported for SY383 grafted on 110R (SY383/110R) [18,23] and for TN112/110R [5,19]. One hundred grafts per combination were performed, as well as one hundred homografts (grafts of each genotype with themselves). All grafts were performed on 27 April 2018 by bench omega-grafting of dormant cuttings under commercial nursery conditions at the Plansel nursery located in Montemor-o-Novo, Portugal (291 m above sea level, 38°39′ N, and 8°13′ W). The nursery provided all plant material except SY383 cuttings which were collected from the Portuguese National Ampelographic Collection (PRT 051), INIA Dois Portos, INRB I.P. (Quinta da Almoinha). All procedures concerning the handling of plant material were carried out by the nursery under phytosanitary guidelines used for their commercial clients. Grafts were dipped in paraffin (containing 0.11% of Quinidol and 0.004% of 2,5-Dichlorobenzoic acid) and underwent 21 days of stratification (at 30 °C and 80%–90% relative humidity) to induce callusing at the graft interface. On 18 May 2018, the grafted plants were transferred to the field nursery in a randomized complete block design (RCBD) with 4 blocks (25 repetitions/block) for hardening under drip irrigation. The main climatic parameters for the field trial were monitored throughout the experiment (Figure S1) using daily meteorological data collected for Montemor-o-Novo at the Évora weather station, Portugal [25] (38°65′ N; 8°21 W; altitude: 247 m) for the period from 22 May to 1 October 2018.

2.2. Growth Parameters

Sprouting and rooting rates of the grafted plants were recorded at the end of the callusing stage—21 days after grafting (DAG) and at the

hardening stage—152 DAG. The sprouting rate at 152 DAG is named “graft take” as, at this time point, sprouted grafts are considered successful. The two time points were chosen because *callus* formation is a prerequisite for a successful graft [7] and because 5 months is considered sufficient time to assess levels of incompatibility in the field [26]. Six biological repetitions per graft combination were randomly selected from each of the 4 blocks (n = 24) and the following growth parameters measured at 21 DAG: (i) Length of the main shoot (cm), (ii) root number, (iii) length of the major root (cm), (iv) stem diameters at the base of the sprouted shoot, at the graft union and 5 cm below the union (mm) and (v) score of callusing on a scale from 0 to 4 based on visual evaluation, where 0 = no *callus*, 1 = 25%, 2 = 50%, 3 = 75%, and 4 = 100% of *callus* formed around the graft union. At 152 DAG, the following data were collected on the survived grafts that were monitored at 21 DAG: (i) Length of the main shoot (cm), (ii) stem diameters 5 cm above and below the union (mm) and at the graft union. The stem diameters were measured with a digital compass (DigiMax, Swiss Precision, CA, USA).

2.3. Internal Characterization of the Union

At 152 DAG, the graft union of the same plants sampled for the growth parameters monitored, were longitudinally sectioned at the graft area. Anatomy on the surface of the union was recorded and evaluated for vascular continuity on both the right and the left part of the pith, adapting the method of Herrero [27]. According to this method, 5 categories (from A to E) were used for evaluation, where category A represents a perfect union in which the graft line is almost invisible. Category B shows few structural imperfections and/or slight discontinuities between wood and bark or cambial invaginations. Category C is characterized by bark discontinuities and D by wood discontinuities. Category E includes

broken/unattached unions and/or unions with dead tissue in the proximity of the union line. Graft unions were scored as follows: unions showing at least one side scored as A or B categories (A/−, B/−) were considered compatible. C/C, C/D, C/E scored unions were considered intermediate while D/D, D/E, E/E unions were considered incompatible.

2.4. Affinity Coefficients (ACs)

The measured stem diameters at 152 DAG were used as data input on the four affinity coefficients (ACs) formulas developed by Branas, Perraudine, Spiegel-Roy and Lavee, and Onaran, which were already reviewed and applied in *Vitis* [14]. Below, the ACs formulae used in this work are listed:

Perraudine: good affinity when AC ≅ 12. If > 12, the rootstock is thicker.

$$AC = [C/A + (C + A)/2B] + 10AC \quad (1)$$

Branas: good affinity when AC ≅ 10. If > 10, the rootstock is thicker.

$$AC = [C/A \times (C + A)/2B] \times 10 \quad (2)$$

Spiegel-Roy and Lavee: good affinity when AC ≅ 0.

$$AC = (C/A) - 1 \quad (3)$$

Onaran: good affinity when AC ≅ 100.

$$AC = (C \times 100)/A = \% \quad (4)$$

where, A is scion diameter (mm), B is graft union diameter (mm), C is rootstock diameter (mm).

2.5. Chlorophyll Fluorescence and Pigments Content

Chlorophyll fluorescence parameters were measured at 152 DAG using the OS-30p+ Chlorophyll Fluorometer (Opti-Sciences, Hudson, NH, USA). After 20 min of dark adaptation, the first expanded leaf in 6 grafts/combination/block was measured according to the OJIP protocol

described in the fluorometer's manual. We ensured that a total of 6 measurements were recorded when fewer than 6 grafts had survived in a given block. Leaf samples for pigment quantification were the same as those used for chlorophyll fluorescence measurements. In total, 1.27 cm^2 of leaf area was excised from the sampled leaf, submerged in 2 mL of 95% ethanol and stored at 4 °C for two weeks. Then, chlorophyll and carotenoids contents were determined using Ultraspec 4000 UV/Visible Spectrophotometer (Pharmacia Biotech, Piscataway, NJ, USA) according to the method of Lichtenthaler [28]. Pigments absorbances were measured between 0.3 and 0.85 [29]. In the case of absorbance values > 0.85, a dilution of the samples was made, and the dilution factor was considered in the quantification.

2.6. Statistical Analysis

Statistical analysis of the collected data for all graft combinations at each time point, except for the results from the internal characterization of the union, was performed in RStudio (RStudio Team, 2015. RStudio: Integrated Development for R. RStudio, Inc., Boston, MA, USA, http://www.rstudio.com/) by Kruskal–Wallis test and multiple comparisons of treatments, in the R-package "agricolae", which uses the criterium Fisher's least significant difference as a post hoc test [30]. For sprouting, graft take, and rooting rates a Fisher's exact test was performed for all graft combinations at each time point. Pearson correlations were carried out between graft take rates and the parameters analyzed at 21 and 152 DAG. To compute the significant levels for Pearson correlation the "rcorr" function in the R-package "Hmisc" was used [31]. For visualization, the R package "corrplot" was used [32]. Data are shown as mean values of original data ± SE (standard error). Significant differences are reported at * $p < 0.05$, ** $p < 0.01$, *** $p < 0.001$.

3. Results

3.1. Grafting onto 110R Rootstock Leads to Higher Graft Take Rates

Several external symptoms have been associated with incompatible graft unions, including a high rate of graft take failures, leaves yellowing, early defoliation, a decline in the vegetative growth, marked differences in vigor and the seasonal biological clock, overgrowth of one of the partners or at the graft zone and the break of the union [7]. Our results showed that at 21 DAG a few homografts sprouted compared with their respective heterografts, suggesting that grafting onto 110R supports and induces early sprouting of the scion genotypes (Figure 1a), which is consistent with other studies [33,34].

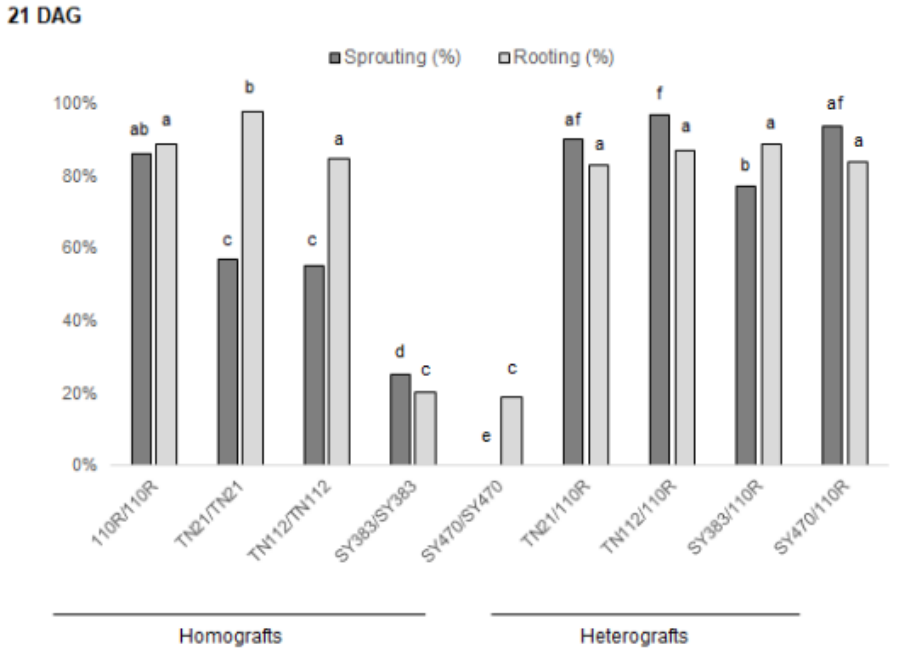

(a)

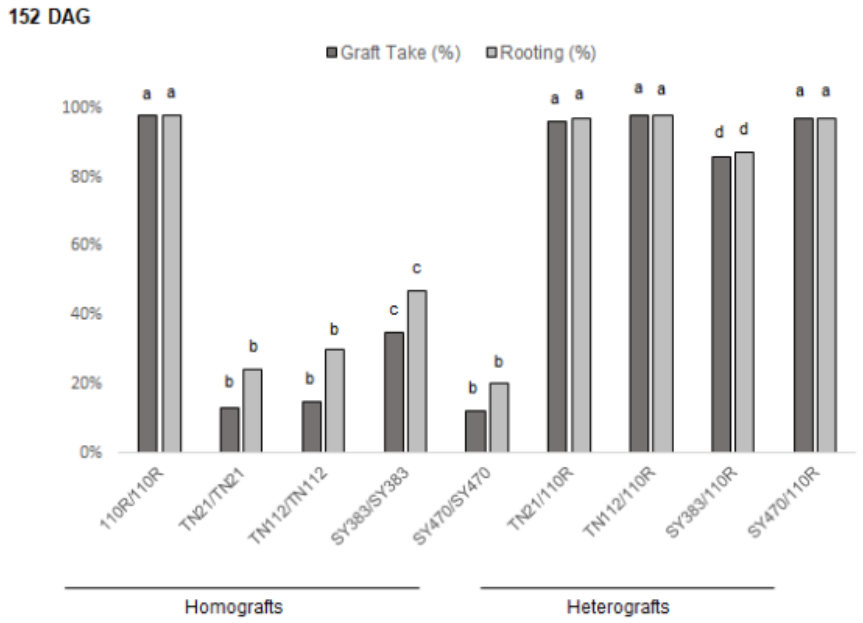

(b)

Figure 1. Percentage of graft take, sprouting, and rooting at 21 and 125 DAG in all graft combinations. (**a**) Sprouting and rooting percentages at 21 DAG; (**b**) graft take and rooting percentages at 152 DAG in the same population analyzed at 21 DAG. Different letters indicate significant differences between all graft combinations with $p < 0.05$ (n = 94–100 per graft combination) according to Fisher's exact test.

Indeed, at 21 DAG, more than 80% of 110R homografts, approx. 50% of the Touriga Nacional homografts, and less than 25% of Syrah homografts sprouted, suggesting that 110R is an early sprouting genotype followed by Touriga Nacional and Syrah. Nevertheless, when Touriga Nacional and Syrah clones were grafted onto 110R, more than 90% of these heterografts sprouted at this time, while the sprouting rate of SY383/110R was just 77% (Figure 1a). At 152 DAG, graft take rates showed a marked difference between homo- and heterografts, which seems to depend on the 110R rootstock genotype rather than to the type

of graft (homo- or heterograft). In line, the success of graft takes in *V. vinifera* homografts ranged from 13% (TN21/TN21) to 35% (SY383/SY383), whereas in heterografts, it ranged from 85% (SY383/110R) to 98% (TN112/110R). Among heterografts, just SY383/110R displayed a significantly lower graft take, while this was not observed for TN112/110R. Interestingly, the rootstock homograft (110R/110R) displayed a graft take success with 98 %, which is in the same order as detected with most heterografts (except SY383/110R) (Figure 1b). This led us to hypothesize that the low graft take of the *V. vinifera* homografts could be due to a lower rooting capacity of these genotypes in comparison with 110R, an American hybrid specifically selected to be used as rootstock [35]. Indeed, this hypothesis was supported by the Pearson correlation calculation between rooting and graft take at 152 DAG, indicating a correlation value of 0.89 ($p < 0.05$).
Concerning *callus* formation degree in the studied graft combinations, we detected a significantly higher *callus* formation in all heterografts (average grade of 4) when compared with the homografts (average grade of 3) (Table 1). *Callus* proliferation was expected not only because of the natural wound response but also because of the effect of 2,5-dichlorobenzoic acid added to the paraffin.

Table 1. Average of *callus* grade, root number, root length, and shoot length detected at 21 and 152 DAG.

	21 DAG				152 DAG
	***Callus* Grade (0–4)**	**Roots Number**	**Root Length (cm)**	**Shoot Length (cm)**	**Shoot Length (cm)**
Graft Combination	***	***	***	***	***
110R/110R	3.9 ± 0.1 abc	4.1 ± 0.6 a	1.6 ± 0.3 a	4.3 ± 0.6 a	78 ± 6.2 cd
TN21/TN21	3.0 ± 0.3 d	5.3 ± 0.9 a	1.6 ± 0.2 a	1.9 ± 0.5 bcd	95 ± 7.4 bc
TN112/TN112	1.5 ± 0.2 e	5.7 ± 1.2 a	1.1 ± 0.2 a	0.9 ± 0.3 cde	127 ± 8.2 ab
SY383/SY383	3.4 ± 0.2 bcd	0.5 ± 0.2 b	0.2 ± 0.1 b	0.4 ± 0.1 de	78 ± 3.8 cd
SY470/SY470	3.3 ± 0.3 cd	0.8 ± 0.3 b	0.3 ± 0.2 b	0.0 ± 0.0 e	139 ± 9.0 a
TN21/110R	4.0 ± 0.0 a	3.0 ± 0.5 a	1.3 ± 0.3 a	2.9 ± 0.4 ab	80 ± 7.7 cd
TN112/110R	4.0 ± 0.0 ab	4.1 ± 0.8 a	1.8 ± 0.4 a	3.5 ± 0.4 a	63 ± 4.1 d
SY383/110R	3.9 ± 0.1 abc	3.8 ± 0.7 a	1.9 ± 0.3 a	2.1 ± 0.4 abc	66 ± 3.9 d
SY470/110R	4.0 ± 0.0 a	3.9 ± 0.6 a	1.8 ± 0.3 a	4.3 ± 0.5 a	78 ± 4.6 cd
Graft Type	***	ns	ns	***	***
Homograft	3.0 ± 0.1 a	3.3 ± 0.4	1.0 ± 0.1	1.5 ± 0.2 a	97 ± 3.9 a
Heterograft	4.0 ± 0.0 b	3.7 ± 0.3	1.7 ± 0.1	3.2 ± 0.2 b	72 ± 2.7 b

± SE standard error; 21 DAG n = 24; 152 DAG n = 11–24. Significant differences according to Kruskal–Wallis test are indicated by asterisks symbols *** $p < 0.001$; "ns" indicates non-significant differences.

It is commonly thought that grapevine grafts will develop their final root system only when plotted in a field. However, the development of adventitious roots can be observed already at 21 DAG and might be indicative of the rooting capacity of the genotypes under study. Indeed, while the individual graft combination had a strong effect, the type of graft (homo- or heterograft) did not produce a statistically significant difference in root development at 21 DAG. The only significantly lower rooting performance was detected with Syrah homografts compared to all other combinations. Here the mean values were below 1 for SY383/SY383 and SY470/SY470 combinations with 0.5 ± 0.2 and 0.8 ± 0.3, respectively (Table 1). Nevertheless, no differences were detected comparing Syrah scions heterografts with other heterografts suggesting that the scion does not influence the rooting ability of the rootstock indicating that this is an autonomous trait of the rootstock.

The length of the main scion shoot depended on the graft type at both 21 and 152 DAG and suggests an influence of the used rootstock on scion's growth. At 21 DAG, homografts displayed a significantly lower shoot length than heterografts (i.e., 1.5 vs. 3.2 cm) (Table 1). This difference is in accordance with the observed delayed sprouting of homografts. Interestingly, the situation inverted at 152 DAG, with the homografts displaying a significantly higher shoot length than heterografts (i.e., 97 vs. 72 cm) (Table 1). This suggests that the expansion growth rate of homografts was higher than that of heterografts, which is consistent with reports from other studies [36].

With respect to the stem diameters evaluated, a significant difference was detected between all different graft combinations above, below, and at the graft union at both time points (Table 2).

Table 2. Mean values of the Stem Diameters (SD) detected at 21 and 152 DAG.

	21 DAG			152 DAG		
	SD Above	**SD Graft Union**	**SD Below**	**SD Above**	**SD Graft Union**	**SD Below**
Graft Combination	***	***	**	***	***	***
110R/110R	3.21 ± 0.18 ab	14.26 ± 0.35 a	9.47 ± 0.29 ab	5.08 ± 0.37 c	18.18 ± 0.88 ab	10.86 ± 0.44 bc
TN21/TN21	1.55 ± 0.32 cd	10.94 ± 0.38 cd	8.82 ± 0.17 ab	6.88 ± 0.48 abc	15.67 ± 0.68 bc	11.01 ± 0.46 abc
TN112/TN112	1.46 ± 0.41 bcd	9.38 ± 0.29 d	8.42 ± 0.15 b	6.77 ± 0.40 bc	13.88 ± 1.04 c	11.45 ± 0.47 abc
SY383/SY383	1.46 ± 0.46 bcd	12.01 ± 0.49 bc	9.70 ± 0.29 a	7.59 ± 0.40 ab	17.80 ± 0.51 ab	12.90 ± 0.44 ab
SY470/SY470	0.00 ± 0.00 d	11.20 ± 0.44 cd	11.20 ± 0.44 ab	10.61 ± 0.90 a	18.98 ± 0.79 ab	14.0 ± 0.72 a
TN21/110R	3.55 ± 0.27 a	13.9 ± 0.27 a	13.90 ± 0.27 a	5.33 ± 0.33 c	17.99 ± 0.62 ab	10.24 ± 0.37 c
TN112/110R	4.25 ± 0.30 a	13.85 ± 0.34 a	13.85 ± 0.34 ab	5.39 ± 0.33 c	17.58 ± 0.63 abc	10.14 ± 0.46 c
SY383/110R	3.26 ± 0.48 a	13.31 ± 0.29 ab	13.31 ± 0.29 a	5.91 ± 0.35 c	18.05 ± 0.68 ab	10.30 ± 0.30 c
SY470/110R	2.85 ± 0.28 abc	14.09 ± 0.29 a	14.09 ± 0.29 ab	6.20 ± 0.28 bc	19.28 ± 0.52 a	10.17 ± 0.39 c
Graft Type	***	***	**	***	*	***
Homograft	1.54 ± 0.17 a	11.56 ± 0.23 a	9.05 ± 0.11 a	7.18 ± 0.28 a	16.99 ± 0.4 a	12.04 ± 0.25 a
Heterograft	3.47 ± 0.18 b	13.79 ± 0.15 b	9.56 ± 0.14 b	5.7 ± 0.16 b	18.23 ± 0.31 b	10.21 ± 0.19 b

± SE standard error; SD above, below, and at the graft union measured at 21 (n = 24) and 152 DAG (n = 11–24) for all graft combinations and graft type. Significant differences according to Kruskal–Wallis test are indicated by asterisks * $p < 0.05$, ** $p < 0.01$, *** $p < 0.001$.

At 21 DAG, all heterografts showed larger stem diameters than homografts in all sections measured (i.e., 3.5 vs. 1.5 mm above the union; 13.8 vs. 11.6 mm at the graft union; and 9.6 vs. 9.1 mm below the union) (Table 2). Interestingly, the situation was different at 152 DAG, since homografts displayed larger stem diameters than heterografts above the union (7.2 vs. 5.7 mm) and below (12 vs. 10.2 mm). Notably, all heterografts showed significantly increased stem diameters (18.2 mm) compared with homografts (17 mm) at the graft union. Over time, the stem diameter growth of the homografts was 2.5 times greater than in heterografts above the graft union (i.e., 5.9 mm increase in homografts vs. 2.2 mm increase in heterografts) (Figure S2). Below the union, the increase was four times greater in the homografts compared to the heterografts (3 mm vs. 0.7 mm, respectively). However, heterografts showed a similar stem diameter growth to that of homografts at the graft interface (4.4 mm vs. 5.3 mm, respectively) (Figure S2).

3.2. Graft Unions Are Frequently Incomplete at Five Months after Grafting

Anatomic studies are frequently performed to assess graft success in cherry [37], peach [38], apricot [36], pear, and quince [39]. In grapevine, grafting anatomy has also been investigated, mainly by non-destructive methods such as X-ray tomography and MRI [16,17]. Nevertheless, the five graft categories (A, B, C, D, and E) established by Herrero (1951), with “A” showing a perfect union and “E” showing unattached unions and/or unions with death tissue [27] have not been applied to *Vitis* so far (Figure 2a).

Using this approach, just SY470 homografts scored as compatible for all replicates. TN21/TN21 and SY470/110R graft unions scored as compatible and intermediate, while the unions of all the other graft combinations displayed all three classes from compatible unions to

intermediate compatible and incompatible unions (Figure 2b). Thus, using this categorization, the most compatible combinations were SY470 and TN21 homografts, and TN112/110R heterografts, with 100%, 83%, and 83% of compatibility, respectively. On the other side, the graft combinations with a high degree of incompatibility were SY383 and 110R homografts (33% and 21% respectively), and TN21/110R and SY383/110R heterografts both with 17% of incompatible unions. Given that homografting should result in the highest graft compatibility value as the growth rate and vasculature pattern should be equal between rootstock and scion, it is surprising that there is enormous variability within the combinations, regardless of whether they are homo- or heterografts. Additionally, bark (category C) and wood (category D) discontinuities in the graft zone were frequently observed. These findings suggested that grafted grapevines might require long times to complete the healing of a union.

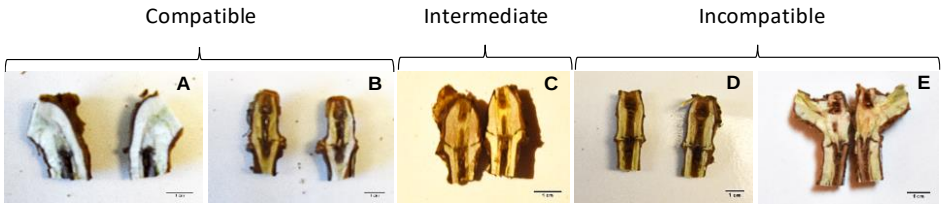

(a)

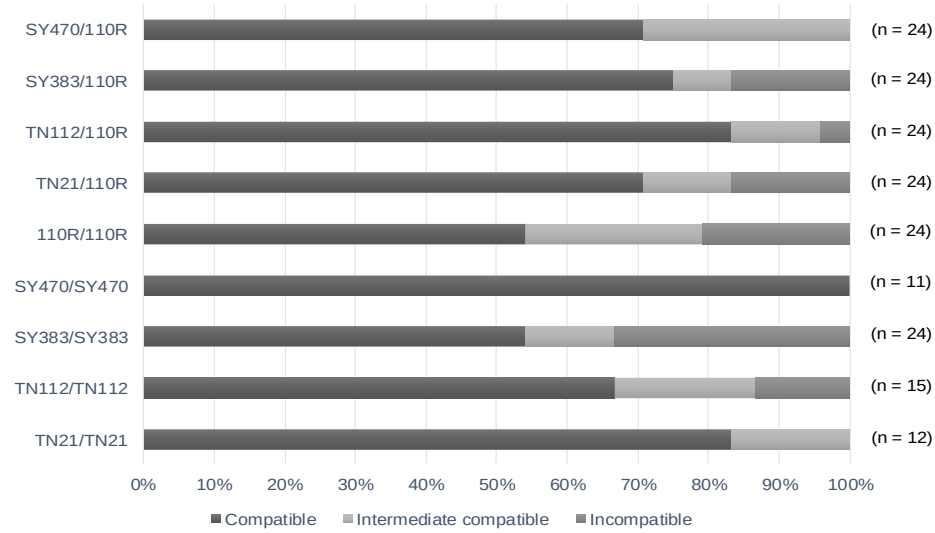

(b)

Figure 2. Internal characterization of the graft union. (**a**) Example images of the category A to E charactering the internal graft unions. Category A represents a perfect union in which the graft line is almost invisible. Category B shows few structural imperfections and/or slight discontinuities between wood and bark or cambial invaginations. Category C is characterized by bark discontinuities and D by wood discontinuities. Category E includes broken/unattached unions and/or unions with dead tissue in proximity of the union line. (**b**) Proportion (%) of compatible, intermediate, and incompatible classes detected per graft combination

3.3. Affinity Coefficients (ACs) Calculated for the Same Graft Combination Vary According to the Formula Used

Looking for the early determinants of long-term graft success of different graft combinations, several AC formulas based solely on stem diameter measurements of scion and rootstock have been proposed and applied in vineyards [14,16] and orchards [40], since growth differences above and below the graft union are regarded as a sign of incompatibility [14].

ACs calculated using the Parraudine formula indicated good compatibility for all analyzed combinations, since all calculated values were close to 12 (Table S1). ACs calculated using Branas' formula identified 110R and SY383 homografts as the more compatible combinations, while TN112/TN112 and SY470/110R were the combinations with the worse calculated affinity since their coefficients were far from the ideal value (10). Using Branas' coefficient, significant differences were found among graft combinations and also between graft type, suggesting homografts as more compatible than heterografts (Table S1). No statistical significant difference was detected between homo- and heterografts when the formula of Parraudine, Spiegel-Roy and Lavee, and of Onaran were used, although differences were detected among graft combinations (Table S1). In summary, the ACs calculated for the same graft combination vary according to the formula used, and they are not reliable indicators of graft (in)compatibility for the used graft combinations.

3.4. Chlorophylls Analysis Is a More Sensitive Indicator of Stress than the Analysis of Chlorophyll Fluorescence

In this study, chlorophyll fluorescence parameters, fast chlorophyll fluorescence induction curve (OJIP curve), and the quantification of leaf pigments were tested to screen the graft combinations for their compatibility behavior. The main chlorophyll fluorescence parameters investigated were: Vj (variable fluorescence at the J step), PI (Performance Index), Fv/Fm and Fv/Fo (maximum quantum yield of photosystem II – PSII). Nevertheless, no significant differences were detected for any of the parameters, with the exception of Fv/Fo, for which a significant difference ($p < 0.01$) was found for SY470 homografts compared with 110R and SY383 homografts (data not shown). This combination stood out by having the lowest values of the maximum quantum efficiency of PSII (Fv/Fm = 0.72) and, in particular, a significantly

lower Fv/Fo (2.74). Fv/Fo is considered a more sensitive parameter for plant stress, capable of amplifying small variations detected by Fv/Fm, since it is normalized over the minimal fluorescence (Fo) [41]. The optimal Fv/Fm value for stress-free plants is around 0.83 [42]. In our study, Fv/Fm values for all graft combinations varied from 0.72 to 0.77, suggesting that all graft combinations were subjected to stress at the moment of the measurements. It has been shown that some types of plant stress affect specific parts of the OJIP curve. For example, severe nitrogen stress displays a K strep at 300 μs [43]. To investigate whether grafting and/or incompatibility could have a similar effect, OJIP curves for all graft combinations were plotted. Nevertheless, the transients were almost overlapping, denoting that homografts' OJIP curve does not differ from heterografts' and no unusual step was observed on the OJIP traces (Figure S3) suggesting that, in our study, OJIP curves of grafted grapevines are not affected by the graft combination.

Methods to quantify chlorophylls in plants are used to estimate the effect of different stress factors on the efficiency of photosynthesis [44]. Furthermore, it was proposed that measurements of chlorophyll concentrations in scion leaves allow the identification of graft incompatibility in *Prunus* species [38]. To evaluate this on *Vitis* grafts, we measured chlorophyll a (Chl(a)), b (Chl(b)), total (Chl(a+b)), and carotenoids (Carot) concentrations in leaves formed on scions of the different graft combinations. The ratios Chl(a)/Chl(b) and Chl(a+b)/Carot were also calculated. In TN21, TN112, SY470 homografts and in SY470/110R heterografted plants, the detected Chl(a) concentrations were lower than in the other graft combinations. The same homografts also displayed a lower amount of Chl(b) and overall, homografts are significantly less enriched in Chl(b) than heterografts (Table 3).

Table 3. Mean values of chlorophyll and carotenoid content per graft combination and graft type.

	Chl(a) (mg/cm^2)	Chl(b) (mg/cm^2)	Carot (mg/cm^2)	Chl(a)/Chl(b)	Chl(a+b)/Carot
Graft Combination	**	***	ns	***	***
110R/110R	0.023 ± 0.001 a	0.01 ± 0.001 ab	0.004 ± 0.000	2.6 ± 0.1 a	9.5 ± 0.9 ab
TN21/TN21	0.019 ± 0.001 ab	0.007 ± 0.001 bc	0.005 ± 0.000	2.7 ± 0.1 ab	5.4 ± 0.2 cd
TN112/TN112	0.019 ± 0.001 ab	0.008 ± 0.001 bc	0.004 ± 0.000	2.6 ± 0.1 ab	6.3 ± 0.5 bcd
SY383/SY383	0.022 ± 0.001 a	0.011 ± 0.001 ab	0.004 ± 0.000	2.4 ± 0.1 a	10.2 ± 3.0 abc
SY470/SY470	0.016 ± 0.001 b	0.005 ± 0.000 c	0.004 ± 0.000	2.9 ± 0.1 b	5.1 ± 0.1 d
TN21/110R	0.022 ± 0.001 a	0.011 ± 0.001 ab	0.004 ± 0.000	2.1 ± 0.1 a	8.2 ± 1 abc
TN112/110R	0.022 ± 0.001 a	0.014 ± 0.001 a	0.004 ± 0.000	1.7 ± 0.1 a	14.7 ± 4.0 a
SY383/110R	0.022 ± 0.001 a	0.011 ± 0.001 ab	0.005 ± 0.000	2.1 ± 0.1 a	7.0 ± 0.7 bcd
SY470/110R	0.020 ± 0.001 ab	0.009 ± 0.001 ab	0.004 ± 0.000	2.3 ± 0.1 ab	7.4 ± 0.6 abcd
Graft Type	ns	***	ns	***	ns
Homograft	0.020 ± 0.001	0.009 ± 0.000 a	0.004 ± 0.000	2.6 ± 0.1 a	8.0 ± 0.9
Heterograft	0.021 ± 0.001	0.011 ± 0.000 b	0.004 ± 0.000	2.1 ± 0.1 b	9.3 ± 1.1

± SE: standard error; significant differences according to Kruskal–Wallis test are indicated by asterisks ** $p < 0.01$ and *** $p < 0.001$; “ns” indicates non-significant differences (n = 24). Abbreviations: Chl(a) = chlorophyll a; Chl(b) = chlorophyll b; Carot = carotenoids.

With exception of SY383 genotypes showing no changes in chlorophyll content regardless of the rootstock, it seems that grafting onto 110R leads to higher amounts of Chl(a) and Chl(b) in the scion when compared with the respective homografts (Table 3). Although this effect is only significant for Chl(b), this implies increased root uptake and/or translocation of nitrogen or other micronutrients across the graft junction in plants grafted onto 110R rootstock. The decreased contents in both Chl(a) and Chl(b) in the SY470 homografts (Table 3) could also explain the detected reduced quantum yield of PSII in these plants. Indeed, a reduction in the quantum yield of PSII is generally associated with the stress-induced degradation of chlorophylls, which has been partially attributed to the sensitivity of the membranes to oxidative stress [41].

Carotenoids, necessary for photoprotection in photosynthesis, play an important role as precursors of signaling during plant development under abiotic/biotic stress [45]. However, no differences were detected in carotenoids contents with respect to the graft combinations (Table 3). Therefore, the statistical differences found among graft combinations for the Chl(a+b)/Carot ratio are more likely related to the differences in chlorophyll content. The analysis of pigment contents in leaves seems a more sensitive indicator of stress than the analysis of chlorophyll fluorescence, even if just Chl(b) contents were differentiating homo- from heterografts.

3.5. Graft Take Correlates with Callus Formation and with the Improvement of Scion–Rootstock Translocation

We next performed a statistical correlation analysis with respect to the graft take rates on the parameters recorded at 21 DAG and 152 DAG. Figure 3a shows that root and shoot length, the measurements of stem diameters, and the degree of *callus* development were all positively correlated with graft take at 21 DAG. However, root length and the stem

diameter below the union displayed low correlation coefficients ($r \leq 0.3$), while the highest correlations were obtained for stem diameter at the graft zone and above the union, the degree of *callus* development and shoot length ($r = 0.65$, 0.57, 0.54, and 0.52, respectively). Considering that the measurements of stem diameters above the unions were done only on sprouted scions at 21 DAG and that stem diameters at the graft zone increased with the degree of callusing, we conclude that overall graft take correlated best with scion growth and with the proliferation of *callus* tissue around the union.

Given that many grafts fail before scion sprouting, it is clear why shoot growth positively correlated with graft take at 21 DAG. Nevertheless, shoot length negatively correlated ($r = -0.51$) with graft take at 152 DAG (Figure 3b), with the stem diameters above and below the union ($r = -0.49$ and $r = -0.45$ respectively), and with the Chl(a)/Chl(b) ratio ($r = -0.36$). Positive correlations with graft take at 152 DAG were found for the stem diameters at the graft zone and Chl(a) and Chl(b) contents, although only the Chl(b) content disclosed a correlation coefficient higher than 0.3 (Figure 3b). Interestingly, correlation coefficients with graft take rates measured at 152 DAG seem higher at 21 DAG than at 152 DAG, suggesting that early predictions do not necessarily imply low confidence of the prediction.

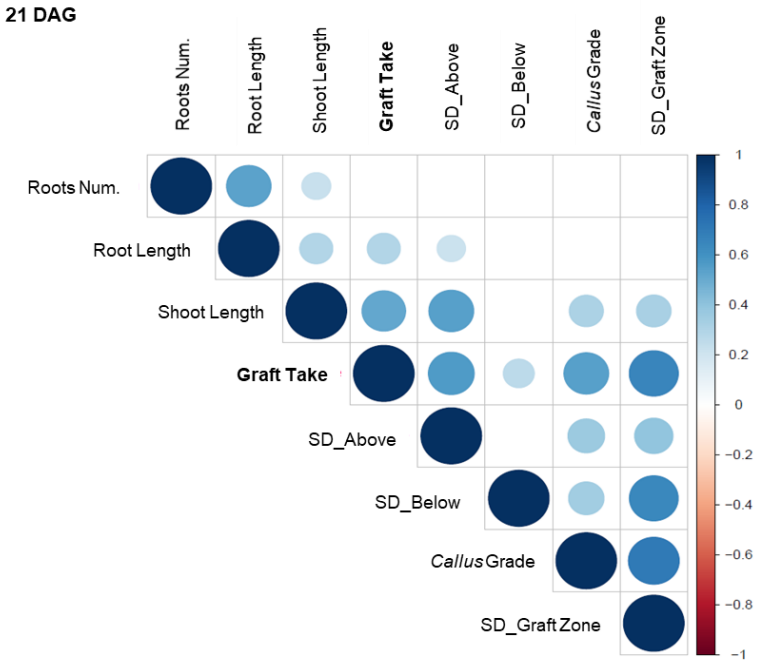
21 DAG
Roots Num.
Root Length
Shoot Length
Graft Take
SD_Above
SD_Below
Callus Grade
SD_Graft Zone
1
0.8
0.6
0.4
0.2
0
−0.2
−0.4
−0.6
−0.8
−1

(a)

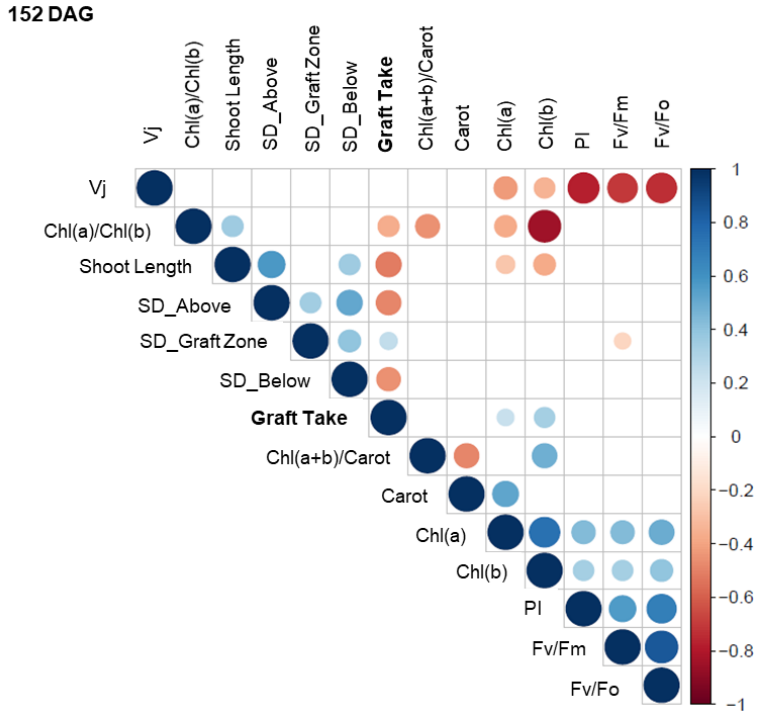
152 DAG
Vj
Chl(a)/Chl(b)
Shoot Length
SD_Above
SD_Graft Zone
SD_Below
Graft Take
Chl(a+b)/Carot
Carot
Chl(a)
Chl(b)
PI
Fv/Fm
Fv/Fo
1
0.8
0.6
0.4
0.2
0
−0.2
−0.4
−0.6
−0.8
−1

(b)

Figure 3. Pearson correlation of the graft take value versus all the parameters investigated at 21 and 152 DAG. (**a**) at 21 DAG: roots number, length of the major root, shoot length, stem diameters (SD) above, below and at the graft zone and *callus* score. (**b**) Pearson correlation of the graft take values versus the parameters investigated at 152 DAG: shoot length, stem diameter (SD) above, below and at the graft zone, Chlorophyll a (Chl(a)), Chlorophyll b (Chl(b)), carotenoids (Carot), ratio Chl(a) and Chl(b), ratio total chlorophylls and Carot, and the following chlorophyll fluorescence values: Vj, PI, Fv/Fm, Fv/Fo. Positive correlations are displayed in blue and negative correlations in red colors. The size of the circles and color intensities are proportional to the correlation coefficients. Correlations with *p* value > 0.01 are considered insignificant and are left blank.

4. Discussion

Much effort has been dedicated to the search of physiological [11,17], metabolic [18,19,46], and molecular [5,21,22] markers to predict in an early growth stage graft compatibility in grapevine with the aim of improving rootstock selection and propagation. To reveal grafting-related physiological symptoms that might enable nurseries to predict whether a graft combination is likely to succeed, we applied several methods at two time points (21 DAG and 152 DAG) to score graft compatibility of graft combinations known to show distinct compatibility behavior [5,18,19,23]. Surprisingly, at 5 months after grafting (152 DAG), graft take rates did not match our expectations since *V. vinifera* homografts had lower graft take rates than heterografts. Notably, the rootstock homograft (110R/110R) performed as well as heterografts that have the 110R rootstock. We noticed a correlation of the 110R rooting ability with graft success, which might explain the low take rates detected with the *V. vinifera* homografts (<40%). Here, it should be noted that all grafted plants were cultivated at

the same field lot over the same growth period. Thus, we can exclude exogenous factors such as soil quality or local stresses. In addition, it can be excluded that insufficient water supply could have impacted the root formation as all grafted plants were grown under drip irrigation. Considering that exogenous factors were similar to all grafted plants and that we found a significant correlation between used rootstock and the rooting capacity of heterografts, we encourage the use of homografts as compatibility controls in viticulture just for studying qualitative attributes and not to quantify graft success.

It is widely known that rootstocks are selected for rooting and grafting capacity, abiotic and biotic stress tolerance, and their ability to impact the phenotype of the grafting scion [47]. In this work, 110R rootstock anticipates the sprouting of the heterografted scion and exerts control over scion growth. It is conceivable that the early dormancy break of the rootstock (110R) is responsible for the increased heterograft scion bud burst response. In our study, cuttings with only one bud were grafted onto the rootstock, implying dependence of bud break on rootstock reserves. Thus, it seems that the sooner the rootstock will break dormancy, activating carbon supply for the scion, the sooner they may sprout. The analysis of the internal anatomy of the graft union led us to realize that graft healing is not yet complete at five months after grafting. Milien et al. (2012) [17] compared the anatomy of “good“ and “bad” grafts eight months after grafting and observed that the omega-cut line was visible in both graft types and that, on “bad” grafts, connectivity was incomplete and necrotic tissue was present at the graft junction. The inspection of grapevine graft unions through MRI also revealed areas in the graft zone with no vascular connection even in 2 years-old grafts [16]. Our results are in agreement with other studies on woody species, in which graft incompatibility may not become apparent for several years [3]. Thus, graft (in-)compatibility

studies in grapevines should include later time points than five months after grafting.

Concerning the methods applied to predict graft compatibility, several AC formulas based solely on stem diameter measurements of scion and rootstock have been proposed and applied in vineyards [14,16] and orchards [40], since growth differences above and below the graft union are regarded as a sign of incompatibility [14]. Nevertheless, in this work, the ACs were not suitable predictors to assess graft incompatibility levels of the used graft combinations as they resulted in contradicting conclusions.

An alternative approach is the use of methods to quantify chlorophylls in plants as an indicator of the effect of different stress factors on the efficiency of photosynthesis [44]. Grafting causes stress to the grafting partners, since the mechanical wound results in localized cell death, loss of water, solutes, and disruption of the vascular system [3]. Repair of graft junctions, *callus* formation, and lack of vascular continuity imply a high metabolic demand that has to be sustained by the photosynthetic activity of the scion [3]. Light energy absorbed by chlorophyll drives photosynthesis (photochemistry) but is also re-emitted (fluorescence) and dissipated by heat. Since these processes compete with each other, the yield of chlorophyll fluorescence gives information on the quantum efficiency of photochemistry [48]. For this reason, chlorophyll fluorescence imaging and the determination of leaf chlorophyll concentrations using the Soil Plant Analysis Development (SPAD) can be early diagnosis tools of graft incompatibility [38,49]. Notably, we found chlorophyll concentration measurements a more sensitive parameter to identify changes between different graft combinations than the measurements of chlorophyll fluorescence.

Overall, homografts were found less enriched in leaf chlorophylls than heterografts, although just Chl(b) was significantly different. The fact that

both types of chlorophylls are reduced in the same graft combinations suggests that Chl(b) is not converted into Chl(a) in the context of the Chl(b)-to-Chl(a) pathway [50]. Rather, it might be indicative of a reduced root-to-shoot translocation of water and soil nutrients, particularly of nitrogen, since chlorophyll is one of the most important points of its accumulation [44]. Nevertheless, many mineral deficiencies are also known to produce specific pigment distribution within the same plant [51] and the selective mineral uptake of different rootstocks [8] might be equally implicated. Furthermore, a decrease in chlorophylls content is a common phenomenon under drought stress, and it is frequently associated to an increase in Chl(a)/Chl(b) ratio since the reduction of Chl(b) is greater than that of Chl(a) under drought stress [45]. Although, this is consistent with our results, since the graft combinations with the lowest values of chlorophylls (i.e., TN21, TN112, SY470 homografts and SY470/110R heterografts) also displayed the highest values of Chl(a)/Chl(b) ratio.

The growth parameters that best correlated with graft take rates were shoot length and the degree of callusing at 21 DAG, and a higher Chl(b) content and a lower swelling above and below the union at 152 DAG. As anticipated, this might imply that graft success correlates with the improvement of the scion–rootstock translocation via vasculature. However, it should be noted that positive correlations between graft take and scion growth at 21 DAG must be carefully evaluated, since grapevine scion sprouting relies on rootstock reserves. Excessive scion growth would deplete metabolite reserves before a functional root system can be established, which taken together would lead to a graft failure due to plant death.

The formation of a *callus* bridge between the grafted plant parts represents the beginning of the connectivity leading to the formation of a continuous vasculature between the grafting partners [3] and is suspected of predetermining the future compatibility or incompatibility response [52].

Additionally, *callus* formation is considered a prerequisite for the development of a successful graft junction [7]. Accordingly, the degree of *callus* formation was suggested as a valuable indicator of good graft take in grapevines [13,33]. Our results confirmed the reported positive correlations between the degree of callusing and the success of grafting in grapevines. Therefore, considering that grapevine grafts undergo callusing during a relatively short period (21 days), allowing only grafts with well-developed *callus* to proceed to the further hardening stage might be already of economic advantage at a nursery perspective.

Scion and rootstock stem diameters are frequently monitored in field studies to aid the assessment of compatibility levels as a measure of graft success [13,34,36]. Although the swellings often develop above unions with vascular discontinuities, it also can simply appear because of differences in relative scion and rootstocks' growth rates [53]. Therefore, stem swelling of one of the grafting partners is not a reliable indicator of graft incompatibility in other species according to Hartman et al. (2011) [7]. Nevertheless, in this study, stem diameter correlation coefficients with graft take at both time points are among the highest ones and stem swelling above and/or below the graft union was suggested to lead to decreased water and nutrient flow through the union causing wilting [54]. Furthermore, swelling of the scion has been associated with a blockage of carbohydrates at the graft zone and with phloem degeneration [54]. Recently, it was reported that narrow stem size in *Vitis* rootstocks imposes a morphological constraint on the scion via reduced annual vascular formation reflected by the annual ring size, which consequently leads to reduced hydraulic conductivity, limiting physiological performance and yield [55] and, consequently, to limited shoot growth. Whether this would explain the association between incompatibility and the increase in one of the partners' stem diameters still need to be investigated.

Comparison between homo- and heterografted plants with graft take success can be valuable to understand scion–rootstock interactions during graft formation. Our results pointed out a crucial role of the rootstock genotype in the vegetative growth and the Chl(b) content of the scion, although scions did not seem to influence the rooting ability of the rootstock. Heterografts exhibited a higher graft take rate, better *callus* development, and enrichment in Chl(b), which could be explained either by an increased root uptake rate or by a higher healing capacity of the graft union. Nevertheless, the internal anatomy of the union does not support the hypothesis that the healing of heterografts' unions plays a role. In addition, the fact that scion growth was reduced in heterografts does not fit to an increased root-to-shoot translocation in these plants. Moreover, the detected rootstock effect on scion bud burst suggests that scion–rootstock communication takes place as soon as *callus* is formed between the partners and that this communication is able to impose developmental decisions and growth habits on the scion. Overall, it seems that the quality, rather than the quantity, of the scion–rootstock translocation system, is responsible for the detected alterations in plant performance when a different rootstock genotype is used. Finally, the correlations analysis between all these traits may reduce the number of parameters and plants needed to be screened for graft compatibility, which might be of interest for breeders considering the high number of graft replicates needed to assess each combination between different rootstocks and new cultivars from different breeding programs.

5. Conclusions

Standardized methods to detect graft incompatible grapevine combinations at early stages would be very valuable to improve rootstock breeding and nurseries selection. Nevertheless, phenotyping incompatibility in woody species is a challenge, since compatibility

symptoms are often difficult to discriminate from the effect of environmental stresses and often unpredictably arise early or very late after grafting. By applying several methods described as indicative of incompatibility in several crops on grapevine grafts with known compatibility behavior, we found that graft take rates are not always indicative of compatibility and therefore they are not *per se* sufficient to assess compatibility levels in viticulture, where graft success is also dependent on the rooting ability of the rootstock. Moreover, the use of homograft compatibility controls should be carefully evaluated, as they did not show the highest graft take rates. Among the parameters investigated, the grade of *callus* development at 21 DAG as an indicator of graft success, might be most valuable for practical nursery's applications. We encourage the analysis of leaf chlorophyll contents rather than the use of chlorophyll fluorescence measurements. Conversely, we discourage the use of Affinity Coefficients based on stem diameters, although stem diameters were found to strongly correlate with graft success, which could be misleading as swelling is also associated with incompatibility of grafts. In summary, our measurements and assessment of predictive graft success parameters might be useful for both researchers and breeders for evaluating graft (in)compatibilities.

Acknowledgments

The authors thank Jose Valadas and João Carvalho from Plansel Nursery for the acquisition and management of the plants. José Eduardo Eiras Dias, Jorge Cunha and João Brazão from the National Institute for Agricultural and Veterinary Research (INIAV-Dois Portos) for the provision of SY383 cuttings. The authors also thank Fundação para a Ciência e Tecnologia (FCT) for the Ph.D. grant with the reference

PD/BD/128399/2017. The authors acknowledge the research unit GREEN-it “Bioresources for Sustainability” (UID/Multi/04551/2013).

References

1. Lee, J.; Kubota, C.; Tsao, S.J.; Bie, Z.; Echevarria, P.H.; Morra, L.; Oda, M. Scientia horticulturae current status of vegetable grafting : Diffusion, grafting techniques, automation. *Sci. Hortic. (Amst.)* **2010**, *127*, 93–105.
2. Ollat, N.; Bordenave, L.; Tandonnet, J.P.; Boursiquot, J.M.; Marguerit, E. Grapevine rootstocks: Origins and perspectives. *Acta Hortic.* **2016**, *1136*, 11–22.
3. Pina, A.; Cookson, S.; Calatayud, A.; Trinchera, A.; Errea, P. Chapter 5—Physiological and molecular mechanisms underlying graft compatibility. In *Vegetable Grafting Principles and Practices*; Colla, G., Perez-Alfocea, F., Schwarz D., Eds.; CABI Oxfordshire: Wallingford, UK, 2017; pp. 132–154, ISBN-13 978 1 78639 058 5.
4. Waite, H.; Whitelaw-Weckert, M.; Torley, P. Grapevine propagation: Principles and methods for the production of high-quality grapevine planting material. *N. Zeal. J. Crop. Hortic. Sci.* **2015**, *43*, 144–161.
5. Assunção, M.; Santos, C.; Brazão, J.; Eiras-Dias, J.E.; Fevereiro, P. Understanding the molecular mechanisms underlying graft success in grapevine. *BMC Plant Biol.* **2019**, *19*, 1–17.
6. Pina, A.; Errea, P. A review of new advances in mechanism of graft compatibility-incompatibility. *Sci. Hortic. (Amst.)* **2005**, *106*, 1–11.
7. Hartman, H.T.; Kester, D.E.; Davies, F.T.; Geneve, R.G. Principles of grafting and budding. In *Hartmann and Kester’s Plant Propagation: Principles and Practices*; Prentice Hall: Upper Saddle River, NJ, USA, 2011; pp. 415–463.
8. Bianchi, D.; Grossi, D.; Simone Di Lorenzo, G.; Zi Ying, Y.; Rustioni, L.; Brancadoro, L. Phenotyping of the “G series” *Vitis* hybrids: First screening of the mineral composition. *Sci. Hortic. (Amst.)* **2020**, *264*, 109155.
9. Bianchi, D.; Grossi, D.; Tincani, D.T.G.; Simone Di Lorenzo, G.; Brancadoro, L.; Rustioni, L. Multi-parameter characterization of water stress tolerance in *Vitis* hybrids for new rootstock selection. *Plant Physiol. Biochem.* **2018**, *132*, 333–340.
10. Migliaro, D.; De Lorenzis, G.; Di Lorenzo, G.S.; De Nardi, B.; Gardiman, M.; Failla, O.; Brancadoro, L.; Crespan, M. Grapevine non-vinifera genetic diversity assessed by simple sequence repeat markers as a starting point for new rootstock breeding programs. *Am. J. Enol. Vitic.* **2019**, *70*, 390–397.
11. Vršič, S.; Pulko, B.; Kocsis, L. Effects of rootstock genotypes on compatibility, biomass, and the yield of Welschriesling. *Hortic. Sci.* **2016**, *43*, 92–99.
12. Töpfer, R.; Hausmann, L.; Harst, M.; Maul, E.; Zyprian, E.; Eibach, R. New horizons for grapevine breeding. In *Methods in Temperate Fruit Breeding*; Flachowsky, H., Hanke, M.V., Eds.; Vegetable and cereal science and biotechnology; Global Science Books Ltd., UK: Kagawa, Japan, 2011; pp. 79–100.
13. Çelik, Ü. The effects of different grafting methods applied by manual grafting units on grafting success in grapevines. *Turk. J. Agric. For.* **2000**, *24*, 499–504.

14. Gargin, S.; Altindisli, A. A Research on the affinity coefficients of Red Globe grape variety with 140 R, 41 B rootstocks. *BIO Web Conf.* **2014**, *3*, 01004.
15. Vršič, S.; Pulko, B.; Kocsis, L. Factors influencing grafting success and compatibility of grape rootstocks. *Sci. Hortic. (Amst.)* **2015**, *181*, 168–173.
16. Bahar, E.; Korkutal, I. Using magnetic resonance imaging technique (MRI) to investigate graft connection and its relation to reddening discoloration in grape leaves. *JFAE* **2010**, *8*, 293–297.
17. Milien, M.; Renault-Spilmont, A.S.; Cookson, S.J.; Sarrazin, A.; Verdeil, J.L. Visualization of the 3D structure of the graft union of grapevine using X-ray tomography. *Sci. Hortic. (Amst.)* **2012**, *144*, 130–140.
18. Assunção, M.; Canas, S.; Cruz, S.; Brazão, J.; Zanol, G.C.; Eiras-Dias, J.E. Graft compatibility of *Vitis spp.*: The role of phenolic acids and flavanols. *Sci. Hortic. (Amst.)* **2016**, *207*, 140–145.
19. Assunção, M.; Pinheiro, J.; Cruz, S.; Brazão, J.; Queiroz, J.; Eduardo, J.; Dias, E.; Canas, S. Gallic acid, sinapic acid and catechin as potential chemical markers of *Vitis* graft success. *Sci. Hortic.* **2019**, *246*, 129–135.
20. Gökbayrak, Z.; Söylemezoğlu, G.; Akkurt, M.; Çelik, H. Determination of grafting compatibility of grapevine with electrophoretic methods. *Sci. Hortic. (Amst.)* **2007**, *113*, 343–352.
21. Cookson, S.; Ollat, N. Grafting with rootstocks induces extensive transcriptional re-programming in the shoot apical meristem of grapevine. *BMC Plant Biol.* **2013**, *13*, 147.
22. Cookson, S.J.; Clemente Moreno, M.J.; Hevin, C.; Nyamba Mendome, L.Z.; Delrot, S.; Magnin, N.; Trossat-Magnin, C.; Ollat, N. Heterografting with nonself rootstocks induces genes involved in stress responses at the graft interface when compared with autografted controls. *J. Exp. Bot.* **2014**, *65*, 2473–2481.
23. Renault-Spilmont, A.S.; Grenan, S.; Bousiquot, J.M. Syrah decline. *Progrés Agric. Vitic.* **2005**, *122*, 15–16.
24. Catalogue of Vines Grown in France. Available online: http://plantgrape.plantnet-project.org/en (accessed on 11 March 2020).
25. Metereological Dafa for Évora Weather Station. Available online: https://www.meteoblue.com/pt/tempo/archive/export/montemor-o-novo_portugal_2265888 (accessed on 1 October 2018).
26. Bouquet, A. Differences observed in the graft compatibility between some cultivars of Muscadine grape (*Vitis rotundifolia Michx.*) and European grape (*Vitis vinifera L.* cv. Cabernet Sauvignon). *Vitis* **1980**, *19*, 99–104.
27. Herrero, J. Studies of compatible and incompatible graft combinations with special reference to hardy fruit trees. *J. Hortic. Sci.* **1951**, *26*, 186–237.
28. Lichtenthaler, H.K. ChlorolShylls and carotenoids: Pigments of photosynthetic biomembranes. *Methods Enzymol.* **1987**, doi:10.1016/0076-6879(87)48036-1.
29. Lichtenthaler, H.K.; Buschmann, C. Chlorophylls and carotenoids: Measurement and characterization by UV-VIS spectroscopy. *Curr. Protoc. Food Anal. Chem.* **2001**, *1*, 1–8.

30. De Mendiburu, F. *Agricolae: Statistical Procedures for Agricultural Research*; R package version 1.3–2; 2020. https://cran.r-project.org/web/packages/agricolae/agricolae.pdf (accessed on 13 May 2020)
31. Harrell, F.E, Jr. *Hmisc: Harrell Miscellaneous*; R package version 4.4–0; 2020. https://cran.r-project.org/web/packages/Hmisc/Hmisc.pdf (accessed on 13 May 2020)
32. Wei T.; Simko, V. *Visualization of a Correlation Matrix*; R package "corrplot" Version 0.84; 2017. https://cran.r-project.org/web/packages/corrplot/corrplot.pdf (accessed on 13 May 2020)
33. Basheer-Salimia, Rezq and Hamdan, A.J. Grapevine scion-rootstock combinations of palestinian local cultivars and rootstocks resistant to grape phylloxera *daktulosphaira vitifoliae (fitch)* [phylloxeridae : homoptera]. *Dirasat Agric. Sci.* **2009**, *36*, 19–28.
34. Hamdan, A.S.; Basheer-Salimia, R. Preliminary compatibility between some table-grapevine scion and phylloxera-resistant rootstock cultivars. *Jordan J. Agric. Sci.* **2010**, *6*, 1–10.
35. Robinson, J. *The Oxford Companion to Wine*, 4th ed.; Oxford University Press: Oxford, UK, 2015; ISBN 9780198705383.
36. Irisarri, P.; Pina, A.; Errea, P. Evaluación del comportamiento vegetativo y compatibilidad de injerto de variedades de peral sobre los patrones 'BA-29' y 'OHF-87.' *ITEA Inf. Tec. Econ. Agrar.* **2016**, *112*, 243–254.
37. Moreno, M.A.; Tabuenca, M.C.; Cambra, R. Adara, A. Plum rootstock for cherries and other stone fruit species. *HortScience* **1995**, *30*, 1316–1317.
38. Zarrouk, O.; Gogorcena, Y.; Moreno, M.A.; Pinochet, J. Graft compatibility between peach cultivars and *Prunus* rootstocks. *HortScience* **2006**, *41*, 1389–1394.
39. Ermel, F.F.; Catesson, J.K.A.M.; Poëssel, J.L. Localized graft incompatibility in pear/quince (*Pyrus communis/Cydonia oblonga*) combinations : Multivariate analysis of histological data from 5-month-old grafts. *Tree Physiol.* **1999**, *19*, 645–654.
40. Pereira, I.S.I.A.L.; Picolotto, L.; Fachinello, J.C. Incompatibilidade de enxertia induz aumento da suscetibilidade de cultivares de pessegueiro à *Xanthomonas arboricola* pv. *Pruni*. *Cienc. Rural* **2015**, *45*, 1147–1153.
41. Pereira, I.D.S.; Antunes, L.E.C.; Picolotto, L.; Fachinello, J.C. Revista brasileira de engenharia agrícola e ambiental fluorescence of chlorophyll a and photosynthetic pigments in *atriplex nummularia* under abiotic stresses fluorescência da clorofila a e pigmentos fotossintéticos em *atriplex nummularia* sob estresses abi. *Cienc. Rural* **2017**, *21*, 232–237.
42. Maxwell, K.; Johnson, G.N. Chlorophyll fluorescence—A practical guide. *J. Exp. Bot.* **2000**, *51*, 659–668.
43. Strasser, R.J.; Tsimilli-Michael, M.; Srivastava A. Chapter 12—Analysis of the chlorophyll a fluorescence transient. In *Chlorophyll A Fluorescence: A Signature of Photosynthesis*; Springer: Dordrecht, The Netherlands, 2004; pp. 321–322.
44. Pavlović, D.; Nikolić, B.; Đurović, S.; Waisi, H.; Anđelković, A. Chlorophyll as a measure of plant health : Agroecological aspects. *Pestic. Phytomed. (Belgrade)* **2014**, *29*, 21–34.

45. Ashraf, M.; Harris, P.J.C. Photosynthesis under stressful environments : An overview. *Photosynthetica* **2013**, *51*, 163–190.
46. Davis, A.R.; Perkins-veazie, P.; Box, P.O.; West, H.; Levi, A.; King, S.R. Grafting effects on vegetable quality. *Hortscience* **2008**, *43*, 1670–1672.
47. Warschefsky, E.J.; Klein, L.L.; Frank, M.H.; Chitwood, D.H.; Londo, J.P.; von Wettberg, E.J.B.; Miller, A.J. Rootstocks: Diversity, domestication, and impacts on shoot phenotypes. *Trends Plant Sci.* **2016**, *21*, 418–437.
48. Murchie, E.H.; Lawson, T. Chlorophyll fluorescence analysis : A guide to good practice and understanding some new applications. *J. Exp. Bot.* **2013**, *64*, 3983–3998.
49. Calatayud, Á.; San, A.; Pascual, B.; Vicente, J.; López-galarza, S. Use of chlorophyll fluorescence imaging as diagnostic technique to predict compatibility in melon graft. *Sci. Hortic. (Amst.)* **2013**, *149*, 13–18.
50. Ito, H.; Tatsuyuki, O.; Tanaka, A. Conversion of Chlorophyll b to Chlorophyll a via 7-Hydroxymethyl Chlorophyll. *J. Biol. Chem*. **1996**, *271*, 1475–1479.
51. Rustioni, L.; Grossi, D.; Brancadoro, L.; Failla, O. Iron, magnesium, nitrogen and potassium deficiency symptom discrimination by reflectance spectroscopy in grapevine leaves. *Sci. Hortic. (Amst.)* **2018**, *241*, 152–159.
52. Pina, A.; Errea, P.; Martens, H.J. Graft union formation and cell-to-cell communication via plasmodesmata in compatible and incompatible stem unions of *Prunus spp. Sci. Hortic. (Amst.)* **2012**, *143*, 144–150.
53. Andrews, P.K.; Serrano Marquez, C. Volume 15—Graft incompatibility. In *Horticultural Reviews*; Janick, J., Ed.; John Wiley & Sons, Inc.: Oxford, UK, 1993; pp. 183–232, ISBN 978-0-471-57338-8.
54. Pereira, I.D.S.; Antunes, L.E.C.; Picolotto, L.; Fachinello, J.C. Incompatibilidade de enxertia em *Prunus* Graft incompatibility in *Prunus*. *Cienc. Rural* **2014**, *449*, 1519–1526.
55. Shtein, I.; Hayat, Y.; Munitz, S.; Harcavi, E.; Akerman, M.; Drori, E.; Schwartz, A.; Netzer, Y. From structural constraints to hydraulic function in three *Vitis* rootstocks. *Trees-Struct. Funct.* **2017**, *31*, 851–861.

Supplementary Materials

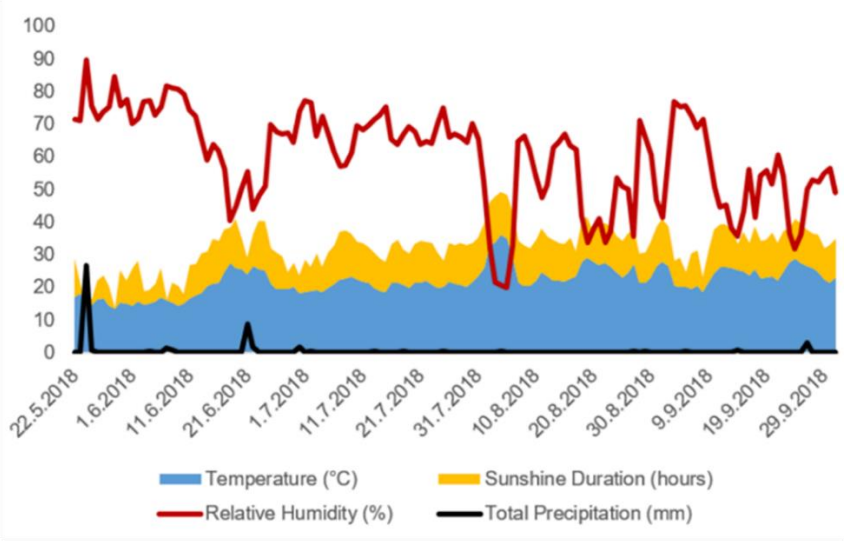

Figure S1. Time course of main climatic parameters (daily means) in the field trial throughout the experiment (May – September 2018).

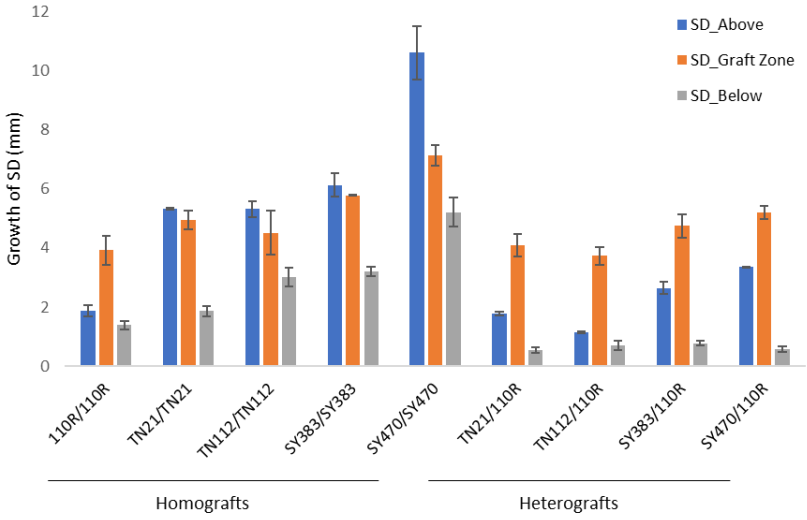

Figure S2. Mean values of Stem Diameter (SD) expansion from 21 to 152 DAG.

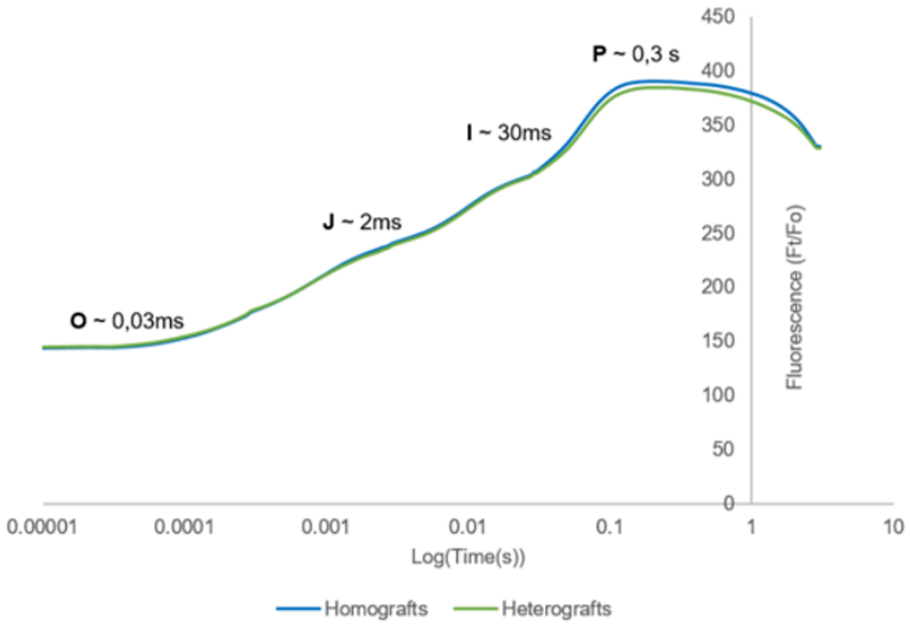

Figure S3. OJIP curves of homo- and heterografts. The curves are plotted on a logarithmic time scale from 10 µs to 3 s. The marks refer to the selected time points used by the JIP-test for the calculation of structural and functional parameters. The signals are the fluorescence intensities: O at 30 s; J at 2 ms; I at 30 ms and P at the maximal fluorescence intensity.

Table S1. Mean values of the affinity coefficients calculated by the formulas of Parraudine, Branas, Spiegel-Roy and Lavee and Onaran.

	Parraudine (Good ≅ 12)	**Branas (Good ≅ 10)**	**Spiegel-Roy and Lavee (Good ≅ 0)**	**Onaran (Good ≅ 100)**
Graft Combination	**ns**	*******	******	******
110R/110R	12.7 ± 0.12	10.0 ± 0.6 a	1.3 ± 0.1 a	225.4 ± 13.0 a
TN21/TN21	12.3 ± 0.13	9.7 ± 0.9 ab	0.7 ± 0.1 abc	168.0 ± 12.7 abc
TN112/TN112	12.8 ± 0.39	18.0 ± 7.2 a	0.8 ± 0.1 abc	175.7 ± 11.1 abc
SY383/SY383	12.3 ± 0.1	10.0 ± 0.3 a	0.8 ± 0.1 abc	177.0 ± 7.3 abc
SY470/SY470	12.0 ± 0.1	9.0 ± 0.7 ab	0.4 ± 0.1 c	139.4 ± 10.4 c
TN21/110R	12.5 ± 0.1	9.0 ± 0.6 ab	1.1 ± 0.1 ab	205.7 ± 11.9 ab
TN112/110R	12.5 ± 0.1	9.0 ± 0.7 ab	1.0 ± 0.1 abc	203.1 ± 14.2 abc
SY383/110R	12.3 ± 0.1	8.5 ± 0.5 ab	0.9 ± 0.1 abc	185.5 ± 9.8 abc
SY470/110R	12.1 ± 0.1	7.2 ± 0.4 b	0.7 ± 0.1 bc	171.3 ± 10.0 bc
Graft Type	**ns**	*******	**ns**	**ns**
Homografts	12.4 ± 0.1	11.3 ± 1.4 a	0.8 ± 0.1	181.1 ± 5.6
Heterografts	12.4 ± 0.1	8.4 ± 0.3 b	0.9 ± 0.1	191.4 ± 5.9

± SE standard error. Significant differences according to Kruskal-Wallis test are indicated by asterisks **p < 0.01 and ***p < 0.001; “ns” indicates non-significant differences, n = 11-24 per graft combination.

Chapter III

The impact of metabolic scion-rootstock interactions in different grapevine tissues and phloem exudates

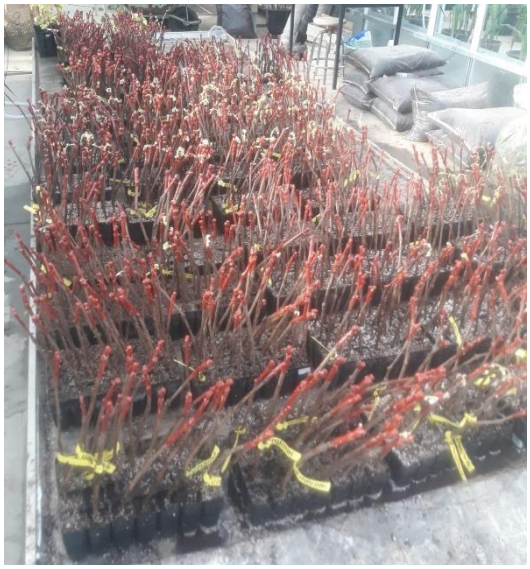

This chapter was published in the *Metabolites* journal:

Tedesco, S.; Erban, A.; Gupta, S.; Kopka, J.; Fevereiro, P.; Kragler, F.; Pina, A. The Impact of Metabolic Scion–Rootstock Interactions in Different Grapevine Tissues and Phloem Exudates. *Metabolites* 2021, *11*, 349. https://doi.org/10.3390/metabo11060349

In this research paper, Sara Tedesco performed the collection of the samples, the statistical analysis, and participated in the writing of the manuscript.

Abstract

In viticulture, grafting is used to propagate Phylloxera-susceptible European grapevines, thereby using resistant American rootstocks. Although scion–rootstock reciprocal signaling is essential for the formation of a proper vascular union and for coordinated growth, our knowledge of graft partner interactions is very limited. In order to elucidate the scale and the content of scion– rootstock metabolic interactions, we profiled the metabolome of eleven graft combination in leaves, stems, and phloem exudate from both above and below the graft union 5–6 months after grafting. We compared the metabolome of scions vs. rootstocks of homografts vs. heterografts and investigated the reciprocal effect of the rootstock on the scion metabolome. This approach revealed that (1) grafting has a minor impact on the metabolome of grafted grapevines when tissues and genotypes were compared, (2) heterografting affects rootstocks more than scions, (3) the presence of a heterologous grafting partner increases defense-related compounds in both scion and rootstocks in shorter and longer distances from the graft, and (4) leaves were revealed as the best tissue to search for grafting-related metabolic markers. These results will provide a valuable metabolomics resource for scion–rootstock interaction studies and will facilitate future efforts on the identification of metabolic markers for important agronomic traits in grafted grapevines.

Keywords: grafting; grapevine; metabolic profiles; phloem exudate; rootstocks; scion-rootstock interactions

1. Introduction

Grafting is an ancient well-established method for plant propagation and improvement. Its discovery likely arose from the attempts of the first agriculturalist for mimicking natural grafting, which allowed the domestication and diffusion of temperate fruit trees [1]. Since then the use of grafting evolved from being merely a means of propagation towards its use to improve resilience against biotic and abiotic impacts [2] and has become a common method used not only in orchards and viticulture but also in horticulture and ornamentals. A prominent example is found with grapevines and the spread of Phylloxera in Europe since the middle of the 19th century. Grafting *V. vinifera* scions onto Phylloxera resistant American rootstocks represents the longest use of a biological control strategy that avoids expensive and elaborate quarantine controls [3]. The use of grafted plants has many agronomical advantages. For instance, grafting is particularly useful for reducing the period of juvenility in perennial plants [4]. The ability of dwarfing rootstocks in reducing scion vigor is widely exploited in commercial fruit production [5]. Grafting also improves plant growth under environmental stresses, such as drought [6,7] and salt stress [8,9]. In addition, the effects of rootstock–scion interaction on growth, fruit quality, and stress tolerance have been widely reviewed [10,11]. Therefore, understanding scion–rootstock interactions is crucial for choosing the most suitable graft combinations for specific environments and good fruit quality [10]. Nevertheless, grafting also constitutes a source for pathogen dissemination given that, by grafting fungal, bacterial, and viral biomes of grafted plants interact and might have a role in the healing of the graft union and the final performance of the plant. Despite this, grafting, when implemented carefully, has greatly contributed to the intensification of agriculture. The effects of grafting, which produces a chimeric organism, are complex and currently largely unpredictable [12].

Chimeric plants produced by grafting have been used to study long-distance movement of signaling molecules, especially via phloem, such as sugars, hormones, proteins, silencing inducing RNAs, and messenger RNAs [13–15]. The identification of the mobile transcription factor, FLOWERING LOCUS T (FT), as the putative “florigen” thought to be the key for the transition to flowering was a major achievement in the past decades and was uncovered by grafting, as FT is produced in leaves but translocated to the shoot apex to exert its function [16]. Crosstalk between the above and below graft parts is conducted by plant vascular systems, xylem, and phloem [17]. While xylem sap is easy to collect, considerable obstacles to access the phloem content lies in the fact that the phloem seals itself upon wounding. However, the phloem exudates from stems, petioles, or floral axes incisions can be collected with the use of chelating agents, such as EDTA, to eliminate sieve tube blockage. It is a well-established method that allowed the unveiling of phloem content and its dynamics in many plant species [18,19]. Nevertheless, it must be taken into account that only relative quantification of the phloem sap can be performed since it is an exudation rather than a direct collection of the phloem sap [18]. New omics approaches have recently been applied in grafting studies to dissect the molecular mechanisms of the early graft-junction formation [20], to unveil the phenomenon of graft compatibility [21–23], and to understand the scion–rootstock interactions leading to the alteration of agronomically important traits [24–26]. Metabolites, as the end-product of gene expression and regulation, have also been investigated in grafted grapevine [27] and citrus trees [17] and were associated to graft formation and fruit quality. Viruses, phenolic compounds, and flavonoids have been proposed as markers for graft incompatibility in *Vitis* [28,29] and *Prunus* [30,31] and secondary metabolism appears to be increased in heterografted grapevines when compared to homografts (i.e., a graft between two individuals of the same

genotype) [32]. Indeed, graft success depends not only on the genotype of each plant part and the grafting protocol used to combine the scion and rootstock but also on the reciprocal signals transmitted between these two plant body parts [2]. However, to date, we have a limited understanding of the signals exchanged between scion and rootstock. Recently, it was shown that grapevine scion–rootstock interactions affect important developmental decisions and growth habits of the scion just 5 months after grafting, at the time when the healing of the graft is not yet complete [33]. In order to shed light on the early metabolic grapevine scion–rootstock interactions between the grafting partners, we investigated changes in the global metabolic profiles in eleven homograft and heterograft grapevine combinations in leaves, stem, and phloem exudates that were collected from both above and below the graft union at 5–6 months after grafting. In particular, we assessed (1) the metabolic profile of homografts and heterografts, (2) the effect of a heterologous grafting partner in the metabolome of a plant in specific tissues and phloem exudates samples, and (3) the metabolic profile of scion and rootstock samples.

2. Material and methods

2.1. Experimental design and plant material

The experimental design comprised of three American rootstocks: Richter-110 (*V. berlandieri* × *V. rupestris*, 110R, JBP/PT clone), *V. rupestris* (RUP), and *V. berlandieri* (BERL); and of six *V. vinifera* cultivars: Syrah clone 383 and 470 (SY383 and SY470, ENTAV-INRA/FR clones), Touriga Nacional clone 21 and 112 (TN21 and TN112, ISA/PT and JBP/PT clones, respectively), and Alfrocheiro (ALF) and *V. vinifera* subsp. *Sylvestris* (SYLV). Certified virus-free cuttings of TN21, TN112, SY470, and 110R were supplied by the Plansel nursery in Montemor-o-Novo, Portugal (291 m above sea level, 38°39′ N, and 8°13′ W). The remaining plants were

collected from the Portuguese National Ampelographic Collection (PRT051), located at Quinta da Almoinha, Dois Portos, Torres Vedras, Portugal (39°02′34.03″ N, −9°10′57.41″ W). The following heterograft combinations, as well as their respective homografts, were performed at the end of April 2018: TN21/110R, TN112/110R, SY383/110R, SY470/110R, ALF/RUP, SYLV/RUP, ALF/BER, and SYLV/BERL. One hundred biological replicates per graft combination were made, except for the grafts with *V. berlandieri* rootstock for which only 20 replicates per combination were available. All grafts were made under commercial nursery conditions by the bench omega-grafting method using dormant cuttings. The grafts were stratified for 21 days to induce *callus* formation at the graft zone [33], plotted in pots (510 cm3 volume), and grown under greenhouse conditions with average day and night temperatures of 20 °C and 23 °C, respectively, and relative humidity of 68 % and 75%, in Oeiras, Portugal, for hardening and to minimize environmental interferences. Supplementary Table S1 summarizes the analyzed graft combinations.

2.2. Sample collection

Samples were collected according to the formation of 10–12 nodes on grafted scions 5–6 months after grafting. Each sample is a pool of 5 grafted plants, scion leaves (1–2 expanded leaves/graft), scion's and rootstock's stem (10–15 cm above and below the graft union, respectively), and phloem exudate from both scion and rootstock sources (15–20 cm above and below the graft union, respectively) were collected as indicated in Figure 1.

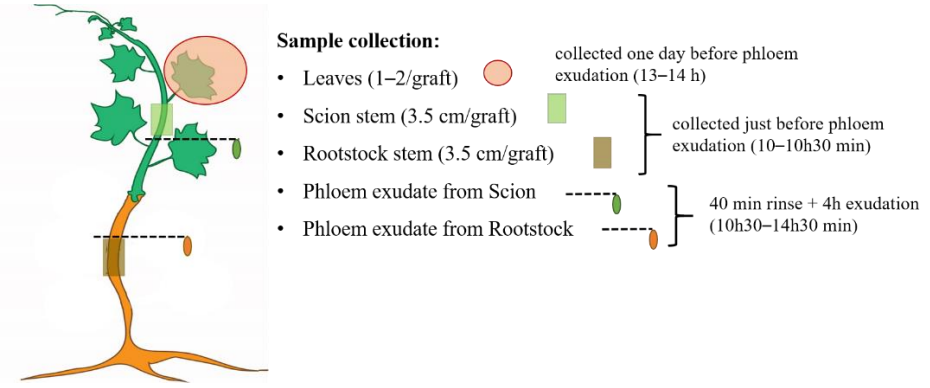

Figure 1. Sample collection scheme. Per graft combination one to two leaves, a segment of 3.5 cm of the scion stem, and 4 h of phloem exudate were collected from scions at 5–6 months after grafting. Rootstock stem samples were harvested from stem segment (length of 3.5 cm) and phloem exudate were collected for 4 h. Leaves were collected one day before phloem exudation to permit the plant to recover. Each sample type was collected at the same circadian phase.

Phloem exudate (five biological replicates per sample) were collected from scion (with 5–6 leaves) and rootstock (with at least 2 scion's healthy leaves) stems cut under EDTA (10 mM EDTA, pH 7.5) solution and submerged in Falcon tubes containing 10 mL EDTA (for scions) and 20 mL EDTA (for rootstocks). The first 40 min of exudate was discarded to avoid contaminations from cut-derived cellular debris. The base of the stems was then submerged under a new EDTA solution and placed on a closed plastic bag filled with water to avoid plant transpiration to facilitate the collection of phloem sap. After 4 h of exudation, the plant material was discarded and the EDTA-phloem sap sample centrifuged (for 5 min at 3400 rcf). Of the supernatant, 10% aliquots (1 mL for scion's phloem exudate and 2 mL for the rootstock) were frozen in liquid nitrogen, and stored at -80 °C until further analysis. The quality of the scion phloem

exudate was previously assessed in EDTA and non-EDTA (water) control samples by monitoring the sugar composition (i.e., sucrose, glucose, and fructose) in the exudate every two hours of collection (up to 6 h) by 1D Proton NMR analysis (data not shown).

2.3. GC-MS Metabolite Profiling of leaves, stems and phloem exudate

Polar metabolite samples were extracted from 85 mg ± 10 mg fresh weight of ground leaves and stem segments as described by Erban et al. (2020) [34]. Briefly, 300 µL of 100% pre-cooled methanol (MeOH), 30 µL of nonadecanoic acid methylester (2 mg/mL stock in $CHCl_3$), and 30 µL of 0.2 mg/mL U-13C-sorbitol in MeOH were added to each sample and mixed for 15 min at 70 °C. The amount of 200 µL of $CHCl_3$ was added and mixed for 5 min at 37 °C. Afterwards, 400 µL of double distilled H_2O was added. The resulting mixture was shaken and centrifuged (for 5 min at 20,800 rcf) to separate predominantly polar and non-polar liquid phases. From the upper polar phase, aliquots of 160 µL were each collected and dried in a Speed Vacuum concentrator overnight. Dry samples were stored at -20 °C. Phloem exudates, namely 1 mL of scion exudate or 2 mL of rootstock exudate were freeze-dried and omitted the extraction procedure. Derivatization of freeze-dried phloem samples and predominantly polar leaf or stem extracts was carried out by methoxyamination and trimethylsilylation [34]. An n-alkane mixture was used to determine retention time indices [34]. Briefly, 40 µL of methoxyamine hydrochloride in pyridine and 20 mg/mL were added to each sample and mixed for 90 min at 30 °C. Afterwards, 80 µL BSTFA-mix, i.e., 70 µL BSTFA plus 10 µL n-alkane-mixture were added and incubated 30 min at 37 °C. The amount of 1 µL of derivatized-sample was analyzed both by 1:30 volume ratio split-injection and by splitless injection modes using a gas chromatography–electron impact ionization-time of flight/mass spectrometry (GC–EI–TOF/MS) instrument. Instrument and instrument settings were as

described previously [34]. ChromaTOF software was used for data acquisition and baseline correction. Processing of chromatography data and peak annotation was carried out using the TagFinder visualization and pre-processing tool [35]. Substance annotation was manually supervised by comparison of retention time indices and mass spectra of reference metabolites from the Golm Metabolome Database, http://gmd.mpimp-golm.mpg.de/, accessed on 26 April 2021 [36]. Metabolite annotations by mass spectral and retention index match are considered verified. Other annotations were by mass spectral match using the AMDIS build 121.86 and MSSearch version 2.0f software (https://chemdata.nist.gov/mass-spc/ms-search/, accessed on 26 April 2021). These annotations are indicated by the prefix “similar to” following the chemical class or the best matching compound [37]. Metabolite names reflect the current identification status of compound or compound class, respectively.

2.4. Comprehensive non-targeted and targeted data analysis of GC-MS profiles

We performed non-targeted data analysis in combination with targeted analyses of metabolites that were represented by the subset of annotated mass features [35,38]. Nontargeted data analysis of all mass features monitored by split and splitless GC-EI-TOF/MS metabolite profiling modes ensured comprehensiveness and included unexpected metabolites and metabolic changes of the predominantly polar metabolite fractions from leaf and stem material or phloem exudates. Stems and leaves datasets were baseline-corrected responses, i.e., arbitrary abundances of chromatographic peak heights of recorded mass-features. These responses were normalized to the response of the U13-sorbitol internal standard and fresh weight after chemical background subtraction using mean responses of non-sample controls. Non sample controls (n = 4 per subset) were empty samples prepared at the metabolite extraction step

and carried throughout the entire analytical procedure. The phloem exudate datasets were identically processed but lacked internal standardization and non-sample controls. These data were normalized to the sum of responses of selected analytes (Supplementary Table S2, spreadsheet “phloem”, cells: KG41-KG56 and KG99-KG101). For statistical analysis, background corrected and normalized data were divided by the median across all samples per mass feature and $\log_{10}$-transformed. Statistical analyses were executed by the R statistical programming software, R version 3.6.2 (www.r-project.org, accessed on 26 April 2021) and RStudio version 1.2.5033 (http://www.rstudio.com/, accessed on 26 April 2021) using the MetaboAnalyst R package v2.0.1 [39]. Data integrity check with default parameters of the package and inter-quantile range filtering was performed followed by one-way ANOVA and Tukey post hoc tests, including FDR-correction of the ‘p.adjust’ R-function (https://www.rdocumentation.org/packages/stats/versions/3.6.2/topics/p.adjust) as the integral part of the MetaboAnalystRv2.0.0 package. The significance threshold was $p < 0.05$. Significantly changed mass features were retrieved from the Tukey multiple-comparison tables. Only those mass features that we recorded in at least 75% of the replicate sets and the mass feature that were simultaneously present in >75% of the replicates of a graft combination and <25% of the replicates of another graft combination were considered. Spurious recordings were omitted from further analyses. In the case of homografted vs. heterografted plants and paired, i.e., graft combination, comparisons of the phloem and stem datasets, the ANOVA and Tukey test were carried out separately for scion and rootstock samples using independently normalized and transformed data subsets.

Principal component analyses (PCAs) were computed using the $\log_{10}$-transformed data sets. PCA was performed by the MetaboAnalyst R

package. Heat maps were generated to analyze relevant differences between metabolic profiles of homografts and heterografts and of the scion comparison to rootstock by applying the ComplexHeatmap R package [40] to a selection of significantly changed metabolites. Specifically, only those metabolites that differentially accumulated significantly and consistently across the diverse graft combinations per group were included. The consistency criterion was an occurrence in at least 80% of the graft combinations per group. Log_{10}-transformed ratios compared to the metabolite means per graft combination were visualized.

Presented results from analyses of paired graft combinations are mean values ± standard error (SE) of data that were maximally normalized. Significant differences are reported at three threshold levels, namely * $p < 0.05$, ** $p < 0.01$, *** $p < 0.001$.

3. Results

Given the impact of the tissue in the distribution of the data (Supplementary Figure S1), the analyses of homografts vs. heterografts and of paired comparisons in phloem and stems dataset were carried out separately for scion and rootstock samples.

3.1. Metabolic Profile of Homografted and Heterografted Grapevines in Tissues and Phloem Exudates Collected from the Scion and Rootstock

The different metabolic profiles in the scion and rootstock tissues and phloem exudates of homografts and heterografts were analyzed for their significant reciprocal changes (95% confidence level). In **leaves**, 23 metabolites (Figure 2A) were found consistently changed between homografts and heterografts. When homografts were compared to heterografts, several sugars were significantly increased, such as 1,3-dihydroxyaceton; and several other not-verified compounds traceable as

disaccharides, carbohydrates, and sugar conjugates (Figure 2A). Aside from carbohydrates, a few compounds related to carboxylic acids, such as a conjugate of propanedioic acid, butan(di)oic acid, butandioic acid di-alkyl-ester, and carboxylic esters (2-deoxyerythropentone-1,5-lactone), were also found significantly increased in homografts. In contrast, among the metabolites that are significantly increased in heterografts comparing to homografts, we detected phosphoric acid monomethyl ester, galactonic acids, and shikimic acids and other not-verified acid compounds such as carboxylic acids, like butanedioic acid among others. In heterografts, phenolic compounds similar to epigallocatechin or gallocatechin and benzoic acid hydroxy, a phenolic acid derived from the phenylpropanoid pathway [41], increased compared to homografts alongside the already mentioned shikimic acid, a central metabolite for the regulation of phenolic metabolism [42].

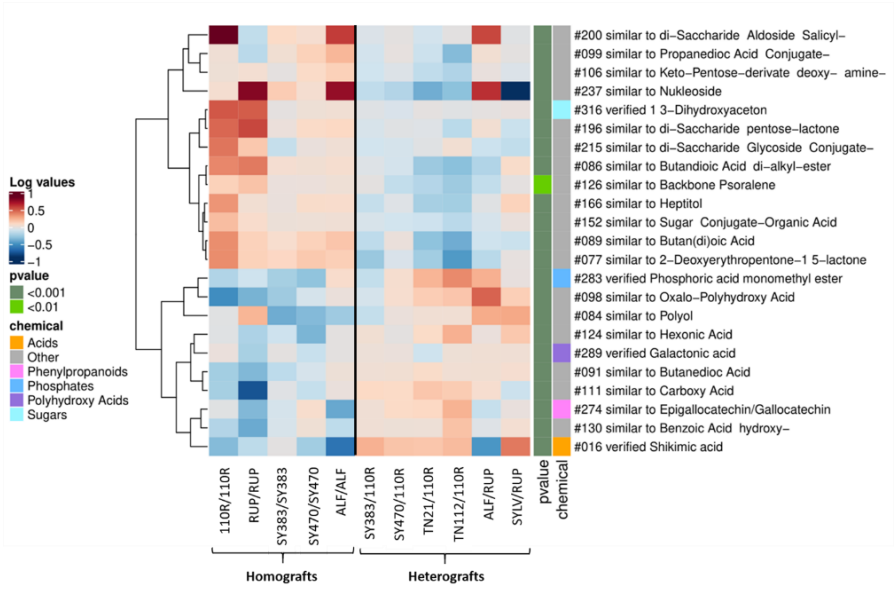

(**A**)

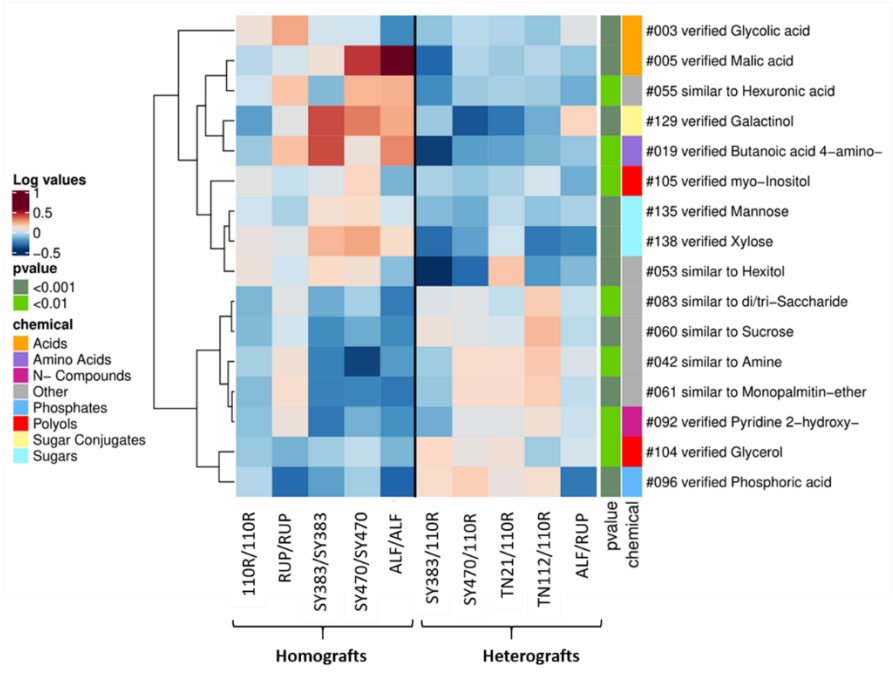

(**B**)

Figure 2. Heat map clustering analysis of homografts versus heterografts at 5–6 months after grafting: (**A**) In the **leaves**; (**B**) and the **rootstock phloem exudate**' datasets. Leaves and phloem rootstocks' metabolites found to be increased or decreased in at least 80% of the homograft combinations and less than 20% of the heterografts (i.e., n = 23 and 16, respectively). Selected metabolites were retrieved from all metabolites found significantly different in at least one of the leaves and phloem rootstock paired-comparison of a homograft versus a heterograft at $p < 0.05$ according to the Tukey post hoc test (i.e., n = 231 and 30, respectively). Mean $\log_{10}$-transformed values per graft combination are plotted, as well as the *p*-value range (<0.01 and <0.001) and the potential chemical class ("chemical") of plotted metabolites. Not-verified metabolites (named with the prefix "similar to") were included in the chemical class

assigned as “Other”. Cluster analysis of metabolites was performed using the Pearson correlation method.

In the **scion phloem exudate** of homografts and heterografts, just one metabolite, the sugar alcohol threitol, was found consistently more abundant in the phloem exudate of homografts (0.09 ± 0.053 SE) than in heterografts (−0.2 ± 0.1 SE; Tukey post hoc test at $p < 0.05$). However, 16 metabolites consistently differed in homografts when compared to heterografts in the **rootstock phloem exudate**. Figure 2B shows that the amino acid 4-amino butanoic acid (GABA), considered an important signal molecule, is consistently more abundant in the phloem exudate of homografts rather than of heterografts together with glycolic and malic acids. Furthermore, sugars, such as mannose and xylose, the sugar conjugate galactinol, and the polyols (sugar alcohols) *myo*-inositol were all increased more in homografts than in heterografts. On the contrary, the metabolites that appeared more abundant in the heterografted combinations were the N-compound 2-hydroxy-pyridine, phosphoric acid, and the polyol glycerol. Regarding the metabolic differences found in the **scion stems**, 19 metabolites were consistently different in homografts versus heterografts (Figure 3A).

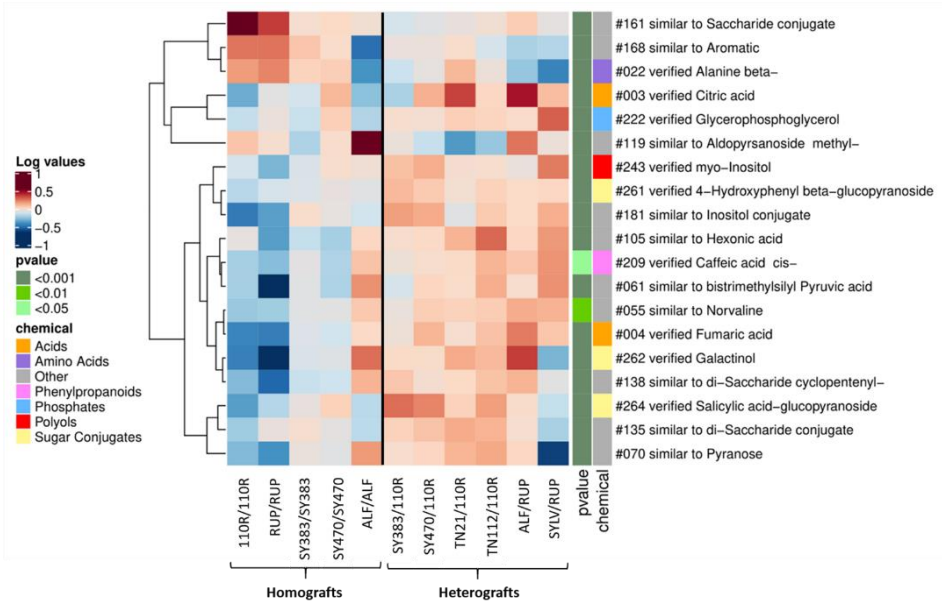

(**A**)

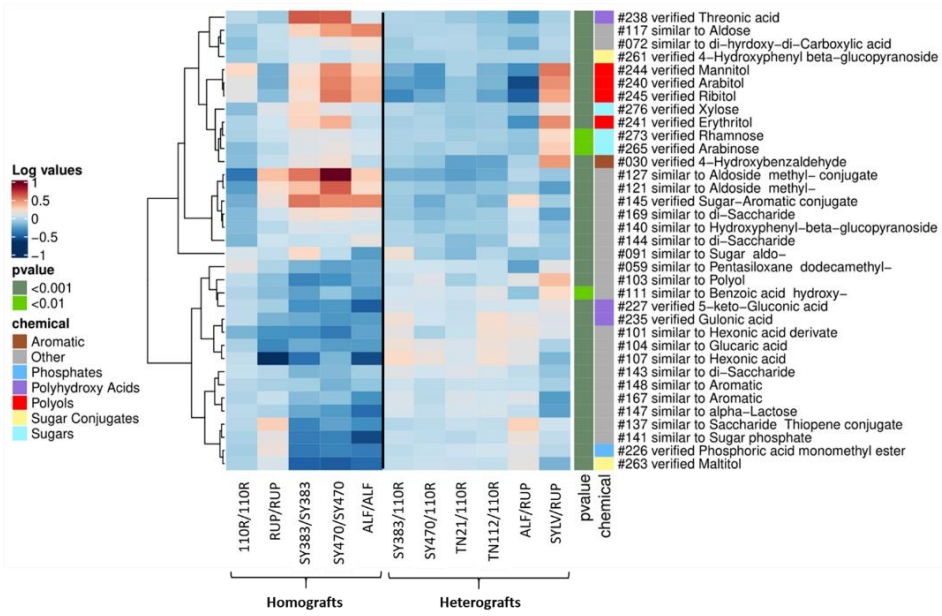

(**B**)

Figure 3. Heat map clustering analysis of homografts versus heterografts at 5–6 months after grafting: (**A**) in the **scion stems**; (**B**) the **rootstock**

stems' datasets. Scion and rootstock stems' metabolites found increased or decreased in at least 80% of the homograft combinations and less than 20% of the heterografts (i.e., n = 19 and 35, respectively). Selected metabolites were retrieved from all metabolites found significantly different in at least 1 scion and rootstock stem paired-comparison of a homograft versus a heterograft at $p < 0.05$ according to Tukey post hoc test (i.e., n = 157 and 159, respectively). Mean $\log_{10}$-transformed values per graft combination are plotted, as well as the *p*-value range (<0.05, <0.01, and <0.001) and the potential chemical class ("chemical") of plotted metabolites. Not-verified metabolites (named with the prefix "similar to") were included in the chemical class assigned as "Other". Cluster analysis of metabolites was performed using the Pearson correlation method.

A higher number of metabolites was increased in heterografts vs. homografts, 16 and 3, respectively. Among these, citric acid, glycerophosphoglycerol, *myo*-inositol, 4-hydroxyphenyl beta-glucopyranoside, *cis*-caffeic acid, fumaric acid, galactinol, and salicylic acid glucopyranoside were all verified (Figure 3A). In addition, 35 metabolites were consistently different between the two groups in the **rootstock stems**. Figure 3B shows that several polyols such as mannitol, arabitol, ribitol, and erythritol; several sugars such as xylose, rhamnose, and arabinose; as well as the sugar conjugate 4-hydroxyphenyl beta-glucopyranoside were all found increased in homografts when compared to heterografts together with threonic acid, 4-hydroxybenzaldehyde, a sugar-aromatic conjugate, and other not-verified compounds. Conversely, polyhydroxy acids such as 5-keto-gluconic acid and gulonic acid, the sugar conjugate maltitol, and phosphoric acid monomethyl ester were increased in heterografts when compared to homografts. Moreover, several not-verified compounds, especially substances attributable as acids,

aromatics, and polyols were found to be increased in heterografts when compared to homografts in the rootstock stems (Figure 3B).

3.2. Grafting Partner Induced Changes in the Scion and Rootstock Metabolome

In order to elucidate how a heterologous grafting partner affects the metabolic composition of the other grafting partner, we compared each homograft tissue (and phloem exudate) with the same tissue (and phloem exudate) of its respective heterograft. In the **leaves** dataset, 8 of 292 identified metabolites were different in homografted SY383 and SY470 when compared with their respective heterografts SY383/110R and SY470/110R and 12 of 292 identified metabolites were found to be different between the leaves of ALF/ALF compared to ALF/RUP at $p < 0.05$ according to the Tukey post hoc test (Figure 4A).

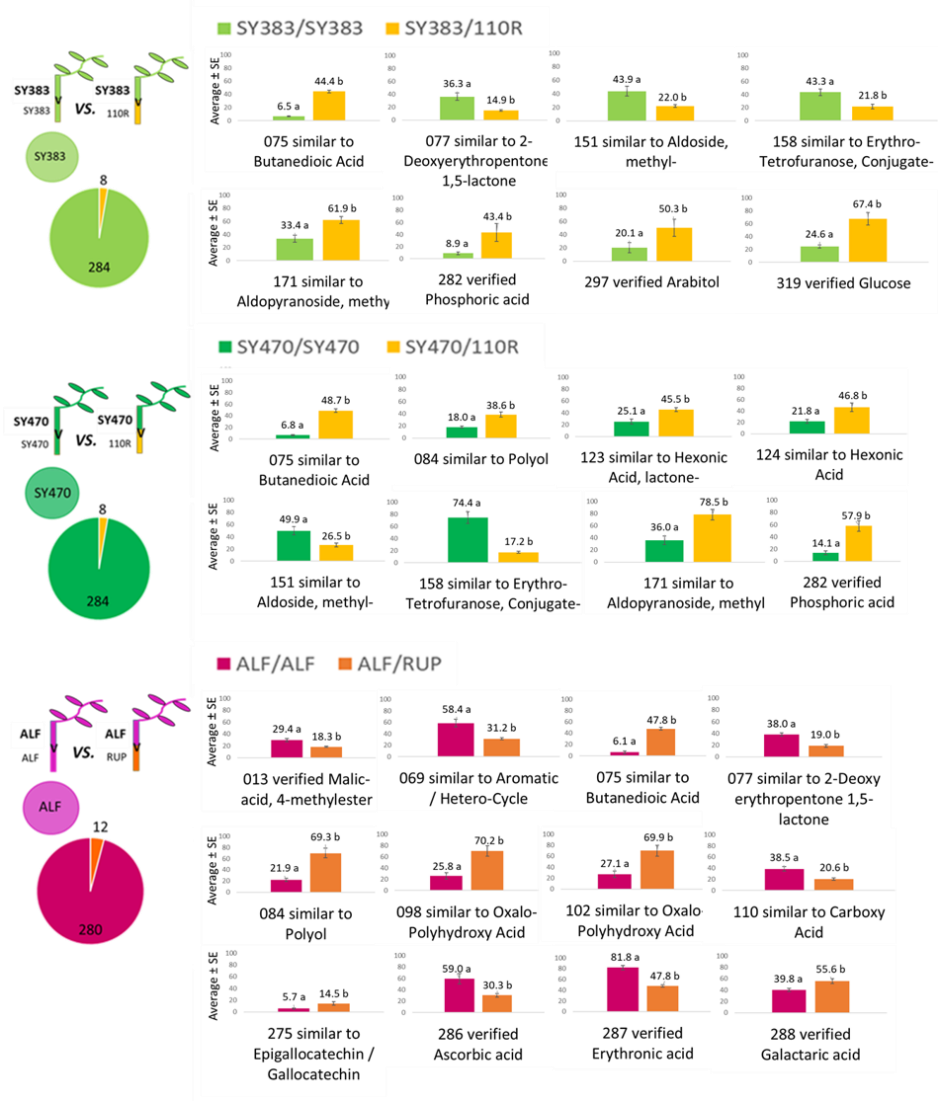
SY383/SY383
SY383/110R
SY383 SY383 VS. SY383 110R
SY383
8
284
075 similar to Butanedioic Acid
077 similar to 2-Deoxyerythropentone 1,5-lactone
151 similar to Aldoside, methyl-
158 similar to Erythro-Tetrofuranose, Conjugate-
171 similar to Aldopyranoside, methy
282 verified Phosphoric acid
297 verified Arabitol
319 verified Glucose
SY470/SY470
SY470/110R
SY470 SY470 VS. SY470 110R
SY470
8
284
075 similar to Butanedioic Acid
084 similar to Polyol
123 similar to Hexonic Acid, lactone-
124 similar to Hexonic Acid
151 similar to Aldoside, methyl-
158 similar to Erythro-Tetrofuranose, Conjugate-
171 similar to Aldopyranoside, methyl
282 verified Phosphoric acid
ALF/ALF
ALF/RUP
ALF ALF VS. ALF RUP
ALF
12
280
013 verified Malic-acid, 4-methylester
069 similar to Aromatic / Hetero-Cycle
075 similar to Butanedioic Acid
077 similar to 2-Deoxy erythropentone 1,5-lactone
084 similar to Polyol
098 similar to Oxalo-Polyhydroxy Acid
102 similar to Oxalo-Polyhydroxy Acid
110 similar to Carboxy Acid
275 similar to Epigallocatechin / Gallocatechin
286 verified Ascorbic acid
287 verified Erythronic acid
288 verified Galactaric acid

(**A**)

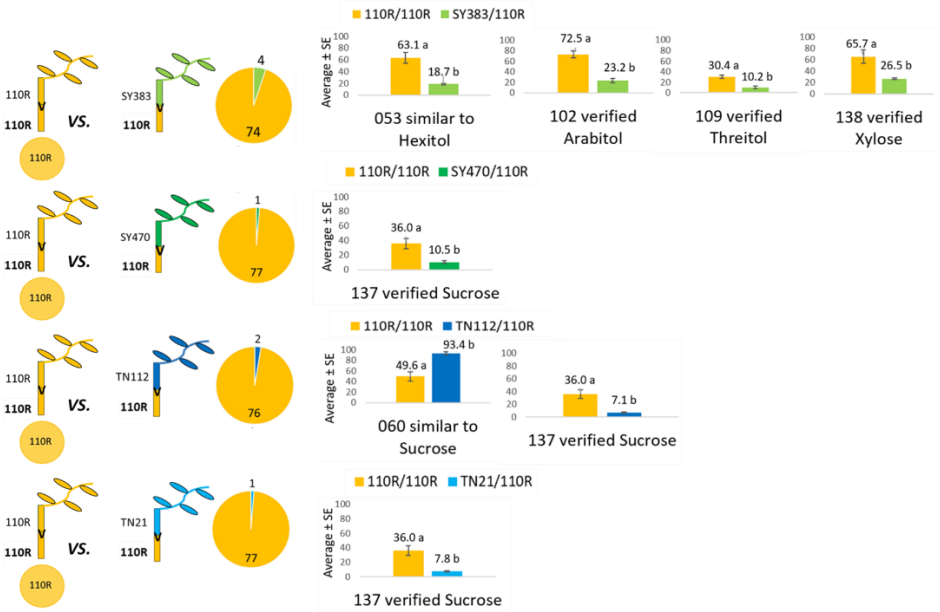

(**B**)

Figure 4. Scale of the effect and significant different metabolites: (**A**) in the **leaves**; (**B**) the **rootstock phloem exudate**' samples of homografts upon grafting with a heterologous partner. Scale of the effect of a heterologous grafting partner in the leaves and phloem rootstocks' metabolome of a homograft and pie graphs with the number of changed and unchanged metabolites (left); bar charts of the mean value of significant different metabolites upon grafting with a heterologous partner (right). The different letters indicate significant differences between the graft combinations at $p < 0.05$ according to the Tukey post hoc test. Data are presented as the average of data normalized to the maximum value for each metabolite. Bars represent the standard error.

The 110R and RUP rootstocks seem to induce a compound similar to butanedioic acid in the leaves of *V. vinifera* cv. Syrah clone 383 and 470 and of cv. Alfrocheiro than when self-grafted. Phosphoric acid and a

compound attributable to aldo-pyranoside methyl were increased while compounds similar to aldoside methyl and erythrotetrafuranose conjugates were reduced in the leaves of both Syrah clones in response to the presence of 110R rootstock. A polyol compound was detected to be increased in SY470 and ALF leaves that are grafted onto 110R and RUP, respectively, rather than when in self-grafted plants. Similarly, a compound traceable as 2-deoxyerythropentone-1,5-lactone was found to be increased in homografts of SY383 and ALF in response to the 110R and RUP rootstocks, respectively. Some metabolites were differently affected by both rootstocks in a genotype specific manner. For instance, 110R leads to an increased content of arabitol and glucose in the leaves of SY383/110R compared to SY383/SY383 but not compared to SY470/110R, where 110R induced an increase in substances similar to hexonic acids and hexonic acid lactone (compared to the leaves of SY470 homografts) (Figure 4A). Interestingly, the **rootstock phloem exudate** showed more metabolic changes in the presence of a heterologous scion than the phloem exudate from the scion (data not shown) in the presence of a heterologous rootstock, according to the source-to-sink (scion and rootstock, respectively) phloem flow. Indeed, when the rootstock phloem exudate of 110R homografts were compared with respective heterografted SY383, SY470, TN112, and TN21 scions, out of the 78 identified phloem exudate metabolites 4, 1, 2, and 1 metabolites were displayed as significantly different, respectively (Figure 4B). Nevertheless, no metabolite was significantly different when compared between the phloem exudate of RUP/RUP and the respective heterografted ALF/RUP exudate. It is worth it to point out that sucrose appeared significantly reduced in the phloem exudates of heterografted 110R rootstocks when compared to the self-grafted 110R/110R exudate, except for SY383/110R. SY383/110R phloem exudate showed reduced xylose and polyols (namely threitol, arabitol, and a compound attributable to hexitol) amounts in comparison to

110R/110R exudate. There was only one not-verified metabolite similar to sucrose found to be increased in TN112/110R phloem exudate with respect to 110R/110R, which might hypothetically compensate for the sucrose depletion seen in heterografts with 110R rootstock (again with SY383/110R being an exception) (Figure 4B). Concerning the effect of rootstocks on **scion stems**, among the 277 identified metabolites only 5 metabolites were found different between the homografted SY383/SY383 and heterografted SY383/110R, 3 metabolites between SY470/SY470 and heterografted SY470/110R, and 22 metabolites were found different in ALF/ALF when compared to the same tissue of ALF/RUP at $p < 0.05$ according to the Tukey post hoc test (Figure 5A).

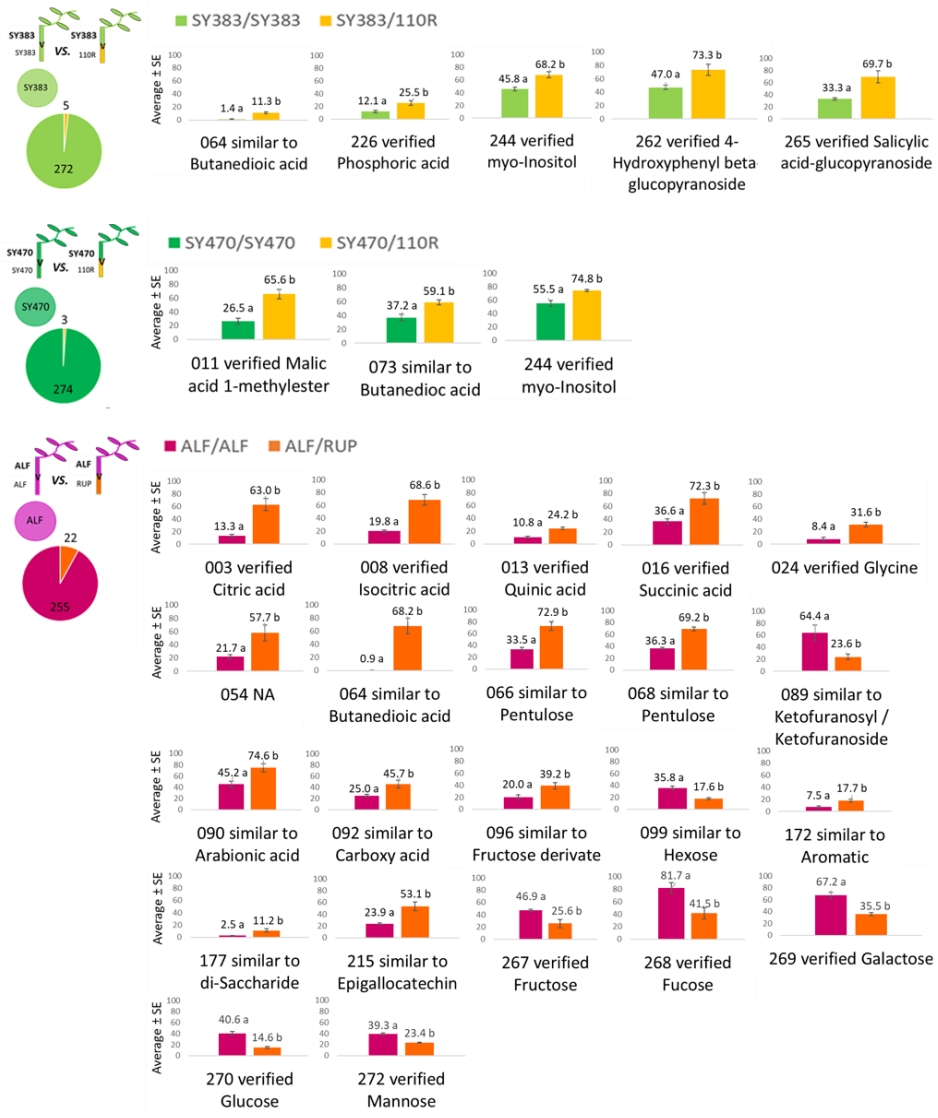
SY383/SY383
SY383/110R
SY383 vs. SY383
SY383 vs. 110R
5
272
Average ± SE
1.4 a
11.3 b
064 similar to Butanedioic acid
12.1 a
25.5 b
226 verified Phosphoric acid
45.8 a
68.2 b
244 verified myo-Inositol
47.0 a
73.3 b
262 verified 4-Hydroxyphenyl beta glucopyranoside
33.3 a
69.7 b
265 verified Salicylic acid-glucopyranoside
SY470/SY470
SY470/110R
SY470 vs. SY470
SY470 vs. 110R
3
274
26.5 a
65.6 b
011 verified Malic acid 1-methylester
37.2 a
59.1 b
073 similar to Butanedioc acid
55.5 a
74.8 b
244 verified myo-Inositol
ALF/ALF
ALF/RUP
ALF vs. ALF
ALF vs. RUP
22
255
13.3 a
63.0 b
003 verified Citric acid
19.8 a
68.6 b
008 verified Isocitric acid
10.8 a
24.2 b
013 verified Quinic acid
36.6 a
72.3 b
016 verified Succinic acid
8.4 a
31.6 b
024 verified Glycine
21.7 a
57.7 b
054 NA
0.9 a
68.2 b
064 similar to Butanedioic acid
33.5 a
72.9 b
066 similar to Pentulose
36.3 a
69.2 b
068 similar to Pentulose
64.4 a
23.6 b
089 similar to Ketofuranosyl / Ketofuranoside
45.2 a
74.6 b
090 similar to Arabionic acid
25.0 a
45.7 b
092 similar to Carboxy acid
20.0 a
39.2 b
096 similar to Fructose derivate
35.8 a
17.6 b
099 similar to Hexose
7.5 a
17.7 b
172 similar to Aromatic
2.5 a
11.2 b
177 similar to di-Saccharide
23.9 a
53.1 b
215 similar to Epigallocatechin
46.9 a
25.6 b
267 verified Fructose
81.7 a
41.5 b
268 verified Fucose
67.2 a
35.5 b
269 verified Galactose
40.6 a
14.6 b
270 verified Glucose
39.3 a
23.4 b
272 verified Mannose

(**A**)

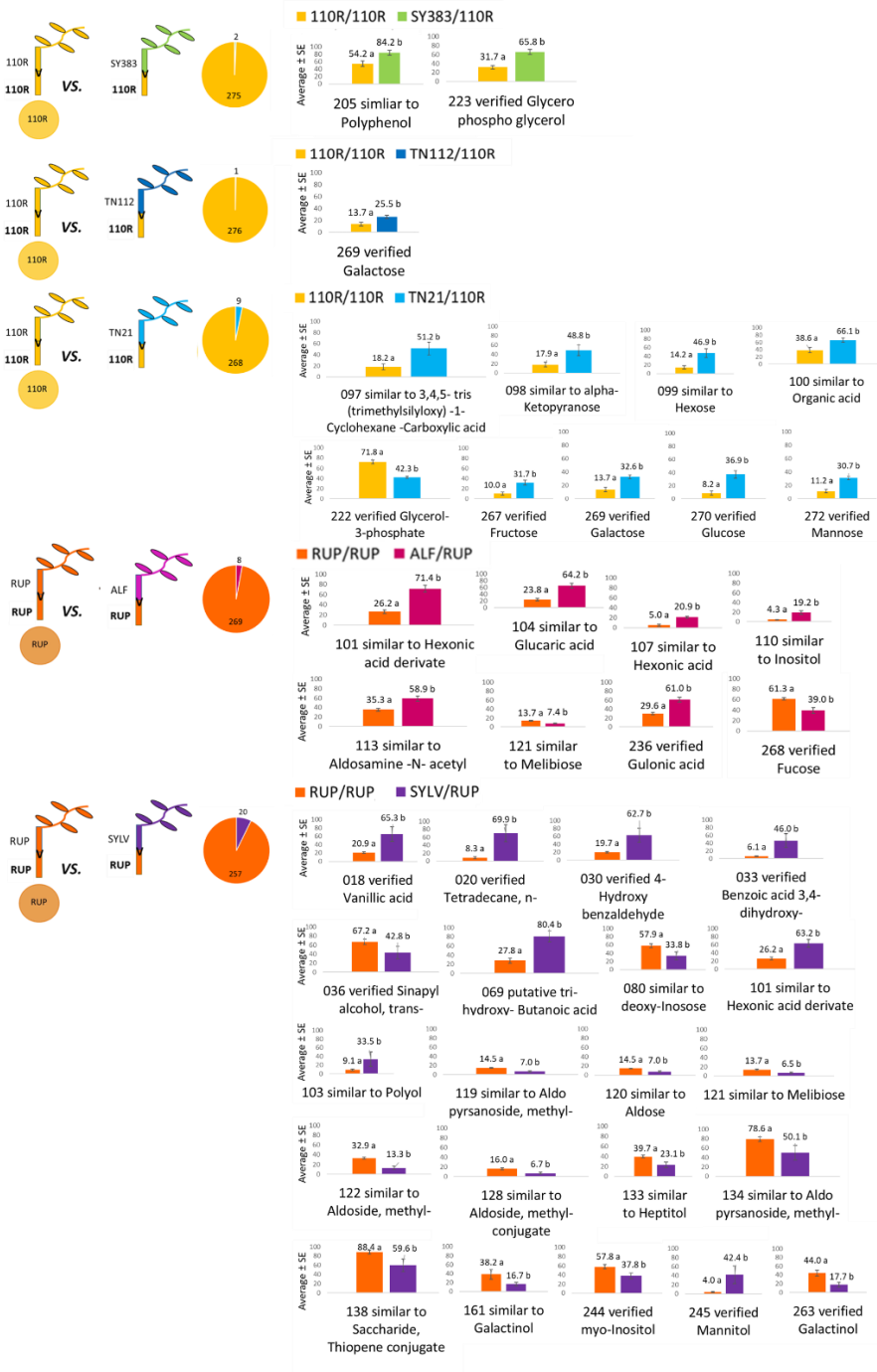
110R/110R
SY383/110R
110R VS. 110R
SY383 VS. 110R
205 simliar to Polyphenol
223 verified Glycero phospho glycerol
110R/110R
TN112/110R
TN112 VS. 110R
269 verified Galactose
110R/110R
TN21/110R
TN21 VS. 110R
097 similar to 3,4,5- tris (trimethylsilyloxy) -1- Cyclohexane -Carboxylic acid
098 similar to alpha- Ketopyranose
099 similar to Hexose
100 similar to Organic acid
222 verified Glycerol- 3-phosphate
267 verified Fructose
269 verified Galactose
270 verified Glucose
272 verified Mannose
RUP/RUP
ALF/RUP
ALF VS. RUP
101 similar to Hexonic acid derivate
104 similar to Glucaric acid
107 similar to Hexonic acid
110 similar to Inositol
113 similar to Aldosamine -N- acetyl
121 similar to Melibiose
236 verified Gulonic acid
268 verified Fucose
RUP/RUP
SYLV/RUP
SYLV VS. RUP
018 verified Vanillic acid
020 verified Tetradecane, n-
030 verified 4- Hydroxy benzaldehyde
033 verified Benzoic acid 3,4- dihydroxy-
036 verified Sinapyl alcohol, trans-
069 putative tri- hydroxy- Butanoic acid
080 similar to deoxy-Inosose
101 similar to Hexonic acid derivate
103 similar to Polyol
119 similar to Aldo pyrsanoside, methyl-
120 similar to Aldose
121 similar to Melibiose
122 similar to Aldoside, methyl-
128 similar to Aldoside, methyl- conjugate
133 similar to Heptitol
134 similar to Aldo pyrsanoside, methyl-
138 similar to Saccharide, Thiopene conjugate
161 similar to Galactinol
244 verified myo-Inositol
245 verified Mannitol
263 verified Galactinol

(B)

Figure 5. Scale of the effect and different significant metabolites: (**A**) in the **scion stems**; (**B**) the **rootstock stems** of homografts, upon grafting with a heterologous partner. Scale of the effect of a heterologous grafting partner in the scion and rootstock stems' metabolome of a homograft and pie graphs with the number of changed and unchanged metabolites (left); bar charts of the mean value of significant different metabolites upon grafting with a heterologous partner (right). Different letters indicate significant differences between the graft combinations at $p < 0.05$ according to the Tukey post hoc test. Data are presented as the average of data normalized to the maximum value for each metabolite. Bars represent the standard error.

As seen in Figure 5A, only not-verified compounds similar to butanedioic acid were found increased in all heterograft combinations (SY383/110R, SY470/110R, and ALF/RUP) when compared to their respective homografts. Similarly, *myo*-inositol was also increased in SY383/110R and SY470/110R heterografts compared to their respective homografts, while phosphoric acid, the phenolic glycoside 4-hydroxyphenyl beta-glucopyranoside, and salicylic acid-glucopyranoside were specifically found increased in SY383/110R with respect to SY383/SY383. Conversely, malic acid 1-methylester was enriched in SY470/110R when compared to SY470/SY470. Several metabolites were specifically altered in ALF stem grafted onto RUP rootstock. For instance, when comparing ALF/ALF to ALF/RUP, several acids such as citric, isocitric, quinic, and succinic acids; as well as several other not-identified compounds including the amino acid glycine and a phenolic similar to epigallocathechin/gallocathechin were increased in ALF/RUP. On the other hand, several sugars such as fructose, fucose, galactose, glucose, and mannose were found depleted in the scion stems of the heterograft ALF/RUP when compared to ALF/ALF (Figure 5A). Regarding the effect

of a heterologous scion on the metabolome of **rootstock stems** (Figure 5B), this was higher in the RUP rootstock than in 110R depending on the scion used. Only two metabolites were found different between the rootstock stem of 110R/110R and SY383/110R, no differences were found in SY470/110R rootstock stem, and one and nine metabolites were found different between 110R/110R homografts and TN112/110R and TN21/110R heterografts, respectively. However, 8 and 20 metabolites changed when RUP was grafted with ALF or SYLV scions, respectively at $p < 0.05$ according to Tukey post hoc test (Figure 5B). The phosphate glycerophosphoglycerol and a substance attributable to a polyphenol increased in SY383/110R relative to the 110R /110R rootstock stem. The sugar galactose was more abundant in the 110R rootstock with TN21 and TN112 scions compared to 110R/110R. Interestingly, TN21 as a scion also induced other metabolic changes in the 110R rootstock stem. In addition to galactose, other sugars (i.e., fructose, glucose, and mannose) were increased in TN21/110R when compared to 110R/110R. In these samples, other not-verified compounds were also found to be increased, while only glycerol-3-phosphate was reduced in TN21/110R when compared to 110R/110R. Changes in RUP rootstock stems were affected in a genotypic-specific manner as only two metabolites, namely compounds traceable as a derivate of hexonic acid and melibiose, were found to be commonly altered by the presence of ALF and SYLV scions. As mentioned, SYLV scion caused more metabolic changes in the rootstock stems of RUP than an ALF scion (Figure 5B). In addition to the sugar conjugate galactinol, the polyol *myo*-inositol, and *trans*-sinapyl alcohol, which were found depleted in the heterograft SYLV/RUP, all the other verified compounds, namely the polyol mannitol, vanilic acid, the aliphatic tetradecane, n-, the aromatics 4-hydroxybenzaldehyde, and benzoic acid 3,4-dihydroxy-, were found increased in the rootstock stems of SYLV/RUP when compared to RUP/RUP.

3.3. Metabolic Profiles of Scion and Rootstock Phloem Exudates and Stems in Grafted Grapevines

To better investigate the scion–rootstock cross-talk and to shed light on the huge impact imposed by the tissue (i.e., scion or rootstock) on the metabolic profiles analyzed (highlighted by the PCAs shown in Figure S1), we compared phloem exudate and stem samples collected from above (scion) and below (rootstock) the graft union. Following the same criterium used for the previous heat maps, significant metabolites with an inverted and consistent behavior among the graft combinations of the scion (_SC) and rootstock (_RT) samples were included in Figure 6. Concerning the composition of the **phloem exudate**, 21 metabolites were consistently found different in samples collected above than in the ones collected below the graft union (Figure 6A).

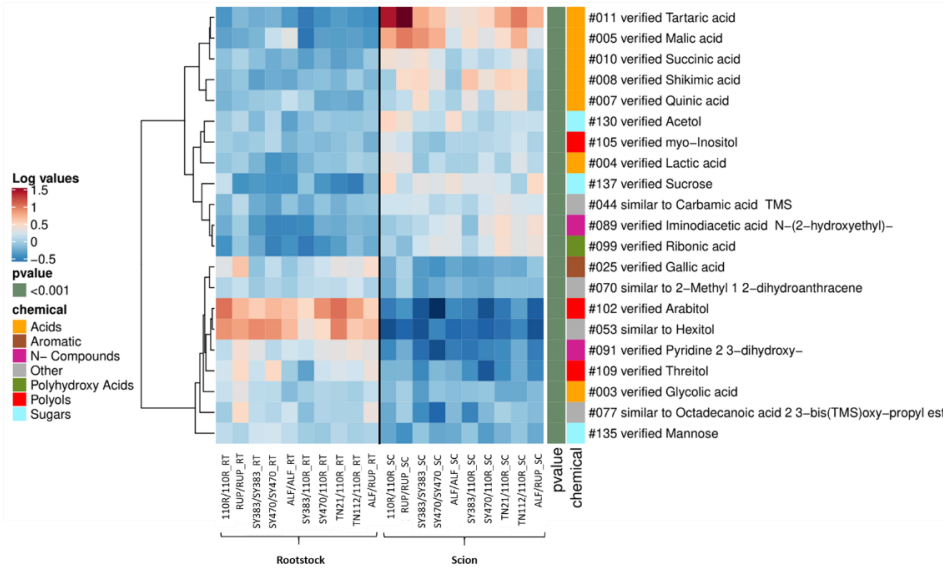

(**A**)

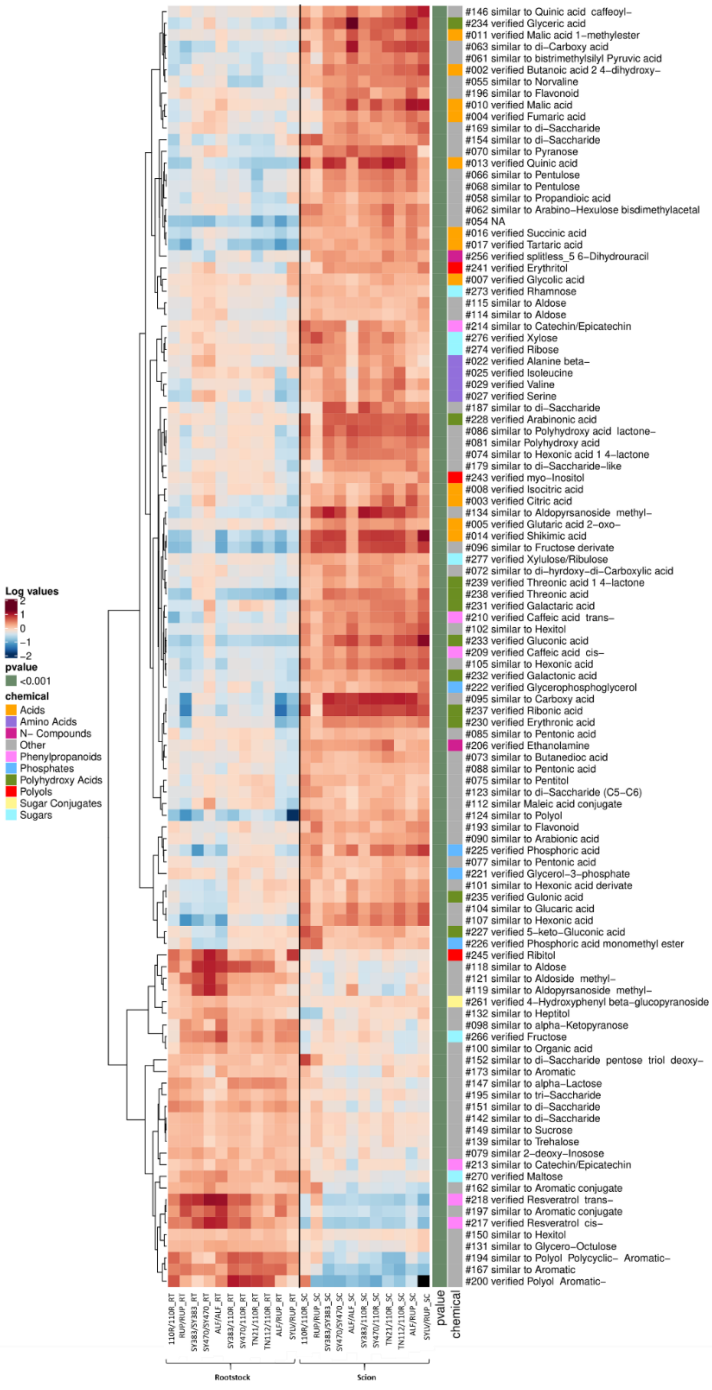
Log values
2
1
0
−1
−2
pvalue
<0.001
chemical
Acids
Amino Acids
N− Compounds
Other
Phenylpropanoids
Phosphates
Polyhydroxy Acids
Polyols
Sugar Conjugates
Sugars
#146 similar to Quinic acid caffeoyl−
#234 verified Glyceric acid
#011 verified Malic acid 1−methylester
#063 similar to di−Carboxy acid
#061 similar to bistrimethylsilyl Pyruvic acid
#002 verified Butanoic acid 2 4−dihydroxy−
#055 similar to Norvaline
#196 similar to Flavonoid
#010 verified Malic acid
#004 verified Fumaric acid
#169 similar to di−Saccharide
#154 similar to di−Saccharide
#070 similar to Pyranose
#013 verified Quinic acid
#066 similar to Pentulose
#068 similar to Pentulose
#058 similar to Propandioic acid
#062 similar to Arabino−Hexulose bisdimethylacetal
#054 NA
#016 verified Succinic acid
#017 verified Tartaric acid
#256 verified splitless_5 6−Dihydrouracil
#241 verified Erythritol
#007 verified Glycolic acid
#273 verified Rhamnose
#115 similar to Aldose
#114 similar to Aldose
#214 similar to Catechin/Epicatechin
#276 verified Xylose
#274 verified Ribose
#022 verified Alanine beta−
#025 verified Isoleucine
#029 verified Valine
#027 verified Serine
#187 similar to di−Saccharide
#228 verified Arabinonic acid
#086 similar to Polyhydroxy acid lactone−
#081 similar Polyhydroxy acid
#074 similar to Hexonic acid 1 4−lactone
#179 similar to di−Saccharide−like
#243 verified myo−Inositol
#008 verified Isocitric acid
#003 verified Citric acid
#134 similar to Aldopyrsanoside methyl−
#005 verified Glutaric acid 2−oxo−
#014 verified Shikimic acid
#096 similar to Fructose derivate
#277 verified Xylulose/Ribulose
#072 similar to di−hyrdoxy−di−Carboxylic acid
#239 verified Threonic acid 1 4−lactone
#238 verified Threonic acid
#231 verified Galactaric acid
#210 verified Caffeic acid trans−
#102 similar to Hexitol
#233 verified Gluconic acid
#209 verified Caffeic acid cis−
#105 similar to Hexonic acid
#232 verified Galactonic acid
#222 verified Glycerophosphoglycerol
#095 similar to Carboxy acid
#237 verified Ribonic acid
#230 verified Erythronic acid
#085 similar to Pentonic acid
#206 verified Ethanolamine
#073 similar to Butanedioc acid
#088 similar to Pentonic acid
#075 similar to Pentitol
#123 similar to di−Saccharide (C5−C6)
#112 similar Maleic acid conjugate
#124 similar to Polyol
#193 similar to Flavonoid
#090 similar to Arabionic acid
#225 verified Phosphoric acid
#077 similar to Pentonic acid
#221 verified Glycerol−3−phosphate
#101 similar to Hexonic acid derivate
#235 verified Gulonic acid
#104 similar to Glucaric acid
#107 similar to Hexonic acid
#227 verified 5−keto−Gluconic acid
#226 verified Phosphoric acid monomethyl ester
#245 verified Ribitol
#118 similar to Aldose
#121 similar to Aldoside methyl−
#119 similar to Aldopyrsanoside methyl−
#261 verified 4−Hydroxyphenyl beta−glucopyranoside
#132 similar to Heptitol
#098 similar to alpha−Ketopyranose
#266 verified Fructose
#100 similar to Organic acid
#152 similar to di−Saccharide pentose triol deoxy−
#173 similar to Aromatic
#147 similar to alpha−Lactose
#195 similar to tri−Saccharide
#151 similar to di−Saccharide
#142 similar to di−Saccharide
#149 similar to Sucrose
#139 similar to Trehalose
#079 similar 2−deoxy−Inosose
#213 similar to Catechin/Epicatechin
#270 verified Maltose
#162 similar to Aromatic conjugate
#218 verified Resveratrol trans−
#197 similar to Aromatic conjugate
#217 verified Resveratrol cis−
#150 similar to Hexitol
#131 similar to Glycero−Octulose
#194 similar to Polyol Polycyclic− Aromatic−
#167 similar to Aromatic
#200 verified Polyol Aromatic−
1109/110R_RT
RUP/RUP_RT
SY383/SY383_RT
SY470/SY470_RT
AU/AU_RT
SY383/110R_RT
SY470/110R_RT
TN212/110R_RT
TN112/110R_RT
AU/RUP_RT
SYU/RUP_RT
1109/110R_SC
RUP/RUP_SC
SY383/SY383_SC
SY470/SY470_SC
AU/AU_SC
SY383/110R_SC
SY470/110R_SC
TN212/110R_SC
TN112/110R_SC
AU/RUP_SC
SYU/RUP_SC
pvalue
chemical
Rootstock
Scion

(**B**)

Figure 6. Heatmap clustering analysis of scion vs. rootstock at 5–6 months after grafting: (**A**) in the **phloem exudate**; (**B**) **stems** datasets. Phloem exudate and stems metabolites found increased or decreased in at least 80% of the scion and less than 20% of the rootstock samples. Selected metabolites were retrieved from all metabolites found significantly different in at least one paired-comparison of a scion vs. a rootstock sample at $p < 0.05$ according to the Tukey post hoc test. Mean $\log_{10}$-transformed values per graft combination are plotted (missing values are visualized in black color), as well as the *p*-value range (<0.001) and the potential chemical class ("chemical") of plotted metabolites. Not-verified metabolites (named with the prefix "similar to") were included in the chemical class assigned as "Other". Cluster analysis of metabolites was performed using the Pearson correlation method.

Figure 6A shows that several acids (i.e., tartaric, malic, succinic, shikimic, quinic, lactic, and ribonic acids) were found increased in the phloem exudate collected from the scion compared to the rootstock. Sucrose, the polyol *myo*-inositol, acetol, and a N-compound (iminodiacetic acid N-(2-hydroxyethyl)) were also found increased in phloem exuded from scions than from rootstocks. Conversely, the sugar mannose and the polyols, threitol and arabitol, were reduced in the phloem from scion than from rootstock. The phenolic compound gallic acid, the N-compound 2,3-dihydroxy-pyridine, and glycolic acid were also found increased in phloem harvested from the rootstock than from the scion (Figure 6A). In **stems**, 111 metabolites were detected to consistently differ among the graft combinations in samples collected from the scion (_SC) and the rootstock (_RT). Many metabolites seem to be increased in the stems collected from the scion rather than from the rootstock (i.e., 82 and 29 metabolites, respectively) as displayed in Figure 6B. Considering the verified metabolites found enriched in the scion stems when compared to the

rootstock stems, we found several acid compounds namely malic acid 1 - methylester, butanoic acid 2,4-dihydroxy-, malic, fumaric, quinic, succinic, tartaric, glycolic, citric, isocitric, shikimic acids, and glutaric acid 2-oxo-. Moreover, polyhydroxy acids such as glyceric, arabinonic, threonic and threonic acid 1,4-lactone, galactaric, gluconic, galactonic, ribonic, erythronic, gulonic acids, and 5-keto-gluconic acid increased in the scion stems rather than in the rootstock stems together with the amino acids alanine beta-, isoleucine, valine, and serine. A few phosphates, namely glycerophosphoglycerol, phosphoric acid, glycerol-3-phosphate, and phosphoric acid monomethyl ester; the phenols, *cis*- and *trans*-caffeic acids; the polyols erythritol and *myo*-inositol; the sugars rhamnose, xylose, ribose, and xylulose/ribulose; the N-compound 5,6-dihydrouracil; and ethanolamine were all found more abundant in the stems collected from the scion than from the rootstock. Other than these, many other not-verified compounds mainly traceable as acids, polyhydroxy acids, and several sugars and their conjugates were higher in scion stems than in rootstocks (Figure 6B). Interestingly, compounds similar to flavonoids and phenolics traceable as catechin/epicatechin, caffeoyl-quinic acid, and the already mentioned *cis*- and *trans*-caffeic acid were more abundant in the scion than in the rootstock stems. Conversely, only a few metabolites were displayed as enriched in rootstock stems when compared to scion stems. Among these, we can find the sugars fructose and maltose, the sugar conjugate 4-hydroxyphenyl beta-glucopyranoside, the polyol ribitol, a polyol aromatic-, and the phenolic compounds *cis*- and *trans*-resveratrol. Likewise, not-verified substances that seem to belong to sugars, sugar conjugates, and aromatics and their conjugates, including a phenolic similar to catechin/epicatechin, appear depleted in the scion stems rather than in the rootstock ones (Figure 6B).

4. Discussion

To elucidate the metabolite content and the changes resulting from scion–rootstock interactions in nursery-grafted grapevines, we have profiled the metabolome of leaves, stems, and phloem exudate collected from above and below the graft union of 11 graft combinations five to six months after grafting. Results from the PCAs (Figure S1), performed for each of the investigated sample type, indicate that grafting had a minor impact on the metabolome of grapevine when tissues or genotypes were compared. The tissue (e.g., scion stem vs. rootstock stem of the harvested material) is the highest variance factor which is expected considering that scion stems are herbaceous tissues and rootstocks stems are lignified. Interestingly, although the phloem composition is not expected to vary much between grapevines, the phloem exudate deviated more than what was expected.

4.1. Heterografting Enhances Defense-Responses in Both Scions and Rootstocks

Concerning the scale of the scion–rootstock interactions in homografts vs. heterografts, rootstocks are more affected by the presence of a selfgrafting or a heterologous grafting partner than scions are. Indeed 13 and 30 significant changes were detected between at least one homograft vs. one heterograft in scion and rootstock phloem exudates, respectively (being 1 and 16 the consistent changed metabolites respectively, on 78 identified metabolites), and 158 and 159 were the metabolic changes detected in scion and rootstock stems, respectively (being 19 and 35 the consistent changes, on 277 identified metabolites). Considering the source-to-sink flow of photoassimilates and that the scion is the photosynthetic producer of the grafted plant, it is not surprising that the rootstock grafting partner, acting as a net sink, was most affected by the presence of a heterologous one. Qualitatively, the profile of homografts vs. heterografts highlighted that sugars are increased in homograft samples both above and below the

graft union when compared to heterografts (Figures 2A,B and 3B) suggesting a more active carbo metabolism in the leaves of homografts and a more effective phloem translocation across their graft interfaces. Indeed, sugars and GABA were found increased in the rootstock phloem exudate of homografts when compared to heterografts. Recently, GABA was also enriched at the graft interface of homografted grapevines compared to the tissues of scion and rootstock [27]. As GABA is considered an important signaling molecule, with roles in plant responses to stress and the carbon:nitrogen balance [43], the enrichment in GABA in the rootstock phloem exudate of homografts might indicate an earlier or a stronger response against the stress induced (directly or indirectly) by grafting in homografts rather than in heterografts. An increased content in carboxylic acids, possible intermediaries of the TCA cycle, and an enhanced phenolic metabolism was found increased in scion leaves and the stems of heterografts when compared to homografts, while below the union, heterografted stems were enriched in polyhydroxy acids. To the best of our knowledge, an enrichment in acid compounds in leaves and stem samples from heterografts when compared to homografts (both above and below the union) was not previously reported in grafting studies, particularly the enrichment in carboxylic acids identified in scion stems. For more than 30 years, metabolites such as sugars and acetate are known to repress the promoter activities of selected photosynthetic genes, while nitrate, amino acids, and several carboxylic acids are known to induce their transcription [44]. Evidence that TCA cycle intermediates act in regulating transcript abundances has been collected in humans [45], yeasts [46], and plants [47,48] and they are considered good candidate signaling molecules since they reflect both the metabolic and redox status of a cell and are transported between compartments [48]. Therefore, it is not an excluded consideration that the carboxylic acids detected in heterografted scion stems might play a role in the perception of a foreign partner and the

adaptation of its gene expression. Caffeic acid, already proposed as related to pathogen resistance in grapevine [49], culminated with other defense-related compounds were found specifically increased in heterografted stems collected a few centimeters above the graft union. Among these, the phenolic glycoside known as arbutin (hydroxyphenyl beta-glucopyranoside) was identified several times in grapevine pathogenesis studies [50], such as upon colonization by endophytic bacteria [51]. Likewise, a glycoside of salicylic acids, important against biotic threats, and the oligosaccharide galactinol involved in antioxidant protection were more abundant in scion stems of heterografts than in self-grafted grapevines. In leaves, other phenolic compounds and shikimic acid were also reported to be increased in heterografts. Below the union, 2-hydroxy-pyridine, a pyridine-based alkaloid compound known to be induced by stress (especially wounding as feeding deterrent) [52], was increased in the rootstock phloem exudate of heterografted vines. Overall, our study confirms an enhanced phenol metabolism in heterografted grapevines supporting the notion that the presence of a non-selfgrafting partner induces a defense-related response, as previously suggested by comparing the transcriptomes of homografted and heterografted grapevines [32]. In this work, we have shown that the presence of a heterologous scion (Figures 2A and 3A) or rootstock (Figures 2B and 3B), not only leads to a local induction of defense-related compounds but also it is detected in leaf tissue and rootstock phloem exudates. Considering that the highest number of intracellular pathogens ever found in a single crop was recorded in grapevines [53], it would be interesting to verify whether the enhanced stress response imputed to heterografted vines might reflect the perception of a foreign biome and/or the interaction of the grafting partner's biomes when these belong to different genotypes. Indeed, many of the identified defense-related compounds such as phenols, sugars, and metabolites from the salicylic acid pathway were

found altered in virus-infected grapevines [54]. Therefore, it is not an excluded consideration that viruses might have a role in the detection of the heterografting-induced defense response. In this regard, viruses were reported to cause graft incompatibility in grapevines [55], which is understandable given that more than 65 viruses have been recorded to infect grapevines, but just a few of these viruses are tested in the EU certification schemes [56].

4.2. Scions and Rootstocks Are Able to Affect Specific Tissues and Phloem Exudates within the Grafted Plant

In the last decades, several lines of research have focused on the rootstock-induced alterations of several important scion agronomical traits and the interest in deliberately altered phenotypes by mean of grafting [2]. In this study, the results highlighted that in grafted grapevines the rootstock is more affected due to the presence of a heterologous partner than the scion when comparing homografts vs. heterografts. However, whether this impact on the metabolome is directly induced by the rootstock genotype *per se* or if it can be attributed to more complex consequences of an altered rootstock metabolism in response to the scion genotype is unknown. In order to better understand the reciprocal impact of one grafting partner to the other, we compared the metabolome of leaves, stems, and phloem exudate collected from both above and below the graft union of homografts with respective heterografts (Figures 4 and 5). Results showed that the scale of the scion–rootstock reciprocal interaction is relatively small and, at certain times, no metabolite was altered in response to a different grafting partner. Nevertheless, such changes are shown to be differentially driven not only by the specific genotypic graft composition but also by the specific samples, suggesting that scions and rootstocks are able to affect specific organs and phloem exudates within the grafted plant (Figures 4 and 5). For instance, the 110R rootstock

phloem metabolome was more affected by the presence of a different scion genotype than its rootstock stem metabolome. In contrast, no metabolomic effect was observed in the phloem exudate when a different scion genotype was grafted onto a RUP rootstock but the effect was higher and genotypically-driven in the rootstock stem metabolomes. It has recently been proposed, based on metabolic changes detected in grafted citrus trees, that an effect of rootstocks on scions might be driven in a distance-dependent manner [17]. However, we found that in grapevines both grafting partners exert their influence in specific organs and phloem exudates independently of their distance but rather depending on the specific graft combination. Qualitatively, a relative high number of changes were consistently detected in scion leaves that were dependent on the rootstock genotype. Hence, among the investigated samples, leaves seem to be the best tissue to search for grafting-related metabolic markers. As it is shown in Figures 4A and 5A, both American rootstocks (110R and RUP) induced an increase in a compound similar to the carboxylic acid butanedioic acid in scion leaves and stems compared to self-grafted plants. This suggests that this increase is a specific response to the American rootstocks. On ALF scion stems, other carboxylic acid intermediates of the TCA cycle and phenolic compounds were also increased when grafted onto RUP rootstock, while the *myo*-inositol content of both Syrah scion stems was found increased when grafted onto 110R indicating an enhanced defense metabolism of cv. Syrah in response to 110R rootstock. Different grapevine rootstocks were already reported to induce different strategies of defense-related responses in scion leaves and were suspected to be potentially involved in the priming phenomenon, which is a defensive measure in which the plant is in a persistently primed state of enhanced defense readiness [57]. Furthermore, carboxylic acids were suggested to act as priming agents in Arabidopsis under *Pseudomona* infections enhancing gene expression of factors regulating

the salicylic and jasmonic acid defense pathways [58]. Related compounds such as 3-hydroxybutanoic acid was proposed as a downy mildew resistance biomarker of grapevine leaves, while isomers of 2,3,4-trihydroxybutanoic acid and *myo*-inositol were related to the susceptibility [59]. Nevertheless, it remains to be shown whether the defense-related responses induced in the scions by the rootstock enhances stress tolerance or if these defense-responses directly respond to the perception of a different grafting partner (or to its biome). As mentioned, the effect of a scion on the rootstock stem metabolome was stronger in RUP rather than in 110R and the changes were mostly dependent on specific scion-rootstock combinations rather than generalized, as only galactose was found increased in 110R stems due to the effect of both Touriga Nacional clones. SYLV scion affected RUP stems more than ALF did and interestingly led to a depletion in the *myo*-inositol content and to a simultaneous increase in its vanillic acid content, which is a phenolic acid. At this time, available evidence showed that the bacteria and fungi of cucumber (*C. sativus L*) rhizosphere soil responded differently to vanillic acid leading to a lower increase in fungi abundance than in the bacterial one [60]. Furthermore, the soil microbes and the root exudates of grapevines were affected when treated with 4-hydroxybenzoic acids [61]. These findings might be related to the fact that *V. vinifera* subspecies *sylvestris* is known to present a higher tolerance towards downy and powdery mildews and black rot pathogens [49]. In this study, although some sugars were depleted in RUP stems in response to a heterologous scion, especially with SYLV, other sugar compounds were also enhanced suggesting a more balanced carbon metabolism in the graft combinations with RUP rootstocks than the ones with 110R. Indeed, while the scion phloem exudate was barely affected by a heterologous rootstock, except for SY383, all grafts composed of 110R rootstock showed a reduction in sucrose in the phloem harvested below the union, which alerts for a

possible unpaired graft union translocation in *V. vinifera* scions grafted onto 110R.

4.3. Phloem Exudate Composition Appears Significantly Altered between Scion and Rootstock

By profiling the metabolome of scion and rootstock samples, 27% of the phloem exudate metabolome (i.e., 21 on 78 metabolites) was consistently found to differ between scion and rootstock and 40% of the stem metabolome (i.e., 111 on 277 metabolites) was consistently changed between the two analyzed groups. Taking into consideration that phloem composition is not expected to vary much within the same plant species, it is astonishing that almost one-third of the phloem exudate metabolome is altered between scion and rootstock samples within the same grafted plant. Nevertheless, it was recently shown that the metabolic composition of grafted Citrus's phloem content was affected by rootstock–scion interactions [17]. Specifically, it seems that the degree of interaction in the rootstock phloem sap of *Citrus* is greater than the metabolites affected in the scion phloem sap. Furthermore, sucrose and GABA were highlighted among the phloem metabolites affected by both scion and rootstock [17]. We have shown that sucrose was significantly depleted in the phloem exudate composition collected below the graft union compared to the above union. Nevertheless, given that the sugar concentrations did not appreciably change in Eucalyptus phloem sap (bled from cut bark) collected at different trunk heights (from 0.1 to 3 m) [62], the implication of grafting, rather than distance to the source, seems to be a more probable explanation for the detected sucrose depletion in phloem exudate collected from the rootstock. In stems, several compounds were enriched in the scion rather than in the rootstock. Among these, carboxylic acids intermediates of the TCA cycle were again enhanced; quinic and shikimic acids involved in phenol metabolism; a number of polyhydroxy acids;

phenolic compounds such as caffeic acids and a catechin/epicatechin-like compounds; and sugars and polyols including *myo*-inositol described as discriminative of grapevine pathogen resistance [49]. These results, once again, suggest the presence of a defense reaction in scion stems coupled with the accumulation of sugars above the union. On the contrary, several other phenolic compounds were accumulated in rootstocks, such as resveraltrol (*cis*- and *trans*-) and another compound similar to catechin/epicathechin. *Trans*-resveratrol production was identified in grapevine leaves after pathogen infection and described as a precursor to fungal toxicity compounds identified as phytoalexins [63,64]. Similarly, catechin and epicatechin were also proposed as grapevine graft incompatibility markers [28] and were found accumulated in pathogen-susceptible *V. vinifera* cultivars together with caffeic acid [49]. Interestingly, phenols were not only enhanced in the rootstock, which is expected due to the lignification of its tissue but also enhanced in herbaceous scion stems, suggesting a possible role in plant defense. Aside from that, differences in scion and rootstock tissues (age and lignification) must also be taken into consideration since the tissue was revealed as the highest variance factor in the PCA (Supplementary Figure S1). In summary, we have shown that in grapevines both grafting partners can exert their influence in specific organs and phloem exudates, according to the specific graft combination. Heterografting seems to affect rootstocks more than scions and we confirmed that both scion and rootstocks perceive the presence of a heterologous grafting partner leading to the induction of defense-related metabolites. This phenomenon is not only restricted to the cells close to the graft interface, as previously proposed [32], but is also detected in distant leaves. We also conclude that leaves are the best choice of tissue to search for grafting-related metabolic markers as they show more consistent changes (Figure 4A). Notably the effect of a scion on a rootstock was genotypically-driven and not

generalizable (i.e., different scions lead to different effects on rootstocks). Surprisingly, the phloem exudate composition was significantly altered between the scion and rootstock and sucrose was found specifically depleted in the rootstock phloem exudate in several *V. vinifera* scions when grafted onto 110R rootstock suggesting an impaired translocation across the graft union of these grafts. Taking into consideration that the phloem is the main route for the exchange of photoassimilates and signals between grafting partners, more studies on the phloem content seem to be necessary to elucidate the grapevine scion–rootstock interactions.

Acknowledgments

The authors thank the Plansel Nursery and the National Institute for Agricultural and Veterinary Research (INIAV-Dois Portos) for the provision and handling of plant material. We acknowledge Isabel Teixeira for her help in the collection of the samples, Ines Fehrle for carrying out the derivatization of the samples, and Yogeswari Rajarathinam for helping in the heat maps R coding.

References

1. Juniper, B.E. The Mysterious Origin of the Sweet Apple. *Am. Sci.* **2007**, 95, 44–51.
2. Assunção, M.; Tedesco, S.; Fevereiro, P. Molecular Aspects of Grafting in Woody Plants. In *Annual Plant Reviews Online*, 1st ed.; Wiley Online Library: New York, NY, USA, 2021; Volume 4, pp. 87–126.
3. Tandonnet, J.P.; Cookson, S.J.; Vivin, P.; Ollat, N. Scion genotype controls biomass allocation and root development in grafted grapevine. *Aust. J. Grape Wine Res.* **2010**, 16, 290–300.
4. Ahsan, M.U.; Hayward, A.; Alam, M.; Hiti-Bandaralage, J.; Topp, B.; Beveridge, C.A.; Mitter, N. Scion control of miRNA abundance and tree maturity in grafted avocado. *BMC Plant Biol.* **2019**, 19, 1–11.
5. Foster, T.M.; McAtee, P.A.; Waite, C.N.; Boldingh, H.L.; McGhie, T.K. Apple dwarfing rootstocks exhibit an imbalance in carbohydrate allocation and reduced cell growth and metabolism. *Hortic. Res.* **2017**, 4, 1–13.
6. Han, Q.; Guo, Q.; Korpelainen, H.; Niinemets, Ü.; Li, C. Rootstock determines the drought resistance of poplar grafting combinations. *Tree Physiol.* **2019**, 39, 1855–1866.

7. Zhang, Z.; Cao, B.; Gao, S.; Xu, K. Grafting improves tomato drought tolerance through enhancing photosynthetic capacity and reducing ROS accumulation. *Protoplasma* **2019**, 256, 1013–1024.
8. Yan, Y.; Wang, S.; Wei, M.; Gong, B.; Shi, Q. Effect of Different Rootstocks on the Salt Stress Tolerance in Watermelon Seedlings. *Hortic. Plant J.* **2018**, 4, 239–249.
9. Zhang, H.; Li, X.; Zhang, S.; Yin, Z.; Zhu, W.; Li, J.; Meng, L.; Zhong, H.; Xu, N.; Wu, Y.; et al. Rootstock alleviates salt stress in grafted mulberry seedlings: Physiological and PSII function responses. *Front. Plant Sci.* **2018**, 871, 1–11.
10. Rasool, A.; Mansoor, S.; Bhat, K.M.; Hassan, G.I.; Rehman Baba, T.; Nasser Alyemeni, M.; Alsahli, A.A.; El-Serehy, H.A.; Paray, B.A.; Ahmad, P. Mechanisms Underlying Graft Union Formation and Rootstock Scion Interaction in Horticultural Plants. *Front. Plant Sci.* **2020**, 11, 590847, doi:10.3389/fpls.2020.590847.
11. Albacete, A.; Martínez-Andújar, C.; Martínez-Pérez, A.; Thompson, A.J.; Dodd, I.C.; Pérez-Alfocea, F. Unravelling rootstock×scion interactions to improve food security. *J. Exp. Bot.* **2015**, 66, 2211–2226.
12. Goldschmidt, E.E. Plant grafting: New mechanisms, evolutionary implications. *Front. Plant Sci.* **2014**, 5, 1–9.
13. Haywood, V.; Kragler, F.; Lucas, W.J. Plasmodesmata: Pathways for protein and ribonucleoprotein signaling. *Plant Cell* **2002**, 14, 303–326.
14. Melnyk, C.W.; Meyerowitz, E.M. Plant grafting. Curr. Biol. 2015, 25, R183–R188.
15. Lough, T.J.; Lucas, W.J. Integrative plant biology: Role of phloem long-distance macromolecular trafficking. *Annu. Rev. Plant Biol.* **2006**, 57, 203–232.
16. Corbesier, L.; Vincent, C.; Jang, S.; Fornara, F.; Fan, Q.; Searle, I.; Giakountis, A.; Farrona, S.; Gissot, L.; Turnbull, C.; et al. FT Protein Movement Contributes to Long-Distance Signaling in Floral Induction of *Arabidopsis*. *Science* **2007**, 316, 1030–1033.
17. Tietel, Z.; Srivastava, S.; Fait, A.; Tel-Zur, N.; Carmi, N.; Raveh, E. Impact of scion/rootstock reciprocal effects on metabolomics of fruit juice and phloem sap in grafted *Citrus* reticulata. *PLoS ONE* **2020**, 15, 1–17.
18. Tetyuk, O.; Benning, U.F.; Hoffmann-Benning, S. Collection and analysis of *Arabidopsis* phloem exudates using the EDTAfacilitated Method. *J. Vis. Exp.* **2013**, 80, e51111.
19. Notaguchi, M.; Okamoto, S. Dynamics of long-distance signaling via plant vascular tissues. *Front. Plant Sci.* **2015**, 6, 161.
20. Melnyk, C.W.; Gabel, A.; Hardcastle, T.J.; Robinson, S.; Miyashima, S.; Grosse, I.; Meyerowitz, E.M. Transcriptome dynamics at *Arabidopsis* graft junctions reveal an intertissue recognition mechanism that activates vascular regeneration. *Proc. Natl. Acad. Sci. USA* **2018**, 115, E2447–E2456.
21. Chen, Z.; Zhao, J.; Hu, F.; Qin, Y.; Wang, X.; Hu, G. Transcriptome changes between compatible and incompatible graft combination of *Litchi chinensis* by digital gene expression profile. *Sci. Rep.* **2017**, 7, 1–12.
22. He, W.; Wang, Y.; Chen, Q.; Sun, B.; Tang, H.R.; Pan, D.M.; Wang, X.R. Dissection of the Mechanism for Compatible and Incompatible Graft Combinations of *Citrus grandis* (L.) Osbeck ('Hongmian Miyou'). *Int. J. Mol. Sci.* **2018**, 19, 505.

23. Assunção, M.; Santos, C.; Brazão, J.; Eiras-Dias, J.E.; Fevereiro, P. Understanding the molecular mechanisms underlying graft success in grapevine. *BMC Plant Biol.* **2019**, 19, 1–17.
24. Shen, Y.; Zhuang, W.; Tu, X.; Gao, Z.; Xiong, A.; Yu, X.; Li, X.; Li, F.; Qu, S. Transcriptomic analysis of interstock-induced dwarfism in Sweet Persimmon (*Diospyros kaki Thunb.*). *Hortic. Res.* **2019**, 6, 1–17.
25. Liu, X.Y.; Li, J.; Liu, M.M.; Yao, Q.; Chen, J.Z. Transcriptome profiling to understand the effect of *citrus* rootstocks on the growth of 'Shatangju' mandarin. *PLoS ONE* **2017**, 12, 1–22.
26. Tzarfati, R.; Ben-Dor, S.; Sela, I.; Goldschmidt, E.E. Graft-induced Changes in MicroRNA Expression Patterns in *Citrus* Leaf Petioles. *Open Plant Sci. J.* **2013**, 7, 17–23.
27. Prodhomme, D.; Fonayet, J.V.; Hévin, C.; Franc, C.; Hilbert, G.; de Revel, G.; Richard, T.; Ollat, N.; Cookson, S.J. Metabolite profiling during graft union formation reveals the reprogramming of primary metabolism and the induction of stilbene synthesis at the graft interface in grapevine. *BMC Plant Biol.* **2019**, 19, 1–12.
28. Assunção, M.; Pinheiro, J.; Cruz, S.; Brazão, J.; Queiroz, J.; Eiras Dias, J.E.; Canas, S. Gallic acid, sinapic acid and catechin as potential chemical markers of *Vitis* graft success. *Sci. Hortic.* **2019**, 246, 129–135.
29. Assunção, M.; Canas, S.; Cruz, S.; Brazão, J.; Zanol, G.C.; Eiras-Dias, J.E. Graft compatibility of *Vitis* spp.: The role of phenolic acids and flavanols. *Sci. Hortic.* **2016**, 207, 140–145.
30. Usenik, V.; Krška, B.; Vičan, M.; Štampar, F. Early detection of graft incompatibility in apricot (*Prunus armeniaca L.*) using phenol analyses. *Sci. Hortic.* **2006**, 109, 332–338.
31. Irisarri, P.; Zhebentyayeva, T.; Errea, P.; Pina, A. Differential expression of phenylalanine ammonia lyase (PAL) genes implies distinct roles in development of graft incompatibility symptoms in *Prunus*. *Sci. Hortic.* **2016**, 204, 16–24.
32. Cookson, S.J.; Clemente Moreno, M.J.; Hevin, C.; Nyamba Mendome, L.Z.; Delrot, S.; Magnin, N.; Trossat-Magnin, C.; Ollat, N. Heterografting with nonself rootstocks induces genes involved in stress responses at the graft interface when compared with autografted controls. *J. Exp. Bot.* **2014**, 65, 2473–2481.
33. Tedesco, S.; Pina, A.; Fevereiro, P.; Kragler, F. A Phenotypic Search on Graft Compatibility in Grapevine. *Agronomy* **2020**, 10, 706.
34. Erban, A.; Martinez-Seidel, F.; Rajarathinam, Y.; Dethloff, F.; Orf, I.; Fehrle, I.; Alpers, J.; Beine-Golovchuk, O.; Kopka, J. Multiplexed Profiling and Data Processing Methods to Identify Temperature-Regulated Using Gas Chromatography Coupled to Mass Spectrometry. *In Plant Cold Acclimation. Methods in Molecular Biology*, 1st ed.; Hincha, D., Zuther, E., Eds; Humana: New York, NY, USA, 2020; Volume 2156, pp. 203–239.
35. Luedemann, A.; Strassburg, K.; Erban, A.; Kopka, J. TagFinder for the quantitative analysis of gas chromatography-Mass spectrometry (GC-MS)-based metabolite profiling experiments. *Bioinformatics* **2008**, 24, 732–737.

36. Kopka, J.; Schauer, N.; Krueger, S.; Birkemeyer, C.; Usadel, B.; Bergmüller, E.; Dörmann, P.; Weckwerth, W.; Gibon, Y.; Stitt, M.; et al. GMD@CSB.DB: The Golm metabolome database. *Bioinformatics* **2005**, 21, 1635–1638.
37. Erban, A.; Schauer, N.; Fernie, A.R.; Kopka, J. Nonsupervised Construction and Application. In *Metabolomics: Methods and Protocols*, 1st ed.; Weckwerth, W., Ed.; Humana Press: Totowa, NJ, USA, 2007; Volume 358, pp. 19–38.
38. Erban, A.; Fehrle, I.; Martinez-Seidel, F.; Brigante, F.; Lucini Más, A.; Baroni, V.; Wunderlin, D.; Kopka, J. Discovery of food identity markers by metabolomics and machine learning technology. *Sci. Rep.* **2019**, 9, 1–19.
39. Chong, J.; Xia, J. MetaboAnalystR: An R package for flexible and reproducible analysis of metabolomics data. *Bioinformatics* **2018**, 34, 4313–4314.
40. Gu, Z.; Eils, R.; Schlesner, M. Complex heatmaps reveal patterns and correlations in multidimensional genomic data. *Bioinformatics* **2016**, 32, 2847–2849.
41. Mandal, S.M.; Chakraborty, D.; Dey, S. Phenolic acids act as signaling molecules in plant-microbe symbioses. *Plant Signal. Behav.* **2010**, 5, 359–368.
42. Santos-Sánchez, N.F.; Salas-Coronado, R.; Hernández-Carlos, B.; Villanueva-Cañongo, C. Shikimic Acid Pathway in Biosynthesis of Phenolic Compounds. In *Plant Physiological Aspects of Phenolic Compounds*, 1st ed.; Soto-Hernández, M., GarcíaMateos, R., Palma-Tenango, M., Eds.; IntechOpen: London, UK, 2019; Volume 395, pp. 116–124.
43. Bouché, N.; Fromm, H. GABA in plants: Just a metabolite? *Trends Plant Sci.* **2004**, 9, 110–115.
44. Sheen, J. Metabolic repression of transcription in higher plants. *Plant Cell* **1990**, 2, 1027–1038.
45. Yang, M.; Soga, T.; Pollard, P.J.; Adam, J. The emerging role of fumarate as an oncometabolite. *Front. Oncol.* **2012**, 2, 1–7.
46. McCammon, M.T.; Epstein, C.B.; Przybyla-Zawislak, B.; McAlister-Henn, L.; Butow, R.A. Global Transcription Analysis of Krebs Tricarboxylic Acid Cycle Mutants Reveals an Alternating Pattern of Gene Expression and Effects on Hypoxic and Oxidative Genes. *Mol. Biol. Cell* **2003**, 14, 958–972.
47. Müller, C.; Scheible, W.-R.; Stitt, M.; Krapp, A. Influence of malate and 2-oxoglutarate on the NIA transcript level and nitrate reductase activity in tobacco leaves. *Plant. Cell Environ.* **2001**, 24, 191–203.
48. Finkemeier, I.; König, A.-C.; Heard, W.; Nunes-Nesi, A.; Pham, P.A.; Leister, D.; Fernie, A.R.; Sweetlove, L.J. Transcriptomic analysis of the role of carboxylic acids in metabolite signaling in *arabidopsis* leaves. *Plant Physiol.* **2013**, 162, 239–253.
49. Maia, M.; Ferreira, A.E.N.; Nascimento, R.; Monteiro, F.; Traquete, F.; Marques, A.P.; Cunha, J.; Eiras-Dias, J.E.; Cordeiro, C.; Figueiredo, A.; et al. Integrating metabolomics and targeted gene expression to uncover potential biomarkers of fungal/oomycetes-associated disease susceptibility in grapevine. *Sci. Rep.* **2020**, 10, 1–15.

50. Filippi, A.; Petrussa, E.; Boscutti, F.; Vuerich, M.; Vrhovsek, U.; Rabiei, Z.; Braidot, E. Bioactive polyphenols modulate enzymes involved in grapevine pathogenesis and chitinase activity at increasing complexity levels. *Int. J. Mol. Sci.* **2019**, 20, 6357.
51. Lòpez-Fernàndez, S.; Compant, S.; Vrhovsek, U. Grapevine colonization by endophytic bacteria shifts secondary metabolism and suggests activation of defense pathways. *Plant Soil* **2016**, 405, 155–175.
52. Noctor, G.; Queval, G.; Gakière, B. NAD(P) synthesis and pyridine nucleotide cycling in plants and their potential importance in stress conditions. *J. Exp. Bot.* **2006**, 57, 1603–1620.
53. Martelli, G.P. Directory of virus and virus-like diseases of the grapevine and their agents. *J. Plant Pathol.* **2014**, 96, 1–136.
54. Wallis, C.M.; Sudarshana, M.R. Effects of Grapevine red blotch-associated virus (GRBaV) infection on foliar metabolism of grapevines. *Can. J. Plant Pathol.* **2016**, 38, 358–366.
55. Rowhani, A.; Uyemoto, J.K.; Golino, D.A.; Daubert, S.D.; Al Rwahnih, M. Viruses Involved in Graft Incompatibility and Decline. In *Grapevine Viruses: Molecular Biology, Diagnostics and Management*; Meng, B., Martelli, G.P., Golino, D.A., Fuchs, M., Eds.; Springer International Publishing: Cham, Switzerland, 2017; pp. 289–302.
56. Martelli, G.P. An Overview on Grapevine Viruses, Viroids, and the Diseases They Cause. In *Grapevine Viruses: Molecular Biology, Diagnostics and Management*, Meng, B., Martelli, G.P., Golino, D.A., Fuchs, M., Eds.; Springer International Publishing: Cham, Switzerland, 2017; pp. 31–46.
57. Chitarra, W.; Perrone, I.; Avanzato, C.G.; Minio, A.; Boccacci, P.; Santini, D.; Gilardi, G.; Siciliano, I.; Gullino, M.L.; Delledonne, M.; et al. Grapevine Grafting: Scion Transcript Profiling and Defense-Related Metabolites Induced by Rootstocks. *Front. Plant Sci.* **2017**, 8, 654.
58. Balmer, A.; Pastor, V.; Glauser, G.; Mauch-Mani, B. Tricarboxylates induce defense priming against bacteria in *Arabidopsis thaliana. Front. Plant Sci.* **2018**, 9, 1–15.
59. Batovska, D.I.; Todorova, I.T.; Parushev, S.P.; Nedelcheva, D.V.; Bankova, V.S.; Popov, S.S.; Ivanova, I.I.; Batovski, S.A. Biomarkers for the prediction of the resistance and susceptibility of grapevine leaves to downy mildew. *J. Plant Physiol.* **2009**, 166, 781–785.
60. Zhou, X.; Wu, F. Artificially applied vanillic acid changed soil microbial communities in the rhizosphere of cucumber (*Cucumis sativus L.*). *Can. J. Soil Sci.* **2013**, 93, 13–21.
61. Guo, X.W.; Wang, B.; Li, K.; Liu, Z.-D.; Han, X.; Xu, S.-J.; Guo, Y.-S.; Xie, H.-J. Effect of 4-hydroxybenzoic acid on grape (*Vitis vinifera l.*) soil microbial community structure and functional diversity. *Biotechnol. Biotechnol. Equip.* **2015**, 29, 637–645.
62. Pate, J.; Shedley, E.; Arthur, D.; Adams, M. Spatial and temporal variations in phloem sap composition of plantation-grown *Eucalyptus globulus*. *Oecologia* **1998**, 117, 312–322.
63. Jeandet, P.; Douillet-Breuil, A.C.; Bessis, R.; Debord, S.; Sbaghi, M.; Adrian, M. Phytoalexins from the *vitaceae*: Biosynthesis, phytoalexin gene expression in

transgenic plants, antifungal activity, and metabolism. *J. Agric. Food Chem.* **2002**, 50, 2731–2741.

64. Chitarrini, G.; Soini, E.; Riccadonna, S.; Franceschi, P.; Zulini, L.; Masuero, D.; Vecchione, A.; Stefanini, M.; Di Gaspero, G.; Mattivi, S.; et al. Identification of biomarkers for defense response to *Plasmopara viticola* in a resistant grape variety. *Front. Plant Sci.* **2017**, 8, 1–11.

Supplementary Materials

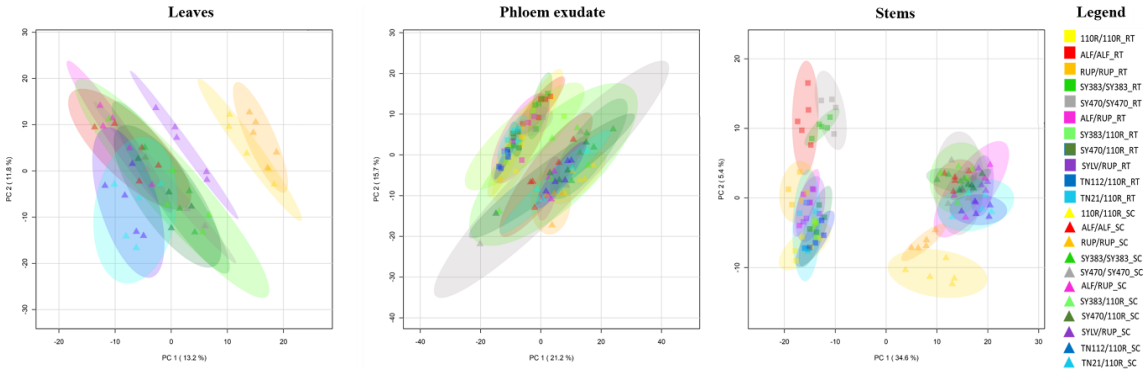

(**a**) (**b**) (**c**)

Figure S1. Scores plot between the first two components of each separate PCA: (**a**) in leaves; (**b**) phloem exudate; and (**c**) stems datasets for all analyzed samples. The variances are shown in brackets and the ellipses show 95% confidence intervals. The square symbol indicates samples collected from the rootstock and the triangle samples collected from the scion. Different colors discriminate the graft combination analyzed. (n = 5 per graft combination, except for SY470 homografts for which n = 4).

Table S1. Graft combination and graft type analyzed.

Graft combination	Scion species	Rootstock species	Graft type
110R/110R	(*V. berlandieri* x *V. rupestris*)	(*V. berlandieri* x *V. rupestris*)	Homograft
ALF/ALF	*V. vinifera* cv. Alfrocheiro	*V. vinifera* cv. Alfrocheiro	Homograft
RUP/RUP	*V. rupestris Du Lot*	*V. rupestris Du Lot*	Homograft
SY383/SY383	*V. vinifera* cv. Syrah, clone 383	*V. vinifera* cv. Syrah, clone 383	Homograft
SY470/SY470	*V. vinifera* cv. Syrah, clone 470	*V. vinifera* cv. Syrah, clone 470	Homograft
ALF/RUP	*V. vinifera* cv. Alfrocheiro	*V. rupestris Du Lot*	Heterograft
SYLV/RUP	*V. vinifera* subsp. *Sylvestris*	*V. rupestris Du Lot*	Heterograft
SY383/110R	*V. vinifera* cv. Syrah, clone 383	(*V. berlandieri* x *V. rupestris*)	Heterograft
SY470/110R	*V. vinifera* cv. Syrah, clone 470	(*V. berlandieri* x *V. rupestris*)	Heterograft
TN112/110R	*V. vinifera* cv. Touriga Nacional, clone 112	(*V. berlandieri* x *V. rupestris*)	Heterograft
TN21/110R	*V. vinifera* cv. Touriga Nacional, clone 21	(*V. berlandieri* x *V. rupestris*)	Heterograft

Table S2. Excel file of raw data, statistic results, and experimental details. Leaves, phloem exudate, and stems datasets are contained in separated spreadsheets. Available at: https://www.mdpi.com/2218-1989/11/6/349#cite

Chapter IV

Dissecting grapevine graft formation and graft incompatibility in vitro

This chapter was prepared to be submitted for future publication.

In this research paper, Sara Tedesco performed the grafting and the phenotyping methods, the molecular detection of viruses, the data analysis, and participated in the writing of the manuscript.

Abstract

For a long time, grafting is used for Phylloxera-control permitting vineyards establishment and the propagation of *Vitis vinifera spp*. However, graft incompatibility problems are affecting grapevine nurseries and growers as well threatening its longevity. Several challenges hinder the identification of graft incompatibility causes, affecting the possibility for its early prediction. In this work, we aimed to evaluate the use of *in vitro* micrografting coupled with histology and histochemistry analysis, in order to unravel physiological markers that forecast incompatible responses in grapevine graft combinations of known compatibility behaviour. The time frame of grapevine micrograft formation and the suitability of the system for graft incompatibility prediction were assessed. Particularly, we highlighted the utility of evaluating the graft interface cellular arrangement and starch content via calcofluor and I_2KI staining, respectively. Surprisingly, heterografts failures displayed viral symptoms while translocated incompatibility symptoms were observed in successful heterografts. In this regard, levels of Grapevine Rupestris Stem Pitting associated Virus (GRSPaV) infections were correlated with graft (un)-success in two Syrah clones grafted onto 110-Ritcher rootstock under field and *in vitro* conditions. Furthermore, wounded and grafted Syrah plantlets pointed out to an impaired sucrose distribution in these plants, possibly implicated with GRSPaV infection. Given the evidences provided, we suggest that grapevine graft incompatibility might be a virus-induced problem which can arise even employing certified virus-free plants.

Keywords: Grafting, GRSPaV, Histology, Micrografting, Syrah, Virus

1. Introduction

Grafting is a technique used since ancient times in horticulture and orchards as a tool for plant propagation and improvement. It was a pivotal discovery for the domestication of temperate fruit trees and enabled the intensification of much of their production as more than 70 woody crops are grown on rootstocks and 20 of the 25 most-produced fruit and nut crops are also grafted under certain circumstances [1]. For more than a century, grafting is being exploited as a biological alternative to control soil-borne Phylloxera in vineyards. More than 80% of the vineyards all over the world are currently composed of *Vitis vinifera* scions grafted onto Phylloxera-resistant American rootstocks or their improved hybrids [2]. Despite these benefits, grafting also constitutes a door for the entrance and the dissemination of pathogens and diseases and graft incompatibility can result in propagation losses affecting the ultimate performance of a grafted plant. Graft incompatibility is defined as the failure to form a successful graft union between two plant parts when all other requirements, such as technique, timing, phytosanitary and environmental conditions are satisfied [3]. Considering that graft incompatibility can manifest in short-term graft failure or long-term vine decline in vineyards, this agronomic trait causes economic losses to breeders and growers and threaten the longevity of the vineyards. Despite centuries of research, the phenomenon of graft incompatibility remains a mystery as well as the mechanisms of graft formation, the interactions between scions and rootstocks, the graft-induced alteration of plant traits, and the occurrence of graft-transmissible diseases, which are still insufficiently understood by the scientific community [4,5]. Graft incompatibility research is mainly limited by the large number of genotypes that can be grafted and thus by the wide range of different physiological, biochemical, and anatomical interactions that can arise hindering the identification of the causes of

incompatibility and the search for methods to early predict incompatible responses [6,7]. Although predicting graft incompatibility would be tremendously useful in rootstock breeding programs, this is a real challenge [5]. Traditionally, graft incompatibility has been classified in translocated and localized in fruit trees [8]. In peach/plum combinations, translocated incompatibility was associated with accumulation of starch above the union, phloem degeneration and early effects on growth [9]. Conversely, localized incompatibility is characterized by poor vascular connections leading to mechanical weakness and subsequent breakdown in apricot (*Prunus armeniaca*) when grafted on other *Prunus* species [10] and starvation of the root system with slow development of external symptoms [11]. Previous to the classification of Mosse, another classification included graft failure due to virus and phytoplasma [12] as a virus-induced graft incompatibility type, which has been reported in orange trees, sweet cherry, walnut, apple trees [8], and in grapevines [13]. However, the virus-induced graft incompatibility type is often excluded in the grafting literature. Grapevine is the crop with the highest number of intracellular pathogens, among which viruses has a major role. Nevertheless the EU grapevine nursery industry is allowed to produce and release “certified” material with a lamentably low sanitary standard [14]. Hence, it is unsure whether the use of certified vines is sufficient to exclude the occurrence of virus-induced graft incompatibility problems in grapevines.

In the last decades, *in vitro* micrografting has been used as an experimental system for graft incompatibility studies and has enabled researchers to bypass several *in vivo* constraints such as minimizing environmental variability and biotic interferences, and allowing an early detection [15–17]. Localized incompatibility was studied using *in vitro* systems through histological observation of the graft union in apricot grafts

[10,18] and pear demonstrating a deficient translocation in incompatible pear/quince grafts [19]. Additionally, translocation of carboxyfluorescein diacetate (CFDA) permitted to identify the time frame of phloem and xylem connections in Arabidopsis micrografts [20]. Several histochemistry analysis have been applied to identify specific compounds implicated in the scion–rootstock interaction, such as cellulose, lignin, phenols, and starch in several fruit trees [10,18,21]. Although grapevine micrografting was recently used to identify incompatible interactions of rootstocks with virus-infected scions of Cabernet Franc [16], few histochemical observations have been performed during graft union development in grapevine so far. In this work, the main goal was to assess the suitability of *in vitro* systems as early detection methods for grapevine graft incompatibility and to identify early cellular signs eventually leading to a perturbed graft union formation**.** For this purpose, we observed the response of certified virus-free homo- and heterografted grapevine micrografts, with known graft compatibility response when grafted onto the worldwide used rootstock Ritcher-110 (110R, *V. berlandieri* x *V. rupestris*).

2. Material and methods

2.1. Plant material and in vitro establishment

Scion branches of certified virus-free plants of four registered *V. vinifera* clones cv. “Touriga Nacional”, clone 21 ISA/PT and clone 112 JBP/PT (TN21 and TN112 respectively) and cv. “Syrah”, ENTAV-INRA/FR clones 383 and 470 (SY383 and SY470 respectively) were collected from the Portuguese National Ampelographic Collection (PRT051), located at Quinta da Almoinha, Dois Portos, Torres Vedras, Portugal (39°02′34.03″N, −9°10′57.41″W) in July 2017. Branches from the rootstock genotype Ritcher-110 (*V. berlandieri* x *V. rupestris*, JBP/PT clone, 110R) were harvested from an ungrafted plant maintained under greenhouse

conditions. At the collection time, young leaves from each plant genotype were frozen in liquid Nitrogen and store at -80 ºC until tested in the virology Laboratory of the National Institute for Agricultural and Veterinary Research (INIAV, Portugal) to confirm the absence of GLRaV1, GLRaV2, GLRaV3, ArMV by DAS-ELISA, and of GFkV by DASI-ELISA using commercially available antisera. 11 nodal segments from all genotypes were excised and left at least one hour under running water to get rid of fungal sporous before proceeding to their *in vitro* establishment. After that, the washed nodal segments were immersed under 100 mL of 30% commercial bleach [v/v] (Domestos® Unilever, Portugal with ≤ 5 % active chlorine) in dH_2O, shaken for 15 minutes, and rinsed in sterile dH_2O three times. Finally, explants were dried in sterile filter paper, placed in test tube containing grapevine culture media and maintained in a growth chamber under 16/8 hours of photoperiod and 24+/-1 ºC. The grapevine culture agarose (7 g/L) jelly media consisted of 1/2-strength macro- and micro-elements of Murashige and Skoog (1962) [22] supplemented with 1 mL/L vitamins [23], 30 g/L sucrose, and 5 mg/L dithiothreitol. The pH of the media was adjusted to 6.0 prior to autoclaving.

2.2. Micrografting and time-points selection

Slit micrografting of SY470 and 110R homografts (i.e. SY470/SY470 and 110R/110R, respectively) were established according to Yildirim et al., (2010) [24]. The graft junction of 4 – 6 biological repetitions of SY470/SY470 micrografts per time point (21, 28, 35, 42 and 49 days after grafting (DAG)), were excised and fixed in formaldehyde - acetic acid – 70% alcohol (1:1:18, FAA), kept at room temperature for 48h and dehydrated on 70%, 80%, 96%, and 100% ethanol solutions for a minimum of 2h immersion per solution. Later on, samples were histologically processed for paraffin embedding, sectioned (10 µm), and stained with 0.5% toluidine blue solution for 20 seconds by the Histology

Service of “Instituto Gulbenkian de Ciencia”, Oeiras, Portugal. The provided stained slides were visualized and captured at various magnifications in bright field using a Leica DM6 B microscope, a Leica DFC7000 T camera and Leica LASX software (Nussloch, Germany) to monitor the healing of the graft union at the collection time points. To assess the functionality of the scion-rootstock vascular connections, micrografting of 110R homografts were performed and 6 – 8 grafts per time-point were sampled at 28, 35, 42, 49, and 60 DAG. One scion’s severed petiole per graft was submerged in a solution of Propidium Iodide (PI) (10 µg/mL in dH_2O) and carboxyfluorescein diacetate (CFDA) dye (1:10 dilution in dH_2O from 5 mg/mL in acetone stock solution) and incubated for 20 minutes. Fresh longitudinal vibratome sections (70 µm) of the graft zone were made and CFDA translocation between the grafting partners was visually assessed and captured in bright field and in fluorescent images at 5X magnification under the same microscope using a Leica L5 fluorescent filter.

2.3. Assessment of graft success and graft development

Micropropagated plants of the clones TN112, TN21, SY383, SY470 and the rootstock 110R were used to establish micrografts from the following homo- and heterografted combinations with known compatibility: TN21/TN21, TN112/TN112, SY383/SY383, SY470/SY470, 110R/110R, TN21/110R, TN112/110R, SY383/110R and SY470/110R from May to August 2018. TN112 grafted onto 110R (TN112/110R) is reported as less graft compatible than its clone TN21/110R [3], and SY383/110R shows more problems of graft incompatibility related to the “Syrah decline” than SY470/110R so that SY383 is no longer available into the market [25]. At 28 and 49 DAG, 5 grafts per combination and time-point were fixed in FAA (excepting 110R/110R for which just one graft was fixed at 49 DAG), dehydrated and histologically processed for paraffin embedded for further

histochemistry analysis. Fixed grafts were chosen among the best-looking ones at 28 DAG while grafts were considered successful when growth of the scion and/or rooting of the rootstock was observed at 49 DAG. Graft success (%) and the collection of phenotypic parameters including growth of the scion (cm), number of roots, and length of the main root (cm) were recorded at 49 DAG. Grafts that would survive in field, such as grafts with roots developed at the graft zone or with rootstock thief branches, were considered successful but not phenotypically screened. Conversely, grafted plants that did not respond to grafting (i.e., no growth of the scion and no rooting observed at 49 DAG) were considered unsuccessful.

2.4. Grapevine Rupestris Stem Pitting associated Virus (GRSPaV) detection in non-grafted plants

Since all plants of Touriga Nacional clones died in 2019, the presence of GRSPaV in leaves of non-grafted remaining *in vitro* plant material (SY383, SY470, and 110R) were assessed by real-time quantitative polymerase chain reaction (RT-qPCR) in September 2020. Isolation of total RNA and DNase treatment were carried out according to Assunção et al., (2019) [3] using leaves of 3 biological repetitions per genotype, being each repetition a pool of leaves from 3 plants. For cDNA synthesis 200 ng of total RNA per sample was used in 20 µl ImProm-II™ Reverse Transcriptase reaction (Promega, Madison, WI, USA) with a universal poly(T) primer (10 mM) following the manufacturer's instructions. RT-qPCR reactions for each cDNA sample and for non-template (water) controls were carried out on a LightCycler 480 system (Roche Diagnostics, Penzberg, Germany) using the published "48V/49C" universal GRSPaV primers [26] to amplify 331 bp of the viral target coat protein (CP) and ubiquitin (UBI) primers (forward: AGTAGATGATGACTGGATTGGAGGT, and reverse: GAGTATCAAAACAAAAGCATCG, 177 bp. NCBI accession:

XM_002273532.2) as reference gene for relative quantification. The selected reference gene primers were previously screened for their efficiency, as well as for their stability across the different genotypes, by RT-qPCR amplification and the web-based RefFinder platform (https://www.heartcure.com.au/reffinder/, accessed at 21.12.2020) [27]. PCR mix contained 10 µl SYBR Green SuperMix (Quanta Biosciences, Gaithersburg, MD, USA), 0.6 µl / primer (10 mM), and 1.25 ng of total RNA equivalent of cDNA template in 20 µl reaction volume. All RT-qPCR reactions were run with the following cycle conditions: 5 min at 95 °C, followed by 45 cycles of 95 °C for 10 sec, 55 °C for 10 sec, and 72 °C for 30 sec. Melting curve analysis (up to 97 ºC) was performed following amplification using LightCycler® 480 Software Release 1.5.1.62 SP3. Cycle Threshold (Ct) values provided by the software were used to compile the relative expression values (fold change) of the target viral transcript in leaves of SY383 and SY470 following normalization to the control sample (leaves of 110R) and to the reference gene (UBI) using the Pfaffl method [28]. Finally, fold change data were transformed into a logarithmic scale (base 2) for graph representation and statistical analyses.

2.5. Histochemical observation of in vitro graft unions and quantification

3 of the 5 paraffin embedded grafts per combination and time-point (28 and 49 DAG) were sectioned at 10 µm under a rotary microtome (Leica RM2255) and stained with different dyes for histochemistry analysis. 0.07% (w/v) calcofluor in dH_2O (30 sec incubation) was used to stain cellulose in the cell wall [29], 0.01% (w/v) acridine orange (30 sec incubation) for lignified cell walls [30], phloroglucinol-HCl (10% phloroglucinol in 100% ethanol for 3 min followed by 3 min incubation in 37% HCl) for lignins [31], 0.5% (w/v) toluidine blue (1.5 min incubation) for phenols, potassium iodide-iodine reaction (I_2KI) (2 g of potassium iodide

(IK) and 0.2 g of iodine (I) were dissolved in 100 mL of distilled water, 10 min incubation) for starch, and 0.1% (w/v) aniline blue (10 min incubation) for callose deposition [32]. The samples were viewed under a Leitz Ortholux II fluorescence microscope (Leitz,Wetzal, Germany) equipped with a Leica DC300 camera. The epifluorescence of calcofluor, acridine orange, and aniline blue staining was detected using a BP355-425 excitation filter and a LP460 emission filter. The assignment of phenotypic scores to graft combinations was based on cellular arrangement detected with calcofluor (i.e., A = low arrangement, B = intermediate, and C = high arrangement), and grade of differentiation using acridine orange (A = low differentiation, B = intermediate, C = high differentiation). Similarly, three phenotypic classes were assigned to toluidine blue and phloroglucinol-HCl stained sections depending on the intensity of staining (A = low staining, B = intermediate, C = high staining), although phloroglucinol-HCl staining was evaluated just at the necrotic layer separating the two grafting partners. An example for each of the attributed phenotypic scores at 28 and 49 DAG is shown in Supplementary Figure S1. I_2KI stained images were used to quantify the number of starch granules per cell. Starch quantification was made by measuring starch granules in grids of equal area using Fiji/ImageJ (National Institute of Health, USA, version 1.52p) in three biological repetitions (captured images) per graft combination. Three randomly chosen grids on the scion and three on the rootstock were selected to record the number of starch granules and of cells per grid used to calculate the final number starch granules per cell. Only completely captured cells and their starch contents were counted in each grid. The same approach and number of samples were used to analyse aniline blue stained images to compile the number of callose deposition per cell. Data are presented as mean value ± SE.

2.6. Plant monitoring in response to wounding and to sucrose

Micropropagated SY383, SY470, and 110R (3.5 months *in vitro*) plants were cut at their shoot base and 3 plants / genotype were placed on a culture box containing new media (supplemented with 3% sucrose) in May 2020. 3 culture boxes were prepared per genotype (total of 9 plants per genotype). Images of the plant phenotype after wounding was recorded at least once every 10 days with a camera (Olympus OM-D EM5 MarkII, Tokyo, Japan) for > 4 months until plant recovery or plant death. Additionally, plantlets of SY383 and SY470 were cut and placed on new culture media supplemented with 3%, 1.5%, and 0% sucrose for a total of 9 plants / genotype / treatment. Visual phenotypic response of these plants to the media treatment was recorded 1 and 3 months after wounding. On June 2020, 6 homografts of SY383 were made and placed on culture media supplemented with 3%, 1.5%, and 0% sucrose. Their phenotypic response was recorded at least once every 10 days with a camera. Note that after one month in culture, SY383/SY383 under 3% sucrose contaminated and their image capturing suspended few weeks later. Image capturing lasted 3 months for the remaining grafts.

2.7. Data analysis and statistics

Statistical analysis of all data was performed in RStudio (RStudio Team, 2015. RStudio: Integrated Development for R. RStudio, Inc., Boston, MA, USA, http://www.rstudio.com/). Phenotypic parameters (i.e., shoot growth (cm), root number, and length of the main root (cm)) from the phenotypic screening on micrografts was done at 49 DAG, number of starch granules / cell and number of callose depositions / cell at 28 and 49 DAG were analysed by Kruskal–Wallis test and multiple comparisons of treatments in the Rpackage “agricolae” [33]. Contingency tables of the phenotypic scores attributed to the level of cellular arrangement, differentiation, and

intensity of staining were used as data input to compute the chi-square test of independence (using the function *chisq.test()*) and evaluate for a significant association between the graft combinations and the attributed scores. Pearson residuals were extracted using the function *chisq.test()* and the package *corrplot* used to visualize and present these results according to Kassambara, 2016 [34]. Student's t-test was performed to compare the presence of the GRSPaV in each sample (SY383 and SY470) in relation to the control sample (110R) and UBI expression levels. Mean of the log2 expression levels ± SE (standard error) are visualized. The remaining data are shown as mean values ± SE. Significant differences at 95% confidence level are reported at * $p < 0.05$, ** $p < 0.01$, *** $p < 0.001$.

3. Results

3.1. Newly formed vascular bundles are functional in grapevine micrografts 28 days after grafting

In order to characterize the time frame of the different stages of grapevine graft formation in *in vitro* micrografted plants, we selected a *V. vinifera* homograft (SY470/SY470) and analysed the anatomic structure of the graft union over time at 21, 28, 35, 42 and 49 DAG by toluidine blue staining. At 21 DAG, *callus* cells proliferated filling the spaces between the scion and the rootstock establishing a *callus* bridge between the SY470/SY470 grafting partners. At 28 DAG, the *callus* cells differentiated into tracheary elements forming vascular bundles which were crossing the necrotic layer formed at the graft interface. The newly formed vascular bundle randomly connected to the pre-existing scion and rootstock vasculature at 35 DAG indicating that both xylem and phloem regeneration occurred in *V. vinifera in vitro* homografts (Figure 1).

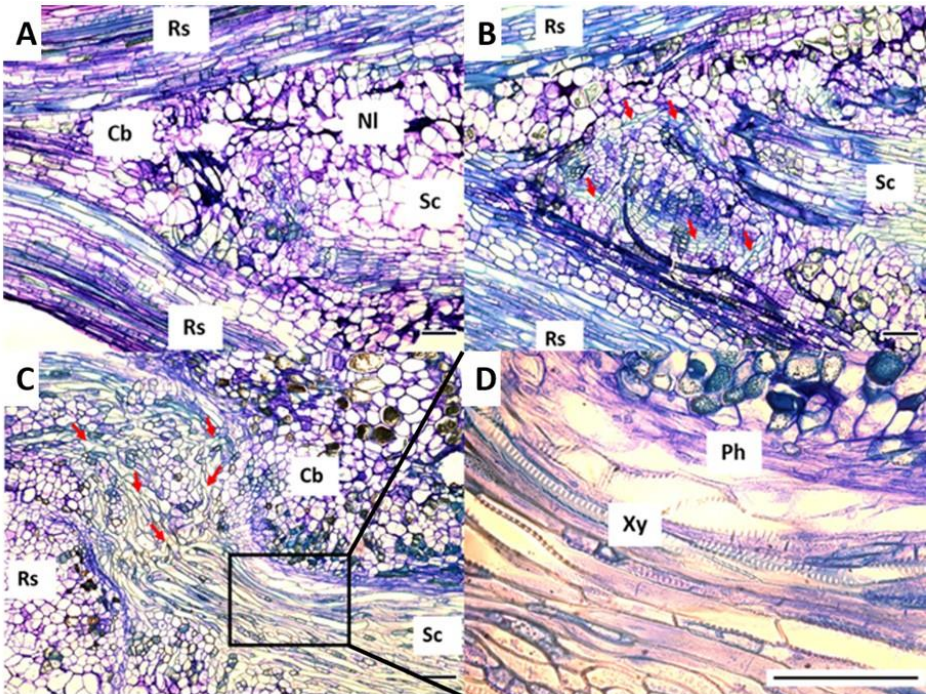

Figure 1. Histological observations of SY470/SY470 graft union stained with toluidine blue at 21 (**A**), 28 (**B**), and 35 DAG (**C**). A magnification of the vascular tissue at 35 DAG is shown in (**D**). Scion (Sc), Rootstock (Rs), *Callus* Bridge (Cb), Necrotic layer (Nl), Phloem (Ph), and Xylem (Xy). Red arrows indicate tracheary elements. Scale bars = 100 µm.

To understand whether the newly formed vascular bundles were functional at the time in which they were detected in histological sections, we monitored CFDA translocation in fresh longitudinal section of 110R/110R harvested at 28, 35, 42, 49, and 60 DAG. Note that loading of CFDA at petioles led to its uptake not only in the phloem but also in the xylem. Despite this, newly formed tracheary elements were able to functionally translocate CF across the graft union already from 28 DAG onwards (Supplementary Figure S2).

3.2. In vitro graft success is higher in homografts and failed grafted plants display a viral phenotype

Graft success ranged from 48% (110R/110R) to 100% (SY383/SY383) in homografts, and from 23% (SY470/110R) to 80% (TN112/110R) in heterografts (Figure 2A) in *in vitro* cultures.

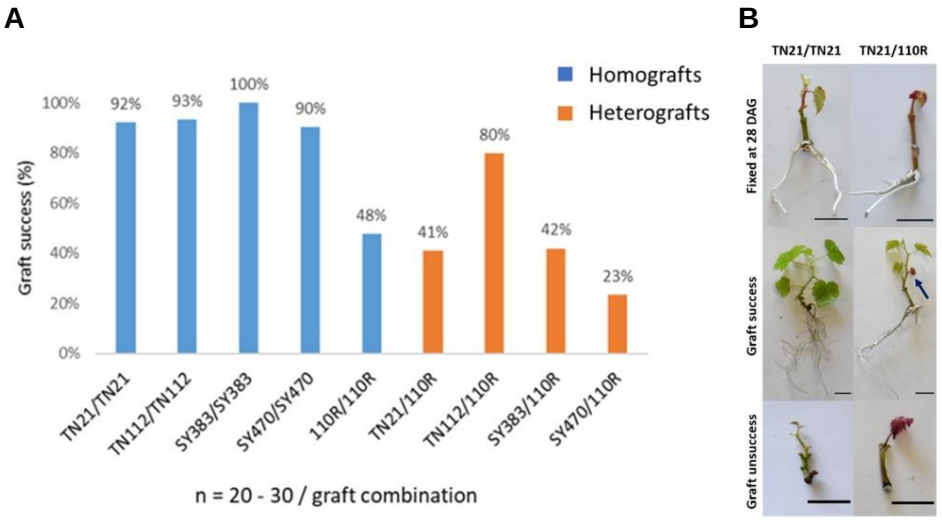

Figure 2. Graft success rate and examples of graft phenotyping. Bar chart of graft success (%) per graft combination at 49 DAG **(A)**. Examples of TN21 homo- and heterografts (i.e., TN21/TN21 and TN21/110R) fixed at 28 DAG, and example of successful and unsuccessful grafts at 49 DAG (**B**). Blue arrow in the successful graft indicates senescence detected at the first leaf. n = 20 – 30 / graft combination. Scale bars = 1 cm.

Notably, TN112 showed a higher graft success than TN21 when heterografted with 110R, and SY383 showed higher success than SY470 when heterografted to 110R under *in vitro* conditions (Figure 2A). Noteworthy, the grafts classified as failures showed a phenotype resembling a viral infection (Figure 2B). Red coloration in scion leaves was visible already at 28 DAG and, interestingly, successful grafts at 49 DAG

often displayed a mature scion leaf that turned red undergoing senescence at the approximate same time of the resume of scion growth looking asymptomatic (Figure 2B). Regarding to the phenotypic parameters collected at 49 DAG on successful grafts, significant differences were found in the number of roots and the main root length depending on both the graft combinations and the type of graft (i.e., homo- or heterografts) (Table 1).

Table 1. Average of roots number, length of the main root (cm), and shoot growth (cm) at 49 DAG per graft combination and graft type (i.e., homo- or heterograft) ± SE. Significant differences according to Kruskal–Wallis test are indicated by asterisks symbols *** $p < 0.001$; ** $p < 0.01$, * $p < 0.05$, and "ns" indicates non-significant differences. "NA" indicate not available data (as 110R/110R tends to develop roots at the graft zone). n > 30 for heterografts and n > 80 for homografts.

		Roots number	Main root length (cm)	Shoot growth (cm)
Graft combination	**Effect**	***	**	ns
	TN21/TN21	1.8 ± 0.19 ab	6.9 ± 0.50 b	2.0 ± 0.24
	TN112/TN112	2.3 ± 0.14 a	7.5 ± 0.35 ab	3.0 ± 0.36
	SY383/SY383	1.2 ± 0.18 b	7.6 ± 1.3 ab	2.9 ± 0.52
	SY470/SY470	1.1 ± 0.31 b	6.2 ± 1.3 ab	2.2 ± 0.40
	110R/110R	NA	NA	NA
	TN21/110R	2.1 ± 0.51 ab	9.5 ± 1.97 ab	2.3 ± 0.88
	TN112/110R	2.8 ± 0.32 a	10.8 ± 1.03 a	2.8 ± 0.53
	SY383/110R	2.8 ± 0.32 a	8.8 ± 2.23 ab	1.4 ± 0.4
	SY470/110R	3.8 ± 1.03 a	6.4 ± 2.06 ab	2.3 ± 0.99
Graft type	**Effect**	**	*	ns
	Homografts	1.7 ± 0.11 a	7.1 ± 0.46 a	2.6 ± 0.20
	Heterografts	2.5 ± 0.23 b	9.5 ± 0.88 b	2.2 ± 0.32

Indeed, in heterografts higher root number (2.5 ± 0.2 SE) and root length (9.5 cm ± 0.88 SE) were detected compared to homografts (i.e., 1.7 ± 0.1 SE and 7.1 cm ± 0.5 SE, respectively). With respect to the graft combinations, Syrah clones homografts poorly rooted when compared to the Touriga Nacional ones and rooted significantly less comparing to TN112 homograft (Table 1). The means of the main root length were more similar among the graft combinations than the number of roots were, as only the main root length of TN21 homograft significantly differed from the one of TN112/110R. In contrast, no significant differences were detected in relation to scion growth measurements at $p < 0.05$ according to Kruskal–Wallis test, although homografts displayed a slightly higher growth (2.6 cm ± 0.2 SE) than heterografts (2.2 cm ± 0.3 SE).

3.3 Syrah clones display high level of GRSPaV infection compared to 110R

In order to elucidate whether the lower graft success of SY470/110R compared to SY383/110R (Figure 2A) could be correlated with GRSPaV infection levels, we measured the presence of GRSPaV transcripts by RT-qPCR on leaves of SY383 and SY470 *in vitro* plantlets. GRSPaV transcript levels in the rootstock genotype (110R) were barely or not detectable (with average raw Ct values above 37) and were used together with the expression level of UBI transcripts to normalize the levels of GRSPaV RNA, in the Syrah leaves. As hypothesized, in SY470 leaves higher levels of GRSPaV transcripts, compared to SY383 leaves, were observed (Figure 3), indicating a negative correlation between the presence of GRSPaV transcripts and the levels of graft success of Syrah plants when grafted onto 110R.

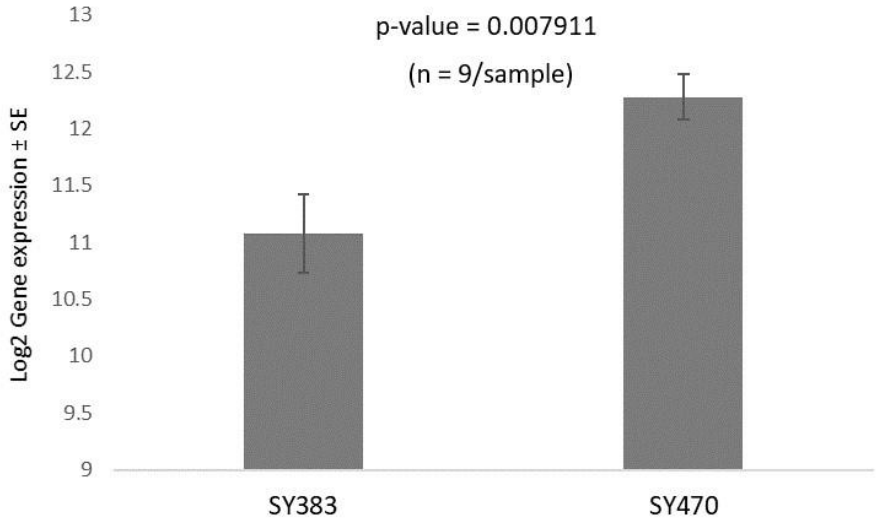

Figure 3. Relative presence of GRSPaV transcripts in leaves of non-grafted SY383 and SY470 *in vitro* plantlets detected by RT-qPCR. Signals were normalized to UBI and to 110R control sample. Data are presented as the mean ± SE of biological and technical replicates. Significant difference between the two Syrah clones was detected at $p < 0.05$ according to Student's t test (n = 3 / graft combination. 1 sample is a pool of 3 plants, 3 technical replicates).

3.4. Heterograft vascular differentiation proceeds slower than in homograft and the necrotic layer persists at 49 DAG

To better understand grapevine graft development and characterize the early cellular signs discriminating homo- and heterografts, as well as more and less graft compatible combinations showing graft success at 49 DAG, we histochemically analysed the graft union of different graft combinations at 28 and 49 DAG. Calcofluor white cell wall staining was used to assess the spatial cellular arrangement and cell shape at the graft union. Based on visual observation, three phenotypic classes were attributed to the inspected tissue cellular arrangement, A = low, B = intermediate, and C = high (Supplementary Figure S1). At 28 DAG, there was a significant

association between the graft combinations and the cellular arrangement according to the chi-square test of independence at $p < 0.05$ (Table 2).

Table 2. Significant associations according to the chi-square test of independence for the qualitative scores attributed at 28 and 49 DAG to the cellular arrangement, cellular differentiation, and intensity of staining in response to the graft combination, graft type (i.e., homo- or heterograft), and time (28 and 49 DAG). Statistical value of the test is reported in case of significant associations, being level of significance indicated by asterisks symbols *** $p < 0.001$; ** $p < 0.01$, * $p < 0.05$, and "ns" indicates non-significant differences. n = 3 observations per graft combination / time-point / staining.

	Graft combination		**Graft type**		**Time**	
Parameter	**28 DAG**	**49 DAG**	**28 DAG**	**49 DAG**	**Homo-**	**Heterograft**
Cell arrangement- *Calcofluor*	29.018 *	ns	ns	ns	ns	ns
Cell differentiation - *Acridine Orange*	ns	ns	ns	ns	6 *	ns
Intensity of staining - *Phloroglucinol HCl*	ns	ns	ns	15.406 ***	ns	7.224 *
Intensity of staining - *Toluidine Blue*	16.586 *	ns	ns	ns	ns	ns

Nevertheless, no significant association was recorded for the graft combinations at 49 DAG. In addition, no significant associations were found between homo- and heterografts at different times or within a same graft type among times (Table 2).

Figure 4A represents an example of calcofluor stained sections used to assess the level of cellular arrangement in the graft combinations.

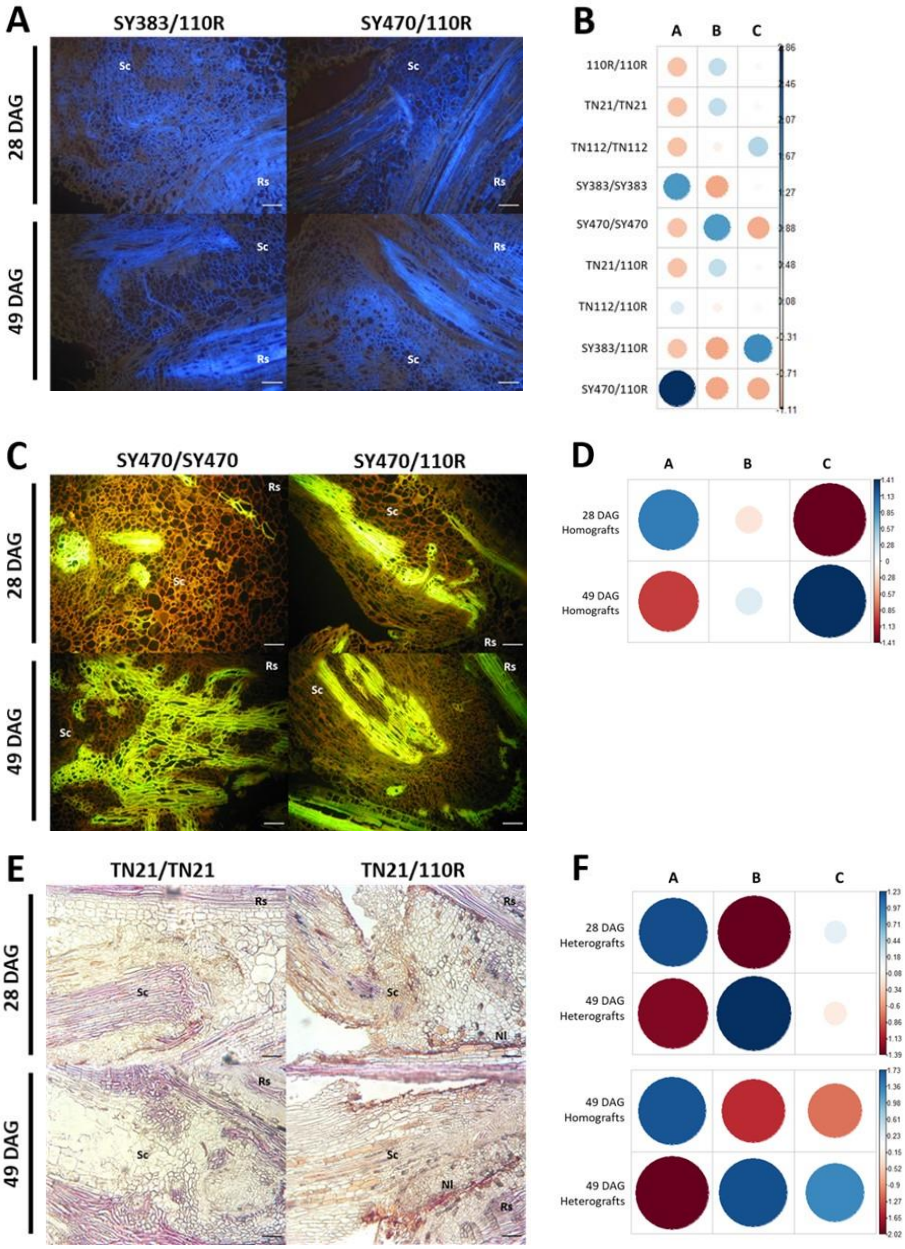

Figure 4. Histochemical staining of the graft union at 28 and 49 DAG, and the Pearson residuals of the significant associations identified according to the chi-square test of independence at $p < 0.05$. Calcofluor stained sections of SY383/110R and SY470/110R (**A**), Pearson residuals of the

graft combinations' cellular arrangement at 28 DAG (**B**). Acridine orange-stained sections of SY470 homo- and heterografts (**C**), Pearson residuals of the homografts' cellular differentiation between times (**D**). Phloroglucinol-HCl stained sections of TN21 homo- and heterografts (**E**), Pearson residuals for the heterografts' intensity of the staining at the necrotic layer between times, and between homo- and heterografts at 49 DAG (**F**). Positive residuals are displayed in blue and negative in red colors. The size of the circles and color intensities are proportional to the value of Pearson residuals. Scale bar = 100 µm.

The highest relative contributions in term of Pearson residuals (Pr) were imputed to SY470/110R for its low cellular arrangement (A score, Pr = 2.858, corresponding to 25.8% of the total contribution) and, secondarily to SY383/110R for its high cellular arrangement (C score, Pr = 1.792, corresponding to 10.1% of the total contribution) at 28 DAG (Figure 4B). The same strategy was used to interpret the results concerning the level of cellular differentiation, and the intensity of staining for phloroglucinol-HCl and toluidine blue dyes. Acridine orange preferentially stained differentiating xylem at the graft junction [30,35]. Therefore, this dye was used to visually evaluate the graft combinations for their level of differentiation from A = low to C = high. The chi-square test of independence showed that just homografts revealed a significant association to the grade of differentiation between the two times of observation (i.e., 28 and 49 DAG). Indeed, the graft union of homografts was significantly more differentiated at 49 DAG than at 28 DAG, although, interestingly, the same did not apply to heterografts (Figure 4C, D). Furthermore, the pattern of vascular differentiation at 49 DAG crossed the boundaries between the scion and the rootstock in homografts, while the new forming vascular bundles were rarely traversing the tissue of heterografts at the same time. Pearson residuals of the scores attributed

to homografts at different times showed that the highest contributions were relative to the homografts with low level of differentiation at 28 DAG (score A, Pr = 0.981 and score C, Pr = -1.414 corresponding to 16% and to 33.3% of the total contribution, respectively) and for their high level of differentiation at 49 DAG (score C, Pr = 1.414 and score A, Pr = -0.981, corresponding to 33.3% and 16% of the total contribution, respectively) (Figure 4D). Phlroglucinol-HCL indicates the presence of lignin in interfascicular fibers, and the stained sections were scored for their intensity of staining limited to the signal at the necrotic layer. The results highlighted a significant association between the level of staining and the type of graft (homo- or heterograft) at 49 DAG and also within the group of heterografts between times (Table 2). Hence, heterografts displayed more staining at the necrotic layer than the homografts at 49 DAG, as well as heterografts seemed more stained at the necrotic layer at 49 than at 28 DAG (Figure 4E). Indeed, Pearson residuals showed that the highest contributions were imputed to the low intensity of staining in homografts (score A, Pr = 1.732 and score B, Pr = -1.512, corresponding to 19.5% and to 14.8% of the total contribution, respectively) differently from the high intensity of staining registered in heterografts at 49 DAG (score B, Pr = 1.766 and score A, Pr = -2.023, corresponding to 20.2% and to 26.6% of the total contribution respectively) (Figure 4F). Similarly, a significant increase in staining was observed in heterografts at 49 DAG in comparison to 28 DAG (score A, Pr = -1.283 and score B = 1.450, corresponding to 22.8% and 29.1% of the total contribution; and score A, Pr = 1.229 and score B, Pr = -1.388, corresponding to 20.9% and 26.6% of the total contribution, respectively) (Figure 4F). Toluidine blue is often used to stain phenolic compounds which should responds with a characteristic green coloration [36]. According to our observations, some green coloration was often colocalized with the forming vasculature at the graft zone, independently by the graft combination or the graft type (data not shown).

3.5 Heterografts scion-rootstock translocation and phloem regeneration is impaired comparing to homografts

Considering that micrografted plantlets were grown on a basal medium supplemented with sucrose, the histochemical localization of starch by I_2KI staining can be a good indication of the sugar transport within the grafting partners. Average number of starch granules / cell and of callose depositions / cell, as well as the significant effect for each of the analysis performed according to Kruskal–Wallis test at $p < 0.05$, is shown in Table 3. Touriga Nacional homografts were more depleted in starch than 110R and Syrah homografts, being SY383/SY383 the graft combination with higher content of starch (101.9 ± 1.8 SE starch granules/cell) at 28 DAG (Table 3). Although TN112/TN112 pointed out to display the lowest number of starch granules per cell (21.3 ± 0.1 SE) at the same time, a significant increase of the starch content was observed in the heterograft TN112/110R (91.2 ± 1.2 SE), while no significant differences were detected comparing TN21 homo- and heterograft (Table 3).

Table 3. Average of number of starch granules / cell, and of callose deposition /cell ± SE at 28 and 49 DAG, per graft combination, graft type (i.e., homo- or heterograft), tissue (i.e., scion and rootstock), and time (i.e., 28 and 49 DAG). n > 30 for heterografts and n > 80 for homografts. Significant differences according to Kruskal–Wallis test are indicated by asterisks symbols *** $p < 0.001$; ** $p < 0.01$, * $p < 0.05$, and "ns" indicates non-significant differences. "NA" indicate not available data. N = 18 observations / graft combination / time-point.

		I_2KI - starch/cell		*Aniline Blue - callose/cell*	
		28 DAG	49 DAG	28 DAG	49 DAG
Graft combination	***Effect***	*****	*****	*****	*****
	110R/110R	81.6 ± 1.6 ab	82.2 ± 1.2 ab	90.1 ± 0.3 ab	77.6 ± 0.3 ab cd
	TN21/TN21	45.8 ± 2.0 bc	52.3 ± 0.2 b	67.0 ± 0.3 ab	96.6 ± 0.2 a
	TN112/TN112	21.3 ± 0.1 c	49.1 ± 0.1 b	72.7 ± 0.1 ab	90.0 ± 0.3 ab
	SY383/SY383	101.9 ± 1.8 a	55.4 ± 0.4 b	80.7 ± 0.3 ab	93.1 ± 0.2 ab
	SY470/SY470	87.3 ± 2.0 ab	53.6 ± 0.4 b	105.2 ± 0.2 a	85.1 ± 0.3 abc
	TN21/110R	70.9 ± 1.1 ab	101.0 ± 2.5 a	73.3 ± 0.2 ab	61.1 ± 0.2 cd
	TN112/110R	91.2 ± 1.2 a	80.9 ± 1.4 ab	73.0 ± 0.2 ab	53.5 ± 0.1 d
	SY383/110R	92.5 ± 2.3 a	88.4 ± 3.3 ab	52.2 ± 0.1 b	67.3 ± 0.1 bcd
	SY470/110R	93.4 ± 2.2 a	97.8 ± 2.4 a	65.2 ± 0.2 ab	70.1 ± 0.4 abcd
Graft type	***Effect***	*****	*****	*****	*****
	Homograft	66.3 ± 1.8 b	59.5 ± 0.7 b	80.6 ± 0.2 a	88.5 ± 0.2 a
	Heterograft	87.0 ± 1.9 a	91.6 ± 2.5 a	65.6 ± 0.2 b	63.1 ± 0.2 b
Tissue	***Effect***	*****	*****	*****	*****
	Scion	66.7 ± 1.5 b	61.4 ± 1.4 b	91.1 ± 0.2 a	94.1 ± 0.3 a
	Rootstock	86.8 ± 2.1 a	90.3 ± 2.3 a	51.6 ± 0.2 b	57.7 ± 0.2 b
Time	***Effect***	*****		***ns***	
	28 DAG	174.7 ± 1.9 a		146.7 ± 0.2	
	49 DAG	124.8 ± 2.0 b		153.2 ± 0.2	

Interestingly, heterografts were significantly more enriched in starch granules than homografts at both 28 and 49 DAG, being the level of significance increased at 49 DAG (Figure 5A).

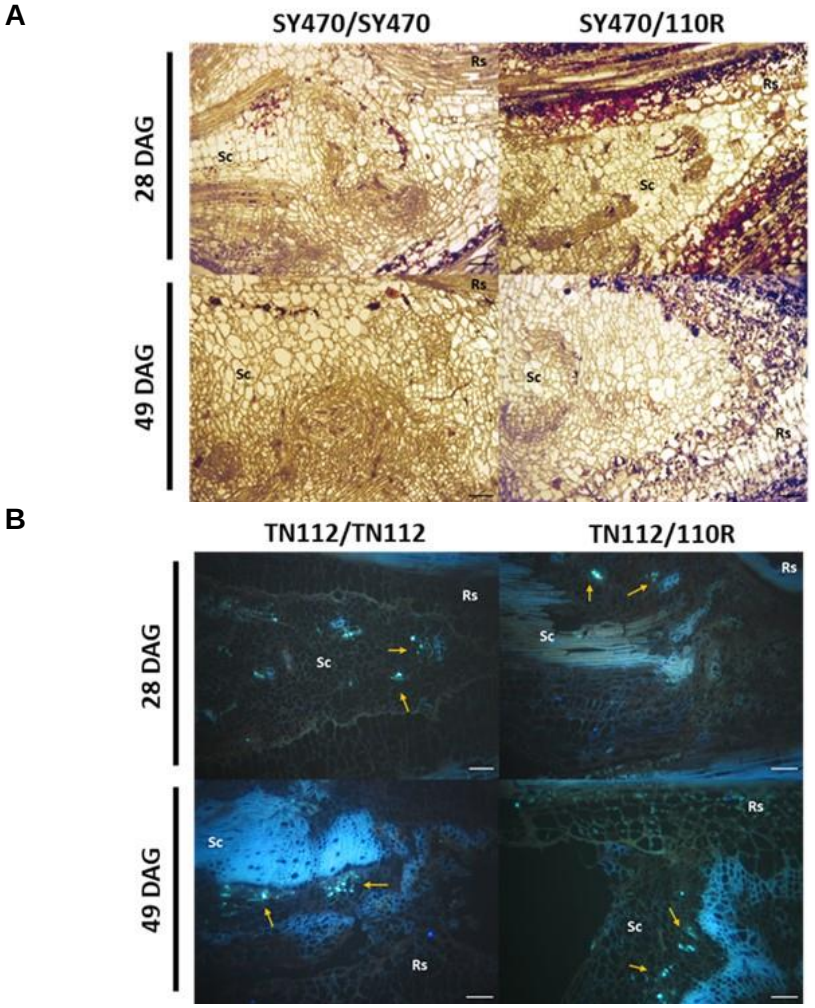

Figure 5. Starch granules and callose deposition at the graft interface revealed by I_2KI staining in the homo and heterografts formed by SY470 (**A**) and for aniline blue staining of callose in the homo- and heterografts formed by TN112 (**B**). Scion (Sc), Rootstock (Rs), yellow arrows indicate callose deposition signals. Scale bar = 100 µm.

The rootstock was always more enriched in starch than the scion, which is most likely due to sucrose supplied from the bottom supported by the basal growth medium. Considering the analysis over time, starch content was significantly higher at 28 DAG than at 49 DAG (i.e., 174.7 ± 1.9 SE and 124.8 ± 2.0 SE, respectively) indicating a better sugar translocation going along with the healing of the union (Table 2, Figure 5A). At 49 DAG, TN21 and SY470 were the only genotypes significant different between homo- or heterografted, being always more enriched in starch than when self-grafted (i.e., 101.0 ± 2.5 SE and 52.3 ± 0.2 SE starch granules in TN21/110R and TN21/TN21, respectively, and 97.8 ± 2.4 SE and 53.6 ± 0.4 SE starch granules in SY470/110R and SY470/SY470, respectively). The callose signal revealed by aniline blue fluorescence had a recurrent pattern being often associated to developing xylem vessels either localized at the outside or the inside of them. This indicated most probably callose involved in the formation of phloem SEs, rather than callose deposited as a defense or stress response (Figure 5B). Indeed, a similar aniline blue signal appeared at the proximity of xylem vessels of non-grafted tissue suggesting that the stain reveals mainly the phloem (data not shown). The callose stain did not significantly vary between 28 and 49 DAG, while a strong significant difference marked scions as being more enriched in callose than rootstocks at both time points (Table 3). Interestingly, in homografts more callose was detected than in heterografts at both time points, with higher statistical significance at 49 DAG than at 28 DAG. Another significant callose deposition difference was detected for the following graft combinations: SY470/SY470 was different from SY383/110R at 28 DAG (i.e., 105.2 ± 0.2 SE and 52.2 ± 0.1 SE of callose deposition / cell respectively), and both TN21/TN21 and TN112/TN112 resulted different from their respective heterografts at 49 DAG (i.e. 96.6 ± 0.2 SE and 61.1 ± 0.2 SE for TN21/TN21 and TN21/110R respectively,

and 90.0 ± 0.3 SE and 53.5 ± 0.1 SE for TN112/TN112 and TN112/110R respectively) (Table 3, Figure 5B).

3.6. Plants responses to wounding and sucrose supply

By *in vitro* culturing SY383, SY470, and 110R, we noticed that both non-grafted Syrah genotypes started to display a red canopy after long term *in vitro* propagation (2 years in culture). Furthermore, all genotypes, when cut (wounded) for a new culture media, displayed leaf reddening and senescence followed by a time of recovery or death (Figure 6).

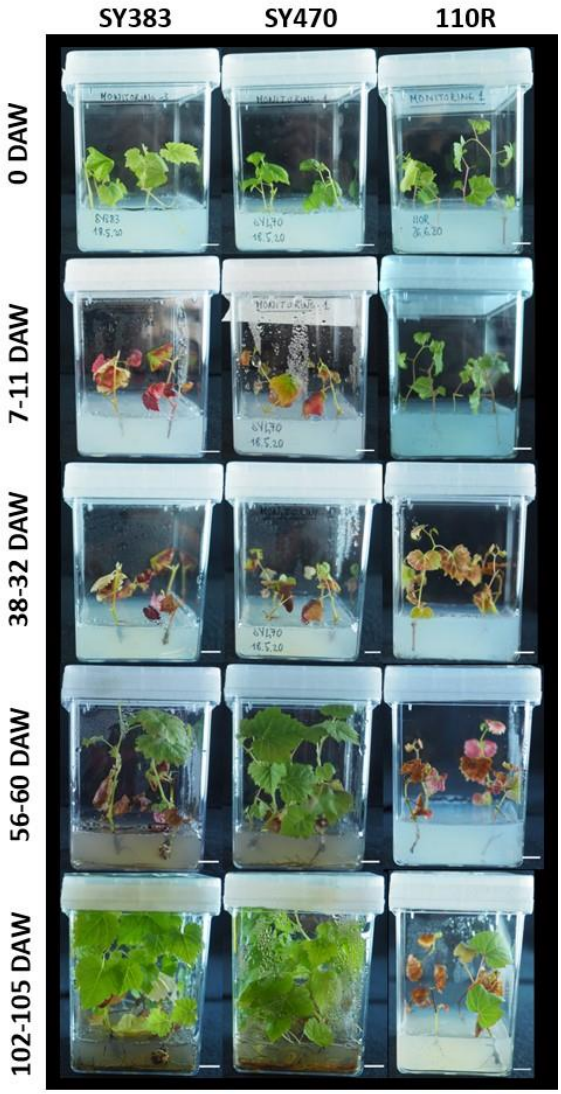

Figure 6. Recovery after wounding of non-grafted plants detected from 0 days after wounding (DAW) until plant recovery or plant death (up to 144 DAW). Examples of non-grafted SY383, SY470, and 110R plants (1 culture box containing 3 plants / genotype is shown) at 0 DAW and after approximately 1 week, 1 month, 2 months, and more than 3 months after wounding. n = 9 / graft combination, scale bar = 1 cm.

A red senescent phenotype was already noticed in both Syrah clones one week after wounding, and both Syrah genotypes started to recover at 55 – 60 days after wounding (DAW). Conversely, symptoms in 110R appeared later (at 18 – 21 DAW) than in Syrah plants and lasted longer, up to 100 DAW, followed by plant recovery or plant death, being plant death more frequent. It is important to take into consideration that such symptoms in Syrah plants started to appear after 2 years under *in vitro* culture, while they took more than 3 years to became apparent in 110R.

To verify that leaf reddening is due to an overproduction of anthocyanins due to sugars accumulation, we monitored the phenotype of SY383 and SY470 one and three months after wounding in 3%, 1.5%, and 0% sucrose enriched media. The results indicated that leaf reddening is clearly dependent by sucrose levels in the media, being the red coloration enhanced in response to increased sucrose content (Supplementary Figure S3A). As wounding led to a mild phenotype resembling the viral phenotype of heterografts (refer to Figure 2B and Figure 6) and responded to sucrose level in the media (Supplementary Figure S3A), we monitored SY383/SY383 homograft in 3%, 1.5%, and 0% sucrose enriched media and visually verified that also graft success was dependent by sucrose content in the media. Indeed, no red symptom were observed in none of the grafts up to 16 DAG, while symptoms started to be visible from 16 DAG on in grafts grown on 3% sucrose (Supplementary Figure S3B). Although plants grown on 3% sucrose were contaminated at 30 DAG, and they could not be analysed further, it become obvious by comparing grafts grown on 1.5% and 0% sucrose up to 86 DAG that homografts not supplement by sucrose could be successfully grafted (Supplementary Figure S3B).

4. Discussion

In the present study, we have characterized the time frame of graft formation in grapevine homografts using certified-virus free *in vitro*

grapevine plantlets of cv. Touriga Nacional (clones 112 and 21), cv. Syrah (clone 383 and 470), and the rootstock 110R. It is widely known that graft union healing is marked by different developmental stages: adhesion between the grafting partners, the formation of a *callus* bridge, and the formation of new vascular bundles leading to a functional long-distance transport system supporting the grafting partners [18]. In this work, we have shown that the *callus* bridge is formed between the grafting partners at 21 DAG. By 28 DAG, some *callus* cells differentiated into tracheary elements forming functional vascular bundles crossing the necrotic layer at the graft interface that translocated CFDA (Supplementary Figure S2). From there on, the new vascular bundles connected further and randomly to the pre-existing vasculature and the union consolidated (Figure 1). This is in line with other studies that reported similar times for grapevine graft union formation under *in vitro* micrografting [16,37]. Considering this and our insights, the time-point of grafts collection was established at 28 DAG in order to study the early cellular events of graft union formation, and 49 DAG to assess the final success of the graft. This later time point (49 DAG) was chosen since incompatible heterografts, compared to homografts, often require more time for healing the graft union [19]. Although it is known that, compared to herbaceous species, woody species require a relative long time to heal the graft union [17], grapevines seem to require even more time to establish a graft union in *in vitro* culture. For instance, 28 days is sufficient for micrografted almond to form a strong graft union [24], cherry micrografts requires 21 days [38], and apple micrografts 20-40 days [39]. Interestingly, also field studies show that grapevine requires long times for the graft union to heal [40], indicating that *in vitro* systems reliably mimic the time frame underlying graft union formation in grapevines. The assessment of graft success highlighted that, as expected, homografts performed better than heterografts, although the graft success rate of rootstock homografts (110R/110R) was lower than that of *V. vinifera*

homografts (i.e., 48% vs. 90-100%, respectively) (Figure 2A). In parallel, we found that TN21 and SY383 performed better than TN112 and SY470 when grafted to 110R rootstock, which is not in agreement with other studies. TN112/110R was reported as less graft compatible than TN21/110R [3], and SY383/110R as more susceptible to the Syrah decline than SY470/110R [25]. Surprisingly, most heterograft failures displayed typical symptoms of viral infections (Figure 2B). Considering that under field conditions SY383/110R displayed lower graft success than SY470/110R [40] and that we found that leaves of SY383/110R (from plants belonging to the same bulk) have higher GRSPaV infection levels than SY470/110R (RNAseq data not shown), we asked whether the incongruence regarding *in vitro* and in field graft success rates could be explained by a correlation with GRSPaV presence in these plants. Indeed, we confirmed by RT-qPCR that the genotype showing less graft success when combined with 110R (SY470) was also the genotype with higher GRSPaV transcripts levels (Figure 3). Conversely, GRSPaV presence on the rootstock genotype (110R) was barely or not detectable. Virus-induced graft incompatibility in grapevines was reported when latent viruses in scions are graft-transmitted to susceptible hypersensitive rootstocks, while the rootstock being the source of a latent virus has never been reported [13]. More experiments have to be performed to verify the role of GRSPaV in the graft success rates of Syrah grafted onto 110R as well as in symptoms of declining Syrah. Here it should be noted that this virus is frequently found in vines affected by “Syrah decline”, although no cause-effect relationship has ultimately been provided [14,26]. Regarding to the physiological parameters investigated, our findings confirmed a lower rooting capacity in homografted *V. vinifera*, particularly in Syrah clones, which was already reported under field conditions [40]. Differently, no significant difference was detected in terms of growth, although homograft growth was slightly higher than that of the heterografts (Table 1). However,

it was not significantly more, as it would be expected considering field data, which might be a direct effect of the carbon source supplied with the culture media. To investigate the early cellular sign of graft union development in grapevine, we evaluated morphological and histological development in different scion-rootstocks combinations (homo- vs. heterografts, compatible vs. incompatible heterografts) at 28 and 49 DAG. Calcofluor staining revealed a significant association between the graft combinations and their cellular arrangement, being the higher contribution imputed to the low cellular arrangement displayed in SY470/110R graft union, which is interestingly the combination with lower graft success rate (Table 2, Figures 2A and 4A). For instance, irregular cell wall thickening and bent cell walls / collapsed cells were already observed by calcofluor fluorescence in incompatible *Prunus* grafts [10,18]. Interestingly, *callus* tissue from *V. vinifera* grafts infected by both GLRaV-1 and grapevine virus A (GVA), was shown to be composed of irregular shaped cells [16]. Acridine orange dye clearly stained the tracheid walls, as reported in other studies [41], underlying the patterns of vascular differentiation across the union (Figure 4C). Results highlighted that while homografts differentiation significantly evolved from 28 to 49 DAG and new vascular bundles were able to cross the boundaries between scion and rootstock, the same did not happened in case of heterografts, suggesting that vascular differentiation proceeds slower in this group and seems blocked at the graft interface. These results are in agreement with other studies on apple [39], tomato [42], and pear/quince grafts [19]. On the other hand, Phloroglucinol-HCl stains indicated that the necrotic layer is significantly more prominent in heterografts than in homografts at 49 DAG, and that heterografts are more stained at the necrotic layer at 49 than at 28 DAG (Table 2, Figure 4E). These results suggested not only that the necrotic layer persists at 49 DAG in heterografted grapevines compared to homografts but also indicates that in heterografts this is even enhanced at

a later stage. The necrotic layer is suggested to be a prerequisite to the formation of continuous secondary plasmodesmata between cells of both grafting partners and to disappear at the moment of *callus* formation in homografts although, in incompatible grafts, its presence seems to block full vascular formation between the grafting partners [7]. Nevertheless, to the best of our knowledge, persistence of a necrotic layer in heterografted grapevines was not previously observed [11]. Observation of I_2KI stained sections revealed that heterografts are significantly more enriched in starch than homografts at both times analysed, especially at 49 DAG. Furthermore, starch content decreased over time in homografts suggesting that starch granules dissolves with the formation of the graft union while the same did not happen in heterografts (Table 3, Figure 5A). The results suggested a negative correlation between graft success and the starch granules content, which might indicate that grapevine graft failures could be a consequence of a reduced sugar translocation between the grafting partners, as it was previously suggested not only for grapevines [11] but also in other species [9,43,44]. This strengthens the use of *in vitro* techniques, and particularly of I_2KI starch staining, as a reliable method to early screen compatible and incompatible grafting partners.

Although accumulation of callose is described as a common stress response such as under viral infections or herbivore attacks [45], callose deposition is also part of phloem vessel formation. Indeed, one of the first observable processes of sieve elements (SEs) formation is an increase in callose that is deposited in platelet around SEs plasmodesmata [46]. Overall callose deposition did not differ between times at the forming SEs at the grapevine graft union which might indicate that from 28 to 49 DAG phloem differentiation proceeds slowly. Results from the quantification of callose deposition also highlighted that scions are more enriched in callose

than rootstocks and that homografts were enriched more than heterografts at both times, especially at 49 DAG (Table 3, Figure 5B). Overall, our results seem to suggest that phloem regeneration is impaired in heterografts compared to homografts especially at 49 DAG and that the effect is stronger in the Touriga Nacional clones. As both auxin and cytokinins (CKs) concur in phloem development and as auxin is known to be transported via phloem while many CKs move root-to-shoot [47,48], a reduced or unbalanced translocation or presence of such hormones across heterografted unions might offer an explanation for the impaired phloem regeneration observed in hetero- but not in homografts. Considering the implications of a reduced phloem translocation in the physiology and longevity of grafted grapevines, and that recently sucrose was found significantly depleted in the phloem exudate of heterografted grapevine species [49], more studies should pay attention to the phloem tissue differentiation process and the molecules transferred via phloem in grafted grapevines.

In addition, we have provided evidence that plants phenotypically responded to wounding thereby displaying a similar but milder phenotype than that displayed by failing heterografted unions (Figure 6). These results confirmed that graft responses are similar to wounding responses as recently suggested and reviewed [5]. The presence of such symptoms on non-grafted plants once more suggests that the Syrah decline might be related to viral infection processes. Possibly, latent viral infections in scion genotypes might manifested later and/or upon stresses such wounding. For instance, Syrah decline symptoms were already reported on own-rooted grapevines in Chilean and Argentinian phylloxera-free vineyards [50]. Furthermore, the detected phenotypic response of wounded and grafted grapevines to different sucrose concentrations in the media (Supplementary Figure S3A and S3B respectively) pointed out for a

possibly impaired carbon translocation via phloem occurring in these plants. Graft incompatibility is often associated with reddening of leaves earlier at the end of the growing season in the field than compatible combinations [9,11], which is also indicative of carbon accumulation in the scion, often associated with poor phloem functioning [5]. In grapevines, leaves reddening was explained as an insufficient connection between the rootstock and the scion inducing sugar accumulation in leaves and secondary metabolic pathways which results in the formation of phenolic compound such as anthocyanin, responsible for the change in leaf color [51]. Nevertheless, leaves reddening is also reported as a typical symptom in grapevine viral infections [52] which are known to lead to a degradation of young phloem cells [53,54]. In grapevine, viruses leads to soluble sugar accumulation in the leaves and deficiency in translocation of these sugars to sink tissues or grape berries [52]. Although more studies are needed to clarify how and in which extent the phloem function of wounded, grafted, and especially heterografted grapevines is impaired, and how this relates to viruses, the evidences provided in this work further suggests the notion that grapevine graft incompatibility is a virus-induced problem which, according to our insights, can arise even employing certified virus free plants. The fact that more than 65 viruses have been recorded to infect grapevines [14], and that just a few of them are tested in the EU certification schemes, opens a panoply of implications related to the preservation of the grapevine germplasm and its certification schemes, which definitively deserve more attention.

5. Conclusions

In this work, we have shown that heterografted grapevine unions showed typical viral symptoms and that successful heterografts displayed a persistent necrotic layer at 49 DAG, a slower vascular differentiation, a lower starch scion-rootstock translocation, and impaired phloem

regeneration compared to homografts. Taken as a whole, these results might suggest the presence of translocated incompatibility symptoms in grapevine heterografts, as previously suggested [11]. Although, whether there is a link between grapevine viruses and the translocated graft incompatibility's imputed to heterografted *Vitis* species, remains to be clarified. Among the histochemical stainings used, we highlighted that calcofluor cellulose staining used to evaluate the cellular arrangement, as well as I_2KI staining for quantifying starch contents, were revealed as the best dyes used in this study as they were able to identify the graft combinations with worse graft success rates. Aniline blue proved to be an easy and fast way to observe phloem vessels in grapevine micrografts, often difficult to localize under histological observations. Overall, we confirm the utility of *in vitro* system in predicting very early grapevine graft compatibility responses. In addition, we encourage its use to address viruses that might be responsible for grapevine graft incompatibility. This should be seen in view of strengthening the certification protocols and thereby preserving our grapevine genetic resources.

Acknowledgments

The authors thank the National Institute for Agricultural and Veterinary Research (INIAV-Dois Portos) for the provision of the plant material. We acknowledge Margarida Basaloco for the candidate reference genes primer design, and Cindy Hauptvogel and Saurabh Gupta in the Kragler laboratory for help in monitoring of plants after wounding and of grafts under different sucrose concentrations and analysing RNAseq data for the presence of viral sequences, respectively.

References

1. Warschefsky, E.J.; Klein, L.L.; Frank, M.H.; Chitwood, D.H.; Londo, J.P.; von Wettberg, E.J.B.; Miller, A.J. Rootstocks: Diversity, domestication, and impacts on shoot phenotypes. *Trends Plant Sci.* **2016**, 21, 418–437.
2. Ollat, N.; Bordenave, L.; Tandonnet, J.P.; Boursiquot, J.M.; Marguerit, E. Grapevine rootstocks: Origins and perspectives. *Acta Hortic.* **2016**, 1136, 11–22
3. Assunção, M.; Santos, C.; Brazão, J.; Eiras-Dias, J.E.; Fevereiro, P. Understanding the molecular mechanisms underlying graft success in grapevine. *BMC Plant Biol.* **2019**, 19, 1–17.
4. Martelli, G.P. Infectious diseases and certification of grapevines. In *Proceedings of the Mediterranean network on grapevine closteroviruses 1992-1997 and the viroses and virus-like diseases of the grapevine a bibliographic report, 1985-1997. Bari : CIHEAM, 1999.* Martelli G.P., Digiaro, M. Eds., pp. 47- 64.
5. Loupit, G.; Cookson, S.J. Identifying Molecular Markers of Successful Graft Union Formation and Compatibility. *Front. Plant Sci.* **2020**, 11, 1–11.
6. Hartman, H.T.; Kester, D.E.; Davies, F.T.; Geneve, R.G. Principles of grafting and budding. In *Hartmann and Kester's Plant Propagation: Principles and Practices*; Prentice Hall: Upper Saddle River, NJ, USA, 2011; pp. 415–463.
7. Pina, A.; Cookson, S.; Calatayud, A.; Trinchera, A.; Errea, P. Chapter 5—Physiological and molecular mechanisms underlying graft compatibility. In *Vegetable Grafting Principles and Practices*; Colla, G., Perez-Alfocea, F., Schwarz, D., Eds.; CABI Oxfordshire: Wallingford, UK, 2017; pp. 132–154, ISBN 13 978 1 78639 058 5.
8. Mosse, B. *Graft-Incompatibility In Fruit Trees With Particular Reference To Its Underlying Causes*. Technical Communication No. 28. Kent: Farnham Royal, Bucks: Commonwealth Agricultural Bureaux, England, 1962.
9. Zarrouk, O.; Gogorcena, Y.; Moreno, M.A.; Pinochet, J. Graft compatibility between peach cultivars and *Prunus* rootstocks. *HortScience* **2006**, 41, 1389–1394.
10. Errea, P., Garay, L., Marın, J.A. Early detection of graft incompatibility in apricot (*Prunus armeniaca*) using *in vitro* techniques *Physiol. Plant.* **2001**, 112, 135–141.
11. Bouquet, A. Differences observed in the graft compatibility between some cultivars of Muscadine grape (*Vitis rotundifolia Michx.*) and European grape (*Vitis vinifera L.* cv. Cabernet Sauvignon). *Vitis* **1980**, 19, 99–104.
12. Herrero, J. La compatibilite entre les sujets porte-greffes et les varieies fruitieres In *Congr. Pomol. Intern. (Namur)* **1956**, 10–13.
13. Rowhani, A.; Uyemoto, J.K.; Golino, D.A.; Daubert, S.D.; Al Rwahnih, M. Viruses Involved in Graft Incompatibility and Decline. In *Grapevine Viruses: Molecular Biology, Diagnostics and Management*; Meng, B., Martelli, G.P., Golino, D.A., Fuchs, M., Eds.; Springer International Publishing: Cham, Switzerland, 2017; pp. 289–302.
14. Martelli, G.P. Directory of virus and virus-like diseases of the grapevine and their agents. *J. Plant Pathol.* **2014**, 96, 1–36.
15. Andrews, P.K.; Serrano Marquez, C. Volume 15—Graft incompatibility. In *Horticultural Reviews*; Janick, J., Ed.; John Wiley & Sons, Inc.: Oxford, UK, 1993; pp.

183–232.
16. Cui, Z.H.; Agüero, C.B.; Wang, Q.C.; Walker, M.A. Validation of micrografting to identify incompatible interactions of rootstocks with virus-infected scions of Cabernet Franc. *Aust. J. Grape Wine Res.* **2019**, 25, 268–275.
17. Assunção, M.; Tedesco, S.; Fevereiro, P. Molecular Aspects of Grafting in Woody Plants. In *Annual Plant Reviews Online*, 1st ed.; Wiley Online Library: New York, NY, USA, 2021; Volume 4, pp. 87–126.
18. Pina, A.; Errea, P.; Martens, H.J. Graft union formation and cell-to-cell communication via plasmodesmata in compatible and incompatible stem unions of *Prunus spp. Sci. Hortic. (Amst.)* **2012**, 143, 144–150.
19. Espen, L.; Cocucci, M.; Sacchi, G.A. Differentiation and functional connection of vascular elements in compatible and incompatible pear/quince internode micrografts. *Tree Physiol.* **2005**, 25, 1419–1425.
20. Melnyk, C.W.; Schuster, C.; Leyser, O.; Meyerowitz, E.M. A developmental framework for graft formation and vascular reconnection in *arabidopsis thaliana. Curr. Biol.* **2015**, 25, 1306–1318.
21. Pina, A.; Errea, P. Differential induction of phenylalanine ammonia-lyase gene expression in response to *in vitro callus* unions of *Prunus spp*. *J. Plant Physiol.* **2008**, 165, 705–714.
22. Murashige, T.; Skoog, F. A Revised Medium for Rapid Growth and Bio Assays with Tobacco Tissue Cultures. *Physiol. Plant.* **1962**, 15, 473–497.
23. Galzy, R. Technique de thermothérapiedesviruses de lavigne. *Ann. Epiphyt.* **1964**, 15, 245–256.
24. Yildirim, H.; Onay, A.; Süzerer, V.; Tilkat, E.; Ozden-Tokatli, Y.; Akdemir, H. Micrografting of almond (*Prunus dulcis Mill.*) cultivars 'Ferragnes' and 'Ferraduel' *Sci. Hortic. (Amsterdam).* **2010**, 125, 361–367.
25. Renault-Spilmont, A.S.; Grenan, S.; Bousiquot, J.M. Syrah decline. *Progrés Agric. Vitic.* **2005**, 122, 15–16.
26. Lima, M.F.; Alkowni, R.; Uyemoto, J.K.; Golino, D.; Osman, F.; Rowhani, A. Molecular analysis of a California strain of Rupestris stem pitting-associated virus isolated from declining Syrah grapevines. *Arch. Virol.* **2006**, 151, 1889–1894.
27. Xie, F., Xiao, P., Chen, D., Xu, L., and Zhang, B. miRDeepFinder: a miRNA analysis tool for deep sequencing of plant small RNAs. *Plant Mol. Biol.* **2012**, 80, 75–84.
28. Pfaffl, M.W. A new mathematical model for relative quantification in real-time RT-PCR. *Nucleic Acids Res.* **2001**, 29, 2002–2007.
29. Hughes, J.; McCully, M.E. The Use of an Optical Brightener in the Study of Plant Structure. *Stain Technol.* **1975**, 50, 319–329.
30. Demarco, D. Histochemical Analysis of Plant Secretory Structures. In *Histochemistry of Single Molecules: Methods and Protocols, Methods in Molecular Biology*; Pellicciari, C.; Biggiogera, M. Eds.; Springer Science+Business Media LLC: Heidelberg, Germany, 2017; pp. 313–330.
31. Ros Barceló, A. The generation of H2O2 in the xylem of *Zinnia elegans* is mediated by an NADPH-oxidase-like enzyme. *Planta* **1998**, 207, 207–216.

32. Leszczuk, A.; Pieczywek, P.M.; Gryta, A.; Frąc, M.; Zdunek, A. Immunocytochemical studies on the distribution of arabinogalactan proteins (AGPs) as a response to fungal infection in *Malus* x *domestica* fruit. *Sci. Rep.* **2019**, 9, 1–14.
33. de Mendiburu, F. agricolae: Statistical Procedures for Agricultural Research. R package version 1.3-2.; 2020. Available at: https://cran.r-project.org/package=agricolae.
34. Kassambara, A. Chi-Square Test of Independence in R; R tutorial, available on-line: http://www.sthda.com/english/wiki/chi-square-test-of-independence-in-r (accessed at 21.03.21).
35. Houtman, C.J.; Kitin, P.; Houtman J.C.D.; Hammel, K.E.; Hunt, C.G. Acridine Orange Indicates Early Oxidation of Wood Cell Walls by Fungi. *PLoS One* **2016**, 11, 7, e0159715
36. Errea, P.; Felipe, A.; Herrero, M. Graft establishment between compatible and incompatible *Prunus spp. J. Exp. Bot.* **1994**, 45, 393–401.
37. D'Khili, S.G.B.; Michaux-Ferrière, N. Etude histochimique de 1 ' incompatibilite au microgreffage et greffage de boutures herbacees chez la vigne. *Vitis* **1995**, 34, 135–140.
38. Gebhardt, K.; Goldbach, H. Establishment, graft union characteristics and growth of *Prunus* micrografts. *Physiol. Plant.* **1988**, 72, 153–159.
39. Richardson, F.V.M.; Mac An Tsaoir, S.; Harvey, B.M.R. A study of the graft union in *in vitro* micrografted apple. *Plant Growth Regul.* **1996**, 20, 17–23.
40. Tedesco, S.; Pina, A.; Fevereiro, P.; Kragler, F. A Phenotypic Search on Graft Compatibility in Grapevine. *Agronomy* **2020**, 10, 706.
41. Zhang, M.; Lapierre, C.; Nouxman, N.L.; Nieuwoudt, M.K.; Smith, B.G.; Chavan, R.R.; McArdle, B.H.; Harris, P.J. Location and characterization of lignin in tracheid cell walls of radiata pine (*Pinus radiata* D. Don) compression woods *Plant Physiol. Biochem.* **2017**, 118, 187–198.
42. Frey, C.; Acebes, J.L.; Encina, A.; Álvarez, R. Histological changes associated with the graft union development in tomato. *Plants* **2020**, 9, 1–13.
43. Schöning, U.; Kollmann, R. Phloem translocation in regenerating *in vitro* - heterografts of different compatibility. *J. Exp. Bot.* **1997**, 48, 289–295.
44. Moing, A.; Salesses, G.; Saglio, P.H. Growth and the composition and transport of carbohydrate in compatible and incompatible peach/plum grafts. *Tree Physiol.* **1987**, 3, 345–354.
45. De Storme, N.; Geelen, D. Callose homeostasis at plasmodesmata: molecular regulators and developmental relevance. *Front. Plant Sci.* **2014**, 5, 138.
46. Lucas, W.J., Groover, A., Lichtenberger, R., Furuta, K., Yadav, S.R., Helariutta, Y. The Plant Vascular System: Evolution, Development and Functions. *J. Integr. Plant Biol.* **2013**, 55, 294–388.
47. Aloni, B.; Cohen, R.; Karni, L.; Aktas, H.; Edelstein, M. Hormonal signaling in rootstock-scion interactions. *Sci. Hortic. (Amsterdam).* **2010**, 127, 119–126.
48. Park, J.; Lee, Y.; Martinoia, E.; Geisler, M. Plant hormone transporters: What we know and what we would like to know. *BMC Biol.* **2017**,15, 1–15.

49. Tedesco, S.; Erban, A.; Gupta, S.; Kopka, J.; Fevereiro, P.; Kragler, F.; Pina, A. The Impact of Metabolic Scion–Rootstock Interactions in Different Grapevine Tissues and Phloem Exudates. *Metabolites* **2021**, 11, 349.
50. Renault-Spilmont, A.; Moreno, Y.; Audeguin, L. Syrah decline: similar symptoms on own-rooted plants. *Prog. Agric. Vitic.* **2010**, 127, 63–67.
51. Bahar, E.; Korkutal, I. Using magnetic resonance imaging technique (MRI) to investigate graft connection and its relation to reddening discoloration in grape leaves. *JFAE* **2010**, 8, 293–297.
52. Basso, M. F., Fajardo, T. V. M., and Saldarelli, P. Grapevine virus diseases:economic impact and current advances in viral prospection and management. *Rev. Bras. Frutic.* **2017**, 39.
53. Esau, K. Some anatomical aspects of plant virus disease problems. *Bot. Rev.* **1938**, 4, 548–579.
54. Esau, K. Some anatomical aspects of plant virus disease problems II. *Bot. Rev.* **1948**, 14, 413–449.

Supplementary Materials

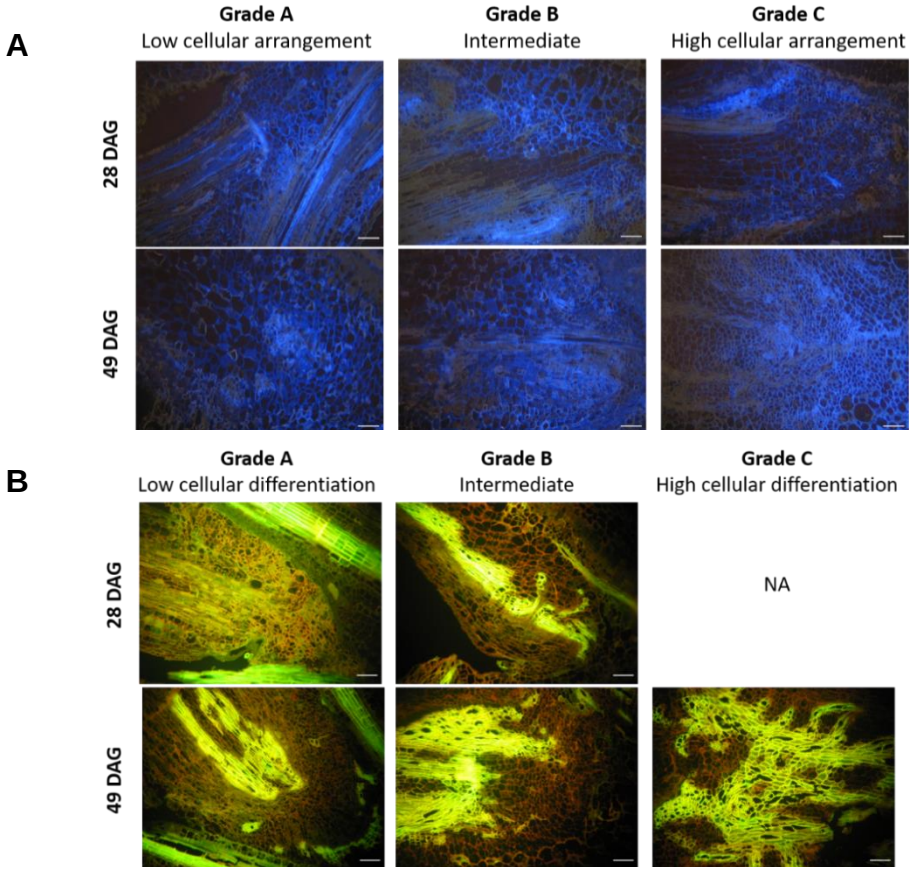

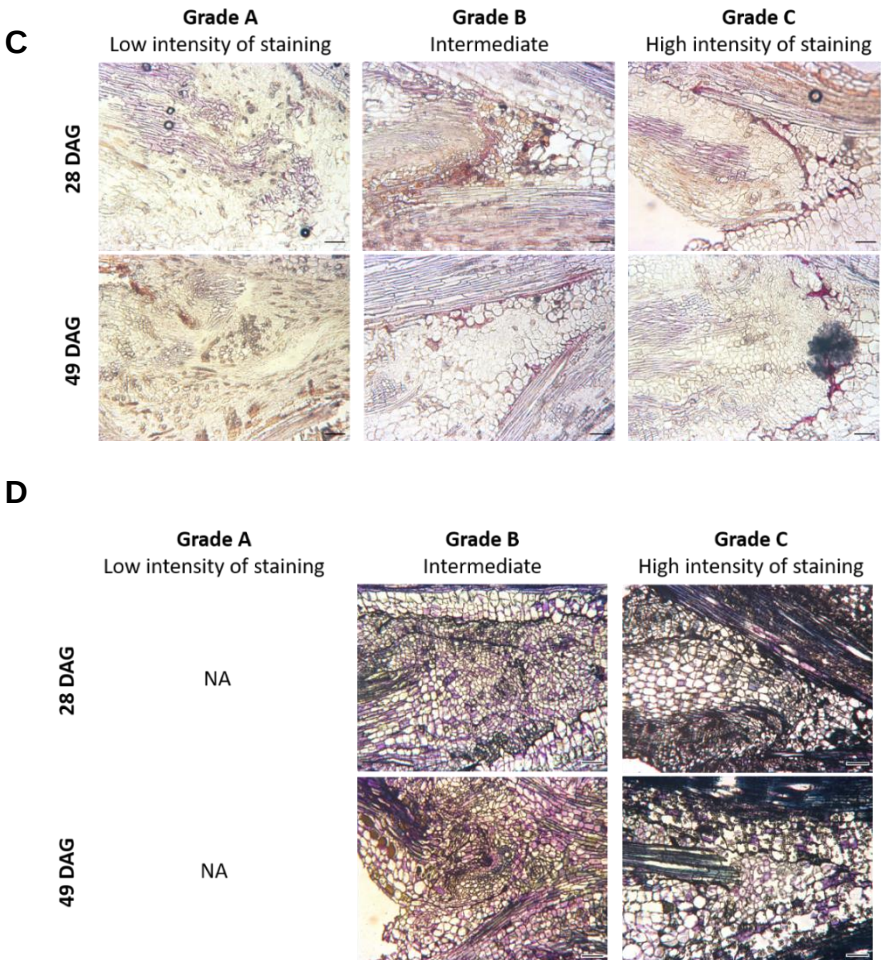

Figure S1. Examples of the attributed phenotypic scores (grade A, B, C) for the histochemical staining at 28 and 49 DAG. Calcofluor staining used to assess the level of cellular arrangement (**A**), acridine orange used to assess the level of cellular differentiation (**B**), Phloroglucinol-HCl used to evaluate the level of cellular staining at the necrotic layer (**C**), Toluidine blue used to assess the level of cellular staining (**D**). Scale bar = 100 µm.

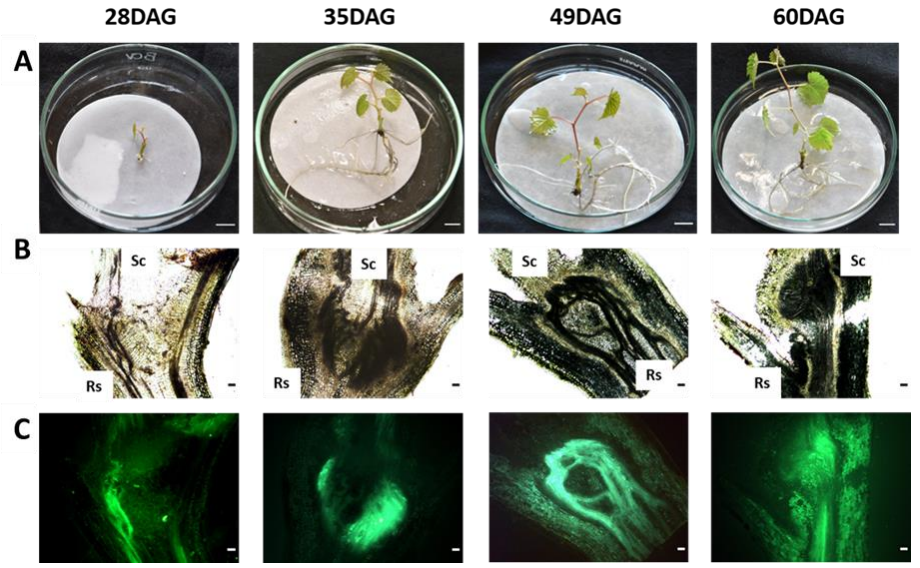

Figure S2. CFDA translocation in 110R/110R micrografts at 28, 35, 49, and 60 DAG. Sampled micrografts at the collection times (**A**), bright field image of fresh vibrotome graft union sections (**B**), and fluorescent image of the same sections showing carboxyfluorescein (CF) translocation across the union (**C**). Scion (Sc), Rootstock (Rs). Scale bars = 1 cm (**A**), and 100 µm (**B, C**).

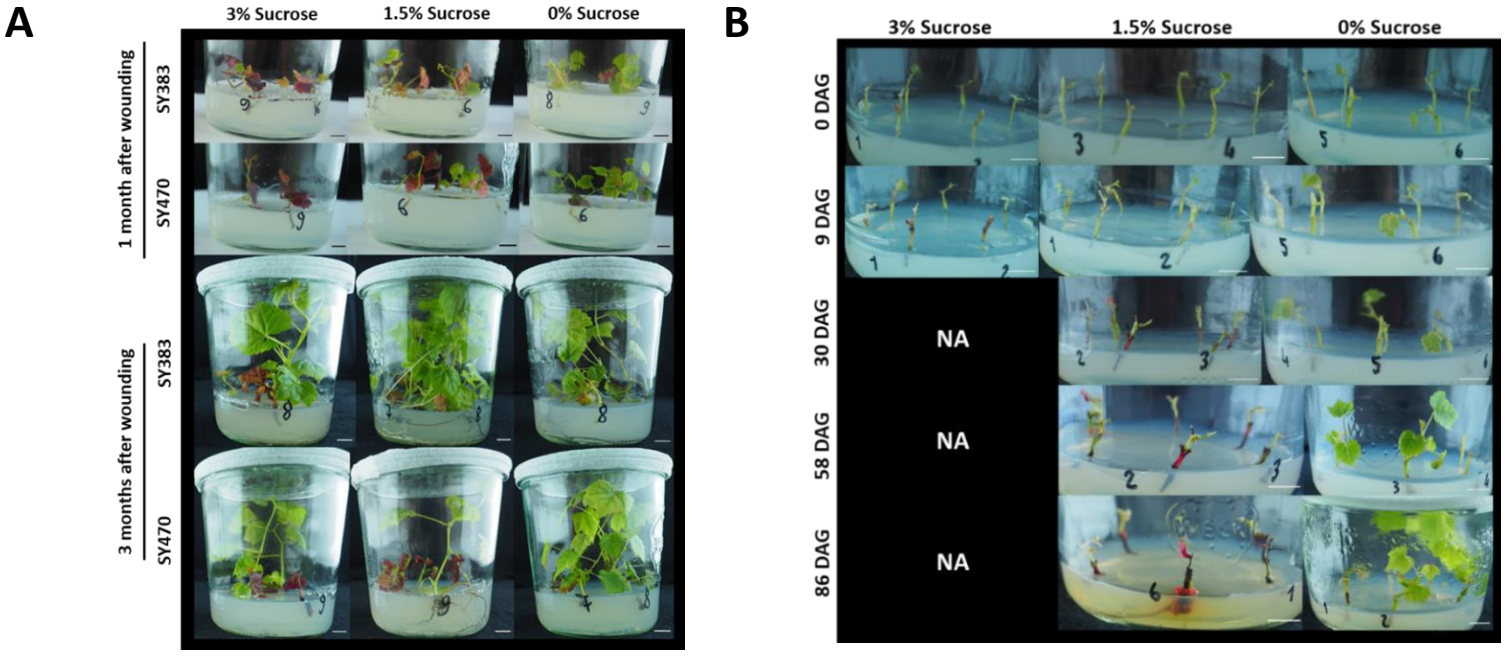

Figure S3. Sucrose effect on wounding and on grafting. Examples of wounded SY383 and SY470 ungrafted plants recorded after 1 and 3 months in culture media enriched with 3%, 1.5%, and 0% sucrose. Scale bars = 1 cm, n = 9 / genotype / treatment) (**A**). Examples of grafted SY383/SY383 recorded from 0 to 86 DAG under 3%, 1.5%, and 0% sucrose enriched media. Examples are given at 0 DAG and after approximately 1 week, 1 month, 2 months, and 3 months after grafting (n = 6 per treatment). Scale bars = 1 cm (**B**).

Chapter V

Conclusions and future perspectives

Grafting has brought incredible advantages to agriculture, being exploited to overcome biotic and abiotic constraints, change cultivar, control tree size, and to clonally propagate plants difficult to propagate with other asexual methods. According to Albacete et al. (2015) [1], rootstocks contribute to food security by increasing yields even under suboptimal growing conditions and by reducing the use of chemicals in agriculture, leading to less pressure on the environment and more efficient use of natural resources, such as soil and water [1]. Therefore, grafting is a precious tool to optimize crop productivity under the present challenges of climate changing. However, our knowledge on the biology of grafting, the scion-rootstock interactions, and the phenomenon of graft incompatibility is still insufficient to deliberately tune plant phenotypes by means of grafting.

Grapevines are propagated by grafting since more than a century to overcome the death of the plant due to the Phylloxera injuries, which would be lethal in *V. vinifera* if not grafted onto American rootstocks showing resistance to Phylloxera. Nevertheless, graft incompatibility, which manifests in short- or long-term graft failure and vine decline, is threatening the longevity of vineyards and causing economic losses to breeders and nurseries. Hence, the development of methods to early detect graft incompatible partners is one of the main applications of the graft incompatibility research, which would be tremendously useful to speed breeding selection and to reduce the source of financial losses by nurseries and growers. Nevertheless, early prediction of graft incompatibility is a challenge given that incompatibility manifestations can range from the complete failure of the union to the development of distress symptoms often difficult to be distinguished from other causes of stress [2], besides the already mentioned lack of predictability in the time of symptoms' appearance. Furthermore, grafting gives rise to a wide range

of different scion-rootstock interactions which often depend on the specific graft combination and are currently largely unpredictable.

This work contributes with new insights on the causes of graft incompatibility in grapevines thereby (1) exploring in field (Chapter II) and *in vitro* (Chapter IV) physiological profiles of compatible and incompatible grapevine combinations aiming to identify phenotypic tools to screen incompatibility in grapevines, and thereby (2) screening metabolic profiles of different graft combinations (Chapter III) to shed light on the early effect of metabolic scion-rootstock interactions in different grapevine tissues and phloem exudates.

Throughout this thesis, we have used two clones of two grapevine cultivars, i.e., cv. Touriga Nacional clone 21 and 112 (TN21 and TN112) and cv. Syrah clones 470 and 383 (SY470 and SY383) being respectively more and less graft compatible when combined onto the same worldwide used 110R rootstock [3,4].

In **Chapter II**, we have applied several methods that have been described as predictive for graft incompatibility in different plant species but not all already (and simultaneously) tested in grapevines. Specifically, several physiological parameters, Affinity Coefficient (AC) calculations based on stem diameter measurements, the internal anatomy of the graft union, and the leaf chlorophyll and carotenoid content, and chlorophyll fluorescence parameters were monitored in the previously described compatible (i.e. TN21/110R and SY470/110R) and incompatible (TN112/110R and SY383/110R) graft combinations in a grapevine nursery context at two times of the propagation process: at the callusing stage (when *callus* tissue is being formed at the graft union) - 21 days after grafting (DAG), and at the hardening stage - at 152 DAG, the selected timing to assess graft success. These time-points were chosen because the formation of

a *callus* bridge between the grafting partners is an essential requirement for successful grafting, representing the beginning of the scion-rootstock connectivity [5]. Also, we considered 152 DAG as a sufficient time to assess compatibility levels since it was previously found that most of the graft failures were occurring within the first 80 DAG [3]. Contrary to our expectations, we found that under field conditions heterografts displayed better graft takes rates than homografts and that this was correlating with a lower rooting capacity imputed to the *V. vinifera* species. Therefore, homografts controls were suggested to be carefully evaluated when used to quantify graft success rates in grapevines [6]. Furthermore, SY383/110R displayed a significant lower graft take rates when compared to other heterografts, although the same did not happen in case of TN112/110R. Concerning the methods applied to predict graft compatibility, we discourage the use of ACs (i.e., formulas based on stem diameters to assess the affinity between proposed grafting partners) as different formulas applied to the same graft combination resulted in contradicting conclusions [6]. Regarding the chlorophylls 'quantification methods, applied as an indicator of the effect of different stress factors on the efficiency of photosynthesis [7], we found the chlorophyll concentration measurements a more sensitive parameter to identify changes between different graft combinations than the measurements of chlorophyll fluorescence.

Among the several growth parameters monitored (i.e., sprouting and rooting rates, length of the main shoot, root number, length of the major root, stem diameters above, below and at the graft union, and score of callusing), shoot length and the degree of callusing at 21 DAG, and a higher Chl(b) content and a lower swelling above and below the union were found to best correlate with graft take rates at 152 DAG. From the internal anatomy characterization of the graft union, we realized that graft

healing is not yet complete at five months after grafting. Hence, a longer time than 5 months seems to be necessary to assess grapevine graft incompatibility under field conditions. Nevertheless, we detected that 110R rootstock was able to anticipate the sprouting of the heterografted scion and exert control over its growth by observing the physiology of these graft combinations, suggesting that important scion-rootstock interactions were already in place at these stages. Considering that standardized methods to phenotype the graft incompatibility trait would be fundamental to improve rootstock breeding and nurseries selection, the identification of predictive graft success parameters, carried out in Chapter II, might aid both researchers and breeders in the early screening of graft incompatibility. For instance, the grade of *callus* development at 21 DAG was revealed as a good indicator of graft success, which might be already of economic advantage at a nursery perspective. The fact that important scion-rootstock interactions were revealed when the healing of the union is not yet complete at early stages after grafting, led us to explore, in **Chapter III**, the scale and the content of early metabolic scion-rootstock profiles of homo- and heterografts in different tissues and phloem exudates. Specifically, we aimed to unveil (i) the metabolic profile of homo- and heterografts, (ii) the reciprocal effect of a heterologous grafting partner in the metabolome of the opposing partner, as well as (iii) the metabolic profile of scion and rootstock samples. Given the previous finding that more than 5 months might be required to assess compatibility levels in grapevines (Chapter II) [6], the metabolic comparison between grafts showing different compatibility behaviours was not included in Chapter III.

In Chapter III, we profiled the metabolome of leaves, stems, and phloem exudate, collected from above and below the graft union of 11 graft combinations at early stages (5-6 months after grafting) of the nursery-grafting grapevine process. The grafts combinations analysed included the

previously described Syrah and Touriga Nacional graft combinations onto 110R, as well as other graft combinations which were covered to increase the genotypic variability under analysis. Specifically, a second American rootstock - *V. rupestris* (RUP), and the *V. vinifera* cultivars: cv. Alfrocheiro (ALF), a progenitor of several cultivars in the Iberian Peninsula [8], and *V. vinifera subsp. Sylvestris* (SYLV), known to present high tolerance towards downy and powdery mildews and black rot pathogens [9], were also part of the experimental design. This approach revealed that grafting has a minor impact on the metabolome of grafted grapevines given that samples in the Principal Component Analysis (PCAs) clearly clustered according to the sampled tissue (i.e., scion or rootstock) and then according to the genotypic graft composition, while the impact of grafting in the PCAs is barely detectable. We found that heterografting affects rootstocks more than scions and both perceive the presence of a heterologous partner leading to the induction of defense-related metabolites (such as phenols, sugars, and metabolites from the salicylic acid pathway) [10]. Therefore, this heterografting-induced defense response is not only restricted at the graft interface, as previously found comparing the transcriptome of homo- and heterografting grapevines [11], but is detected even in phloem exudates and distant leaves. Considering that many of the identified defense-related compounds were several times identified in grapevine pathogenesis studies [9] and in virus-infected grapevines, it is not excluded that the enhanced stress response imputed to heterografted vines might reflect the perception of a foreign biome and/or the interaction of the grafting partners 'biomes when these belong to different genotypes. Regarding the effect of a grafting partner on the other partner's metabolome, we found that in grapevines both grafting partners exert their influence in specific organs and phloem exudate independently of their distance, as previously suggested in *Citrus* [12], but rather depending on the specific graft combination. Leaves were revealed as the best tissue

where to search for grafting-relating metabolic markers as the rootstock-induced changes were more consistent. Differently, scion-induced changes in the rootstock were genotypically driven and not generalizable although all grafts composed of 110R rootstock (except for SY383/110R) showed a reduction of sucrose in the phloem exudate harvested below the union, alerting for a possible unpaired graft union translocation in *V. vinifera* scions grafted onto 110R. Considering that the phloem composition is not expected to vary much within the same plant species, it was astonishing to have further found that almost 1/3 of the phloem exudate metabolome is altered between scion and rootstock samples within the same grafted plant. Also, the fact that sucrose appeared significantly depleted in the rootstock phloem exudate compared to the scion one was not expected. As sucrose is the main transported sugar and the phloem is the main route for the exchange of photoassimilates and signals in plants [13], it is conceivable how a perturbed phloem flow at 5 months after grafting can ultimately affect the performance of grafted grapevines at later stages. Hence, more studies on the phloem content seem necessary to elucidate the grapevine scion-rootstock interactions. This work contributed with new insights on the scale and the content of the scion-rootstock metabolic interactions in grapevines and might facilitate the identification of metabolic markers for important agronomic traits in grafted grapevines.

Finally, **Chapter IV** provide observations and findings collected throughout the entire PhD period. Here, we gave a deeper look into the physiological phenomenon of graft incompatibility in the previously described Touriga Nacional and Syrah graft combinations with 110R, and we further engaged in the challenge of early detecting incompatible partners, but this time, taking advantage from *in vitro* micrografting systems. *In vitro* micrografting has been used as an experimental system for graft incompatibility studies

enabling researchers to bypass several *in vivo* constraints such as minimizing environmental variability and biotic interferences [5,14,15]. In this work, we validated the use of this method, coupled with histology and histochemistry observations of the internal anatomy of the graft union, to unravel physiological markers that forecast incompatible responses in the mentioned graft combinations of known compatibility behaviour. At first, we characterized the time-frame of graft formation in *in vitro* homografts, which permitted us to establish suitable time-points for grafts collection, being these 28 DAG to study the early cellular events of graft union formation, and 49 DAG to assess the final success of the graft. Several of the physiological parameters investigated were in agreement with what recorded on the same graft combinations under field conditions (Chapter II), indicating that *in vitro* systems reliably mimic the time frame and events underlying graft union formation in grapevines. Nevertheless, the assessment of graft success highlighted that TN21 and SY383 better performed when grafted onto 110R comparing to TN112 and SY470, which is not in agreement with previous studies [3,4]. Furthermore, we have surprisingly found that most heterografts graft failures displayed typical symptoms of viral infections and levels of Grapevine Rupestris Stem Pitting associated Virus (GRSPaV) were correlated with graft (un)success in SY383 and SY470 grafted onto 110R under field and *in vitro* conditions. As this virus is frequently found in vines affected by “Syrah decline” although no cause-effect relationship has ultimately been provided [16,17]. Therefore, more studies should be addressed to verify the role of GRSPaV not only in declining Syrah but also in the graft success rates of Syrah grafted onto 110R. Indeed, it is unsure whether the use of certified vines is sufficient to exclude the occurrence of virus-induced graft incompatibility in grafted grapevines; considering that more than 65 viruses have been recorded to infect grapevines, but just a few of these are tested in the EU certification schemes [18]. Histochemical

observations of the graft union of grapevine micrografts pointed out the presence of translocated incompatibility symptoms in heterografted vines, characterized by the persistency of the necrotic layer at 49 DAG, a slower vascular differentiation, a lower starch scion-rootstock translocation, and impaired phloem regeneration compared to homografts. Among the histochemical dyes used, calcofluor, a cellulose staining used to evaluate the cellular arrangement, and I_2KI staining for quantifying starch contents, were able to identify the graft combinations with worse graft success rates among heterografts. In parallel, aniline blue was suggested as an easy and fast way to observe phloem initials in grapevine micrografting. Additionally, we have provided evidence that plants phenotypically responded to wounding. Thereby displaying a similar but milder phenotype than displayed by failing heterografted unions, and that the recorded phenotypic response is dependent on sucrose levels in the media, not only in wounded but also in grafted plants. This further points out at an impaired sucrose distribution via phloem although how and in which extent the phloemic route of wounded and grafted plants is impaired remain to be shown, as well as the possible involvement of viral agents in this phenomenon. All in all, we alert that grapevine graft incompatibility might be a virus-induced problem which can arise even employing certified virus-free plants, we confirm the utility of *in vitro* system in early predicting grapevine graft compatibility responses, and we encourage their use to investigate the viruses that might be responsible for grapevine graft incompatibility in sight of preserving the grapevine germplasm and to strengthen our certification schemes.

The results collected and discussed in this thesis contributed to deepening our knowledge regarding physiological and anatomical aspects of grapevine graft incompatibility as well as about the effect of early metabolic scion-rootstock interactions. Our observations of plants showing different

compatibility behavior permitted us to formulate the hypothesis that graft incompatibility in grapevines might be caused by viral agents and, particularly, that the reported graft incompatibility / vine decline of Syrah grafted onto 110R might be due to the presence of GRSPaV infections. Furthermore, histochemistry analysis of the graft union (Chapter IV) revealed that grapevine graft incompatibility seems to be of the translocated type, which was also suggested by analyzing physiological responses *in vivo* (Chapter II) and indicated due to the sucrose depletion found in the rootstock phloem exudate in the metabolic profiles (Chapter III). Most importantly, our efforts in validating suitable tools to phenotype graft incompatibility in grapevines both under field and *in vitro* conditions represent an important contribution towards the early detection of incompatible grapevine partners as the establishment of adapted phenotypic protocols to quantify the incompatibility trait is one of the main challenges in the field of research besides being fundamental to achieve advanced breeding selection of incompatible partners. Given that viruses seem to be the causal agent of graft incompatibility in grapevine and given the advantages of *in vitro* micrografting in early screening incompatible responses, and virus indexing, we advocate their use to research the viruses that might be involved. Also, it is important to highlight that not only viruses, but also other biomes, might have a role in the graft incompatibility of plants. Indeed, the general *consensus* stating that the higher the taxonomic distance between the grafting partners the higher the odds of incompatibility to manifest, might not be related to the grafting partners themselves, rather to the distance in their biomes.

References

1. Albacete, A.; Martínez-Andújar, C.; Martínez-Pérez, A.; Thompson, A.J.; Dodd, I.C.; Pérez-Alfocea, F. Unravelling rootstock×scion interactions to improve food security. *J. Exp. Bot.* **2015**, 66, 2211–2226.
2. Assunção, M.; Tedesco, S.; Fevereiro, P. Molecular Aspects of Grafting in Woody Plants. In *Annual Plant Reviews online*, 1st ed.; Wiley Online Library: New York, NY, USA, 2021, Volume 4, pp. 87–126.
3. Assunção, M.; Santos, C.; Brazão, J.; Eiras-Dias, J.E.; Fevereiro, P. Understanding the molecular mechanisms underlying graft success in grapevine. *BMC Plant Biol.* **2019**, 19, 1–17.
4. Renault-Spilmont, A.S.; Grenan, S.; Bousiquot, J.M. Syrah decline. *Progrés Agric. Vitic.* **2005**, *122*, 15–16.
5. Pina, A.; Errea, P.; Martens, H.J. Graft union formation and cell-to-cell communication via plasmodesmata in compatible and incompatible stem unions of *Prunus spp. Sci. Hortic. (Amst.)* **2012**, *143*, 144–150.
6. Tedesco, S.; Pina, A.; Fevereiro, P.; Kragler, F. A Phenotypic Search on Graft Compatibility in Grapevine. *Agronomy* **2020**, 10, 706.
7. Pavlović, D.; Nikolić, B.; Đurović, S.; Waisi, H.; Anđelković, A. Chlorophyll as a measure of plant health: Agroecological aspects. *Pestic. Phytomed. (Belgrade)* **2014**, *29*, 21–34.
8. Cunha, J.; Zinelabidine, L.H.; Teixeira-Santos, M.; Brazão, J.; Fevereiro, P.; Martínez-Zapater, J.M.; Ibáñez, J.; Eiras-Dias, J.E. Grapevine cultivar 'Alfrocheiro' or 'Bruñal' plays a primary role in the relationship among Iberian grapevines. *Vitis - J. Grapevine Res.* **2015**, 54, 59–65.
9. Maia, M.; Ferreira, A.E.N.; Nascimento, R.; Monteiro, F.; Traquete, F.; Marques, A.P.; Cunha, J.; Eiras-Dias, J.E.; Cordeiro, C.; Figueiredo, A.; Silva, M.S. Integrating metabolomics and targeted gene expression to uncover potential biomarkers of fungal / oomycetes - associated disease susceptibility in grapevine. *Sci. Rep.* **2020**, 10, 1–15.
10. Tedesco, S.; Erban, A.; Gupta, S.; Kopka, J.; Fevereiro, P.; Kragler, F.; Pina, A. The Impact of Metabolic Scion–Rootstock Interactions in Different Grapevine Tissues and Phloem Exudates. *Metabolites* **2021**, 11, 349.
11. Cookson, S.J.; Clemente Moreno, M.J.; Hevin, C.; Nyamba Mendome, L.Z.; Delrot, S.; Magnin, N.; Trossat-Magnin, C.; Ollat, N. Heterografting with nonself rootstocks induces genes involved in stress responses at the graft interface when compared with autografted controls. *J. Exp. Bot.* **2014**, 65, 2473–2481
12. Tietel, Z.; Srivastava, S.; Fait, A.; Tel-Zur, N.; Carmi, N.; Raveh, E. Impact of scion/rootstock reciprocal effects on metabolomics of fruit juice and phloem sap in grafted *Citrus reticulata*. *PLoS One* **2020**, 15, 1–17.
13. Lemoine, R. Sucrose transporters in plants: Update on function and structure. *Biochim. Biophys. Acta (BBA) Biomembr.* **2000**, 1465, 246–262.

14. Cui, Z.H.; Agüero, C.B.; Wang, Q.C.; Walker, M.A. Validation of micrografting to identify incompatible interactions of rootstocks with virus-infected scions of Cabernet Franc. Aust. J. Grape Wine Res. 2019, 25, 268–275.
15. Richardson, F.V.M.; Mac An Tsaoir, S.; Harvey, B.M.R. A study of the graft union in *in vitro* micrografted apple. *Plant Growth Regul.* **1996**, 20, 17–23.
16. Lima, M.F.; Alkowni, R.; Uyemoto, J.K.; Golino, D.; Osman, F.; Rowhani, A. Molecular analysis of a California strain of Rupestris stem pitting-associated virus isolated from declining Syrah grapevines. *Arch. Virol.* **2006**, 151, 1889–1894.
17. Martelli, G.P. Directory of virus and virus-like diseases of the grapevine and their agents. *J. Plant Pathol.* **2014**, 96, 1–136.
18. Martelli, G.P. An Overview on Grapevine Viruses, Viroids, and the Diseases They Cause. In *Grapevine Viruses: Molecular Biology, Diagnostics and Management*, Meng, B.; Martelli, G.P.; Golino, D.A.; Fuchs, M. eds., Springer International Publishing: Cham, CH, 2017; pp. 31–46.

This research was funded by **Fundação para a Ciência e Tecnologia (FCT)** through the S.T. PhD grant number PD/BD/128399/2017 within the scope of the PhD program Plants for Life (GREEN-IT R&D Unit - Bioresources for Sustainability).

Part of this work had also the financial support of the European Research Council (ERC) Synergy grant ERCSyG 2018_810131–PLAMORF awarded to F.K. and by Gobierno de Aragón—European Social Fund, European Union (Grupo Consolidado A12).